ACTA NATURA ET SCIENTIA

VOLUME: 5 ISSUE: 1 YEAR: 2024

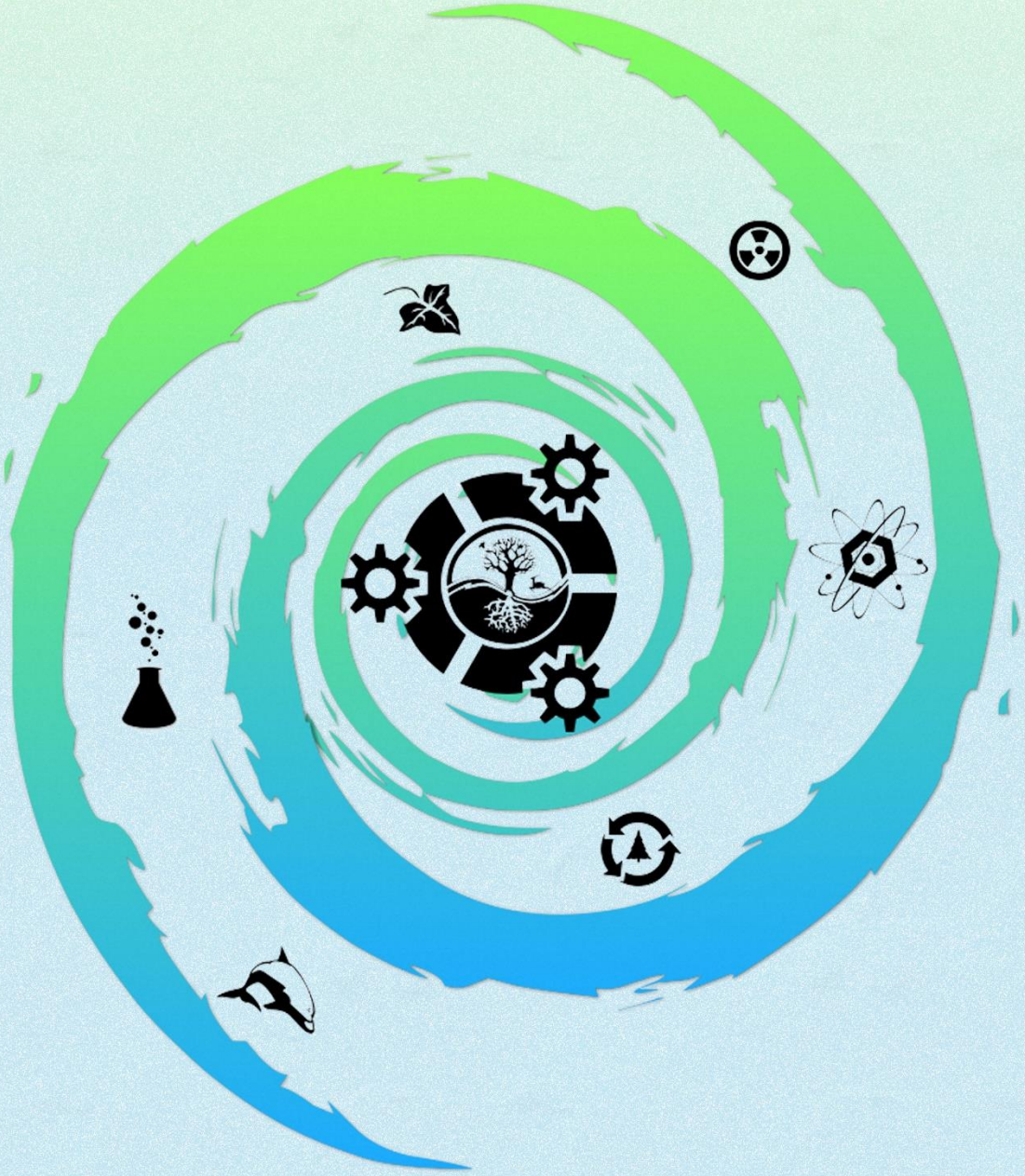

e-ISSN: 2718-0638

www.actanatsci.com

PRENSIP

ACTA NATURA ET SCIENTIA

2024 • VOLUME 5 • ISSUE 1

Acta Natura et Scientia is open access and peer-reviewed scientific journal that publishes high-quality papers in all aspects of nature and science throughout the world.

The aim of *Acta Natura et Scientia* is to contribute to the scientific literature by publishing the finest peer-reviewed researches in all aspects of nature and science depending upon their importance, originality, timeliness, interdisciplinary interests, and significant conclusions.

The publication languages of the journal are English and Turkish.

The journal accepts *Original Research Paper, Short Communication, Review, Case Report* in all aspects of nature and science.

The journal publishes 2 issues per year in June and December.

The double-blind peer-review process is maintained during the review processes.

More detail about *Aim & Scope* of the journal can be found at https://prensipjournals.com/ojs/index.php/actanatsci/aims-scope

AUTHOR GUIDELINES

More detail about *Author Guidelines* of the journal can be found at https://prensipjournals.com/ojs/index.php/actanatsci/author-guidelines

REVIEWER GUIDELINES

More detail about *Reviewer Guidelines* of the journal can be found at https://prensipjournals.com/ojs/index.php/actanatsci/reviewer-guidelines

REVIEW PROCESS

More detail about *Review Process* of the journal can be found at https://prensipjournals.com/ojs/index.php/actanatsci/review-process

FORMAT-FREE SUBMISSION POLICY

More detail about *Format-Free Submission Policy* of the journal can be found at https://prensipjournals.com/ojs/index.php/actanatsci/format-free-submission-policy

OPEN ACCESS POLICY

More detail about *Open Access Policy* of the journal can be found at https://prensipjournals.com/ojs/index.php/actanatsci/open-access-policy

PUBLICATION CHARGES

This journal has no publication charges or submission fees.

PUBLICATION ETHICS

More detail about *Publication Ethics* of the journal can be found at https://prensipjournals.com/ojs/index.php/actanatsci/publication-ethics

LICENSE

ARCHIVING POLICY

More detail about *Archiving Policy* of the journal can be found at https://prensipjournals.com/ojs/index.php/actanatsci/gateway/lockss

INDEXING

Acta Natura et Scientia is indexed by "CAB Abstracts (CABI: Web of Science-Clarivate), Global Health (CABI: Web of Science-Clarivate), Environment Index (EBSCO), Environment Complete (EBSCO), Central & Eastern European Academic Source - CEEAS (EBSCO), Crossref, Scilit, Index Copernicus, Dimensions, Electronic Journals Library (EZB), WorldCat, Bielefeld Academic Search Engine (BASE), OpenAIRE Explore, CiteFactor, Index Medicine, EuroPub, ROAD-Directory of Open Access Scholarly Resources, Eurasian Scientific Journal Index (ESJI), Academic Resource Index-ResearchBib, Directory of Research Journals Indexing (DRJI), Root Indexing, International Services for Impact Factor and Indexing (ISIFI), InfoBase Index, International Institute of Organized Research (I2OR), Cosmos, General Impact Factor, ASOS Indeks, Google Scholar, Scientific Journal Impact Factor (SJIF), International Scientific Indexing (ISI), Advanced Sciences Index, SciMatic, Journal Factor, ScienceGate, International Accreditation and Research Council, İdealOnline, SOBİAD, Lens, SCIPIO (Scientific Publishing & Information Online).

More detail about *Indexing* of the journal can be found at https://prensipjournals.com/ojs/index.php/actanatsci/indexing

PUBLISHER

Prensip Publishing and Consultancy Ind. Trade. Co. Ltd.
Kuzeykent Mah. Orgeneral Atilla Ateş Paşa Cad. No.15 CD, İç Kapı No:31
37150, Merkez, Kastamonu, Türkiye
info@prensip.gen.tr
prensip.gen.tr

ACTA NATURA ET SCIENTIA 2024 • VOLUME 5 • ISSUE 1

TABLE OF CONTENTS

RESEARCH ARTICLES

Acta Nat. Sci. (2024) 5(1): 1-10
DOI: 10.61326/actanatsci.v5i1.1
e-ISSN: 2718-0638

Original Research Paper
info@actanatsci.com
www.actanatsci.com

ACTA NATURA ET SCIENTIA PRENSİP

Calculation of Isothermal Compressibility and Bulk Modulus as a Function of Pressure in a Perovskite-Like Framework of $[(C_3H_7)_4N]$ $[Mn(N(CN)_2)_3]$

Sedat Avcı[1]✉ • Mustafa Kurt[2]

[1] Çanakkale Onsekiz Mart University, Çanakkale Applied Sciences Faculty, Department of Energy Management, 17100, Çanakkale, Türkiye, sedat.avci@comu.edu.tr
[2] Çanakkale Onsekiz Mart University, Engineering Faculty, Department of Electric-Electronic Engineering, 17100, Çanakkale, Türkiye, mkurt@comu.edu.tr

✉ Corresponding Author: sedat.avci@comu.edu.tr

Please cite this paper as follows:
Avcı, S., & Kurt, M. (2024). Calculation of Isothermal Compressibility and Bulk Modulus as a Function of Pressure in a Perovskite-Like Framework of $[(C_3H_7)_4N]$ $[Mn(N(CN)_2)_3]$. *Acta Natura et Scientia*, *5*(1), 1-10. https://doi.org/10.61326/actanatsci.v5i1.1

ARTICLE INFO

Article History
Received: 06.12.2023
Revised: 04.01.2024
Accepted: 08.01.2024
Available online: 22.05.2024

Keywords:
Perovskite-like frameworks
Structural phase transition
Grüneisen value
Bulk modulus
Isothermal compressibility

ABSTRACT

The many distortions in solid material that are most easily triggered by factors like pressure are called its structural degrees of freedom. Zeolites, perovskites, coordination polymers and metal-organic frameworks (MOFs) are all members of the extensive and significant family of solids known as framework materials. In the last decade, it has been shown that perovskite-like framework materials have great potential applicable in solar panel cell production. The Perovskite-like framework, $[(C_3H_7)_4N][Mn(N(CN)_2)_3]$ [TPrA][Mn(dca)$_3$], in short), has recently attracted scientists, due to its magnetism, ferroelectricity, luminescence, switchable dielectric behaviour, multiferroic behaviour, non-linear optical properties and also photovoltaic properties. Exerted pressure causes changes in the structural, optical, and electronic properties of perovskite and perovskite-like compounds. As a result of these effects, these compounds present phase transitions at certain pressures. The [TPrA][Mn(dca)$_3$] compound also exhibits two structural phase transitions at 0.3 GPa and 3.0 GPa pressure. In this study, we calculated some important thermodynamic parameters, which are the isothermal Grüneisen value, isothermal compressibility, and Bulk modulus, as a function of pressure to analyse phase transition dynamics by using observed volume and frequency values from the literature. The Bulk modulus values were determined at 9.86 GPa for the Pcnb -phase and 36 GPa for the P21/n -phase by using calculated isothermal compressibility values. Our results confirm that the perovskite-like [TPrA][Mn(dca)$_3$] compound is a good candidate for solar panel cell production, as corroborated in the literature.

INTRODUCTION

Researchers working on solar panel cell technologies face the challenge of fulfilling the growing worldwide demand for renewable energy and implementing sustainable technologies. To handle this challenge, they are striving to develop new compounds and to improve the power conversion efficiency of photovoltaic (PV) systems while also reducing their operational costs. Within a period of less than a decade, solar cell power conversion efficiencies have reached up to 25% by using perovskite materials as raw materials in the production of solar cells, exceeding that of thin film or multi-layer silicon (Min et al., 2021; Jošt et al., 2022). In addition to the usage of perovskite compounds in PV technologies, scientists and engineers are finding new materials having perovskite and perovskite-like structure attractive because of its intriguing features and potential usage in electrical, optical, and energy storage systems (Grinberg et al., 2013; Shen et al., 2015; Wang et al., 2015). Recent studies have shown that perovskite-like frameworks of $[(C_3H_7)_4N][Mn(N(CN)_2)_3]$ (abbreviated as $[TPrA][Mn(dca)_3]$) exhibit properties similar to perovskites compounds (Mączka et al., 2019). The size and shape of the organic cation, the length and flexibility of the molecular linker, as well as its capacity to form hydrogen bonds with the metal linker framework, all have an impact on the crystal structures and properties of molecular perovskites (Huang et al., 2017; Assirey, 2019; Li et al., 2019). Pressure is one of the main parameters used to manipulate and control the electronic structure and behaviour of perovskite solar cells in the production processes (Oyelade et al., 2020). Molecular crystals, such as perovskites and perovskite-like frameworks, undergo structural phase transitions as the pressure increases, resulting in changes in molecular order. Hence, comprehending the mechanisms behind the phase transition of these types of compounds is highly intriguing, both from the standpoint of crystal engineering and because of their prospective applications. The applicability of $[TPrA][Mn(dca)_3]$ in solar panel cell manufacture can be greatly improved by controlling the structural phase transition that occurs under different pressure settings during the production processes (Bermúdez-García et al., 2015; Agyei-Tuffour et al., 2016, 2017). The Perovskite-like framework $[TPrA][Mn(dca)_3]$ exhibits two structural phase transitions depending on applied pressure. The first transition occurs from tetragonal phase ($P\text{-}42_1c$) to orthorhombic phase (Pcnb) at 0.3 GPa, and the second transition occurs from orthorhombic phase (Pcnb) to monoclinic phase (P21/n) at 3.0 GPa and ambient temperature (Bermúdez-García et al., 2015, 2017a; Mączka et al., 2019). Although there are previous studies related to pressure-induced structural phase transitions, there is currently a lack of comprehensive investigations that adequately clarify the micro dynamics of the phase transition in $[TPrA][Mn(dca)_3]$.

In this work, we calculated the Grüneisen value (γ_T), compressibility (κ), and Bulk modulus by using pressure dependent observed internal Raman and IR modes ($\nu_s(C\equiv N)$, $\nu_{as}(C\equiv N)$, $\delta(CNC)$, $\varrho(CH_2)$ and T(dca)+L(dca)+T(Mn)) in $[TPrA][Mn(dca)_3]$ for $P\text{-}42_1c$, Pcnb and $P2_1/n$ phases as a function of pressure. By using Grüneisen and Einstein approximations for frequency of soft modes in molecular crystals, we also calculated the frequency of the interested modes as a function of pressure and compared the calculated value and observed value to the Raman and IR mode frequencies in [TPrA][Mn(dca)3] given by Mączka et al. (2019).

MATERIAL AND METHODS

Thermodynamics provide a fundamental scientific framework in engineering and basic sciences, although its practical implementation across several fields has given rise to distinct variations characterized by specific terminology and notation. One of the most familiar parameters that is used to define how a crystal lattice's size or dynamics modify under pressure or at a certain temperature in thermodynamics is the Grüneisen value (γ). This parameter is a dimensionless thermodynamic quantity that is named after the German scientist Eduard Grüneisen. Its initial description was established in relation to the nonlinearities of phonons (Grüneisen, 1912). The Grüneisen value can also be defined as an observable thermodynamic parameter in a microscopic model that describes the vibrational

behaviour of atoms within a crystal lattice. Einstein demonstrated that the quantum harmonic oscillator, which represents a mode of crystal vibration in his theory, exhibits a relationship between the frequency of the mode and volume dependence. This relation is characterized by Grüneisen parameter, which can be expressed as a straightforward combination of well-known thermal and mechanical properties (Stacey & Hodgkinson, 2019). Whether the recalling force acting on an atom displaced from its primary position is or is not linearly dependent on the displacement, the frequency of phonons in the crystal will change in association with variations in the crystal's volume. The phenomenon can be used to establish a correlation between the Grüneisen value and the frequency shift of Raman modes by the anharmonic approximation. As mentioned by Stacey & Hodgkinson (2019) and Kurt's (2022) works, the average total energy in an atom is defined as:

$$E = \sum_{n=0}^{\infty} E(n) = \frac{h\nu}{\left[exp(\frac{h\upsilon}{kT})-1\right]} \quad (1)$$

The energy is equivalent to the thermal energy associated with a singular mode in the oscillation of a crystal, characterized by natural frequency and denoted as ν. This frequency is dependent on the volume variation of the crystal, as described in Einstein's theory (Einstein, 1907). Eq. (1) derived from Einstein's model for crystal structure is fundamental to Grüneisen's theory. The Isothermal Grüneisen value corresponding to each Raman or IR internal mode in atomic crystals can be defined as (Stacey & Hodgkinson, 2019):

$$\gamma_T = -\frac{d\, ln\, \upsilon_i}{d\, ln\, V} \quad (2)$$

where υ_i is the frequency for i^{th} mode in a crystal and V is the volume at constant temperature. From here the Grüneisen value is derived at constant temperature γ_T as a function of pressure:

$$\gamma_T = -\frac{V}{\nu}\frac{(\partial\nu/\partial P)_T}{(\partial V/\partial P)_T} \quad (3)$$

where ν is the frequency of Raman or IR internal mode as a function of pressure and V is the volume of a molecular crystal as a function of pressure, under constant temperature T. To calculate the frequency value as a function of pressure for each mode in a molecular crystal, Eq. (2) is integrated. Then frequency is calculated as:

$$\upsilon_T = \upsilon_0\, exp\left[-\gamma_T\, ln\left(\frac{V_T(P)}{V_0}\right)\right] + Const. \quad (4)$$

Eq. (4) includes volume that is dependent on pressure, so an equation for volume as a function of pressure was then derived. Findings of Mączka et al. (2019) for [TPrA][Mn(dca)$_3$] showed that volume exhibit a parabolic variation tendency while pressure is increasing. Therefore, a second-order polynomial function for the observed volume data of the molecular crystal [TPrA][Mn(dca)$_3$] was used in our calculations, as also used previously by scientist in the literature (Yurtseven & Kurt, 2011; Yurtseven & Cebeci, 2015; Yurtseven & Ünlü, 2015; Kurt, 2020):

$$V_T(P) = a_o + a_1 P + a_2 P^2 \quad (5)$$

where the coefficients a_o, a_1 and a_2 are constants at ambient temperature. In order to determine these coefficients, Eq. (5) was fitted to volume data from the literature (Mączka et al., 2019), as shown in Figure 1 and Table 1 for [TPrA][Mn(dca)$_3$]. The volume data of this compound showed discontinuity in the vicinity of 0.3 and 3 GPa pressure. These pressure values also corresponded to the structural phase transition from P-42$_1$c to Pcnb and from Pcnb to P2$_1$/n, respectively.

Table 1. The coefficients of Eq. (5), determined by fitting to the experimental volume data (Mączka et al., 2019) for P-42$_1$c, Pcnb and P2$_1$/n phases in [TPrA][Mn(dca)$_3$].

Phase	a_0 (A^0)^3	$-a_1$ ((A^0)^3/ GPa)	a_2 ((A^0)^3/ GPa^2)	V_0 (A^0)^3
P-42$_1$c	4621.95	467.43	-198.33	4621.95
Pcnb	4507.31	412.72	57.12	4507.31
P2$_1$/n	4088.01	111.98	1.65	4088.01

Table 2. The coefficients of Eq. (6), determined by fitting to the experimental frequency data (Mączka et al., 2019) for ν_s(C≡N), ν_{as}(C≡N), δ(C-NC), ϱ(CH2) and T(dca)+L(dca)+T(Mn) internal modes for P-42$_1$c, Pcnb and P2$_1$/n phases in [TPrA][Mn(dca)$_3$].

	Mode	T(dca)+ L(dca)+ T(Mn)	ϱ(CH$_2$)	δ(CNC)	ν_{as}(CN)	ν_s(CN)
Pcnb	b_0 (cm^{-1})	178.37	773.84	846.78	2159.82	2244.96
	b_1 (cm^{-1}/GPa)	11.08	9.03	10.53	7.65	3.80
	-b_2 (cm^{-1}/GPa^2)	1.27	0.93	1.13	0.37	-0.41
	ν_0 (cm^{-1})	178.37	773.84	846.78	2159.82	2244.96
P2$_1$/n	b_0 (cm^{-1})	198.53	772.46	864.57	2183.73	2251.94
	b_1 (cm^{-1}/GPa)	3.65	7.41	-0.22	-2.44	2.84
	b_2 (cm^{-1}/GPa^2)	0.08	-0.31	0.46	0.70	-0.07
	ν_0 (cm^{-1})	198.53	772.46	864.57	2183.73	2251.94

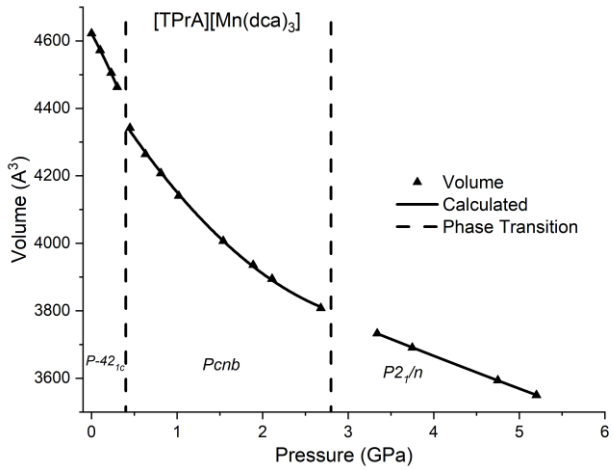

Figure 1. Calculated and observed (Mączka et al., 2019) volume data for P-42$_1$c, Pcnb and P2$_1$/n phases in [TPrA][Mn(dca)$_3$].

Eq. (3) also contains a frequency function that is dependent of pressure. In addition, the observed Raman modes data of ν_s(C≡N), ν_{as}(C≡N), δ(CNC), ϱ(CH$_2$) and T(dca)+L(dca)+T(Mn) for [TPrA][Mn(dca)$_3$] showed a parabolic change with pressure. The frequency of the Raman and IR internal modes in [TPrA][Mn(dca)$_3$] was defined as a second-order polynomial depending on pressure, like the volume function (Eq. 5). To obtain frequency as a function of pressure, the experimental data was iterated to the following equation:

$$\nu_T(P) = b_o + b_1 P + b_2 P^2 \quad (6)$$

where b_0, b_1 and b_2 are constants. In order to determine these constants for each Raman mode including ν_s(C≡N), ν_{as}(C≡N), δ(C-NC), ϱ(CH$_2$) and T(dca)+L(dca)+T(Mn), the experimental data taken from the literature (Mączka et al., 2019) were fitted to Eq. (6) for each phase in [TPrA][Mn(dca)$_3$], as shown in Figure (2) and presented in Table 2. Subsequently, the isothermal Grüneisen values from 0 to 6 GPa for the interested Raman and IR Modes in [TPrA][Mn(dca)$_3$] were determined with Eq. (4) through the calculated volume and frequency with the coefficients (presented in Tables 1 and 2) derived from the experimental data, which varied as a function of pressure, as shown in Figure 3.

Compressibility and bulk modulus are also very important thermodynamic parameters needed to understand the thermoelastic and thermodynamic properties and behaviour of solids under high pressure and temperature, like the Grüneisen parameter. Compressibility (defined as "isothermal compressibility" at constant temperature) refers to the extent to which a fluid or solid changes its volume in response to a change in pressure or mean stress in thermodynamics. The Isothermal Compressibility relation is very well known in thermodynamics and is expressed as follows:

$$\kappa_T = -\left(\frac{1}{V}\right)\left(\frac{\partial V}{\partial P}\right)_T \quad (7)$$

where V is volume and P is pressure at constant temperature. Defining compressibility with a negative sign ensures that compressibility is positive when an increase in pressure leads to a decrease in volume. The isothermal compressibility can be related to the internal mode of molecular crystals by deriving from Eq. (3) and (7) as in the following equation:

$$\kappa_T = \frac{1}{\gamma_T}\frac{1}{v}\left(\frac{\partial v}{\partial P}\right) \quad (8)$$

By using Eq. (8), the isothermal compressibility for [TPrA][Mn(dca)$_3$] from 0 GPa to 6 GPa at constant temperature can be calculated, as shown in Figure 4. The bulk modulus refers to the proportion of the rise in pressure related to the subsequent decrease in volume of a material and describes the degree of resistance of a substance to compression. Moreover, the bulk modulus is known as a measure of elastic characteristics due to its ability to return a compressed material to its initial volume under zero pressure. The relationship between compressibility and bulk modulus can be expressed as:

$$\beta = \frac{1}{\kappa} \quad (9)$$

The bulk modulus of [TPrA][Mn(dca)$_3$] for Pcnd and P2$_1$/n phases was calculated for pressures between 0 to 6 GPa by utilizing the calculated values of isothermal compressibility, as shown in Figure 5. The intercept and slope of the bulk modulus for both phases is also presented in Table 3.

Table 3. Intercept (K_0) and slope (K_0'), determined by fitting calculated Bulk modulus for P-42$_1$C, Pcnb and P2$_1$/n phases in [TPrA][Mn(dca)$_3$].

Phase	K_0 (GPa)	K_0'	Pressure Interval (GPa)
Pcnb	9.89	4.95	0.3<P<2.5
P2$_1$/n	36.07	0.26	3.0<P<6

RESULTS AND DISCUSSION

Pressure is an important parameter that can be employed to manipulate the electrical configuration and characteristics of organic-inorganic perovskite solar cells in production process es (Xiao et al., 2017). Exerting pressure on perovskite results in the compression of molecules. This leads to a higher degree of packing and a decrease in the distances between atoms, ultimately altering the electronic orbitals and bonding configurations. Therefore, applying pressure on perovskites in the production processes can cause alterations in the structural, optical, magnetic, and electrical characteristics of both organic and inorganic perovskite compounds (Huang et al., 2017). Applying pressure can enhance the interlayer contact inside solar cell designs (Tan & Cheetham, 2011; Xiao et al., 2014). By acquiring insight into the impact of pressure on the layers of organic-inorganic perovskite compounds, material properties can be adjusted by relating to compression. Studies related to characteristics of organic-inorganic perovskite under high pressure serve as a guiding framework for the subsequent design, synthesis, and application of materials with the structure and/or features of these perovskites (Oyelade et al., 2020).

For the current study, first the frequency of the Raman and IR modes in a perovskite like framework [TPrA][Mn(dca)$_3$] was calculated depending on pressure for P-42$_1$C, Pcnb and P2$_1$/n phases by using the corresponding Eq. 4. Grüneisen values for ν_s(C≡N) (2244.4 cm^{-1}), ν_{as}(C≡N) (2158.1 cm^{-1}), δ(CNC) (844.7 cm^{-1}), ϱ(CH$_2$) (774.1 cm^{-1}) and T(dca)+L(dca)+T(Mn) (174.1 cm^{-1}) were used, and modes are shown in Figure 2.

The calculated frequency values for the interested internal modes tended to increase with increasing pressure, as expected for all structural phases. Also, these calculations are compatible with the experimental measurements by Mączka et al. (2019). Although there were not any significant jumps in the frequency measurements at 0.3 and 3.0 GPa for interested modes in [TPrA][Mn(dca)3], XRD, volume and dielectric measurements with pressure, other studies have shown a soft structural phase transition from P-421C to Pcnb at 0.3 GPa, and a distinct structural phase transition from Pcnb to P21/n at approximately 3.0 GPa (Bermúdez-García et al., 2015, 2017a, 2017b, 2018; Mączka et al., 2019). Results of the current study show that pressure significantly influences the lattice structure and electronic configuration of perovskite-like framework, as well as the ordering of molecular orientation in

[TPrA][Mn(dca)3]. In addition, the rise in Raman frequencies of the interested modes is likely directly correlated with the applied pressure. Although the phase transition at 0.3 and 3 GPa could not be clearly seen from Raman frequency measurements, Grüneisen values calculated with Eq. (3) show that there were obvious phase transitions at these pressure values, as in the literature, and as also shown in Figure 3.

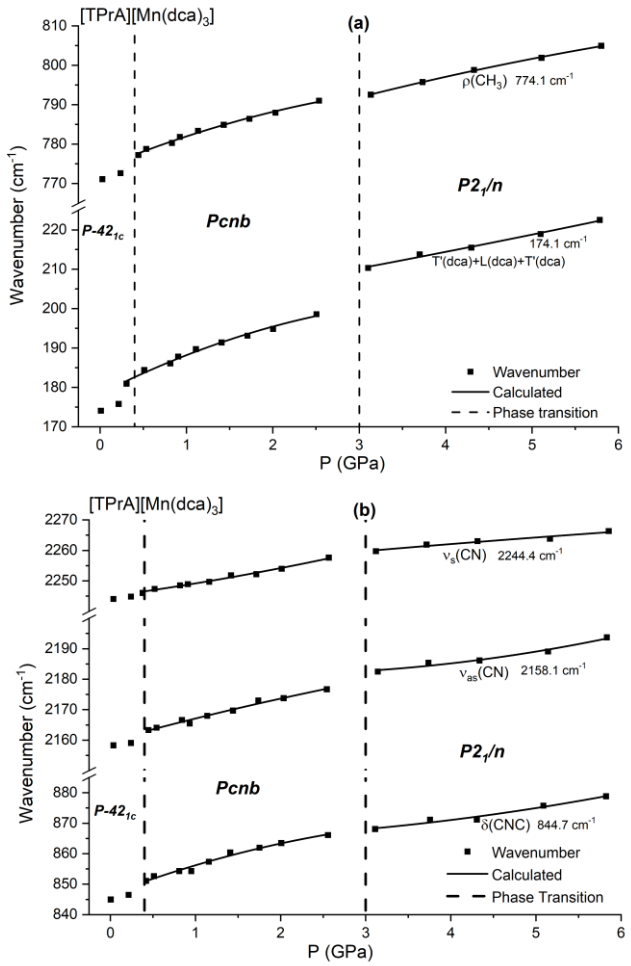

Figure 2. Calculated and observed (Mączka et al., 2019) frequency data of ν_s(C≡N), ν_{as}(C≡N), δ(C-NC), ϱ(CH2) and T(dca)+L(dca)+T(Mn) for P-42$_1$c, Pcnb and P2$_1$/n phases in [TPrA][Mn(dca)3].

As explained in detail above, the Grüneisen value is usually used to connect microscopic structure to macroscopic measurements, so the calculated Grüneisen values as a function of pressure really demonstrate these phase transitions for all internal modes (Figure 3). For ν_s(C≡N) (2244.4 cm^{-1}), ν_{as}(C≡N) (2158.1 cm^{-1}), δ(CNC) (844.7 cm^{-1}) and ϱ(CH$_2$) (774.1 cm^{-1}) internal modes in [TPrA][Mn(dca)$_3$], the calculated Grüneisen value almost exhibited a similar tendency with increasing pressure; however, the T(dca)+L(dca)+T(Mn) (174.1 cm^{-1}) IR mode had a very distinct trend. The cause of this behaviour for T(dca)+L(dca)+T(Mn) IR mode might be interference of the three bonds and energy exchange between these three modes.

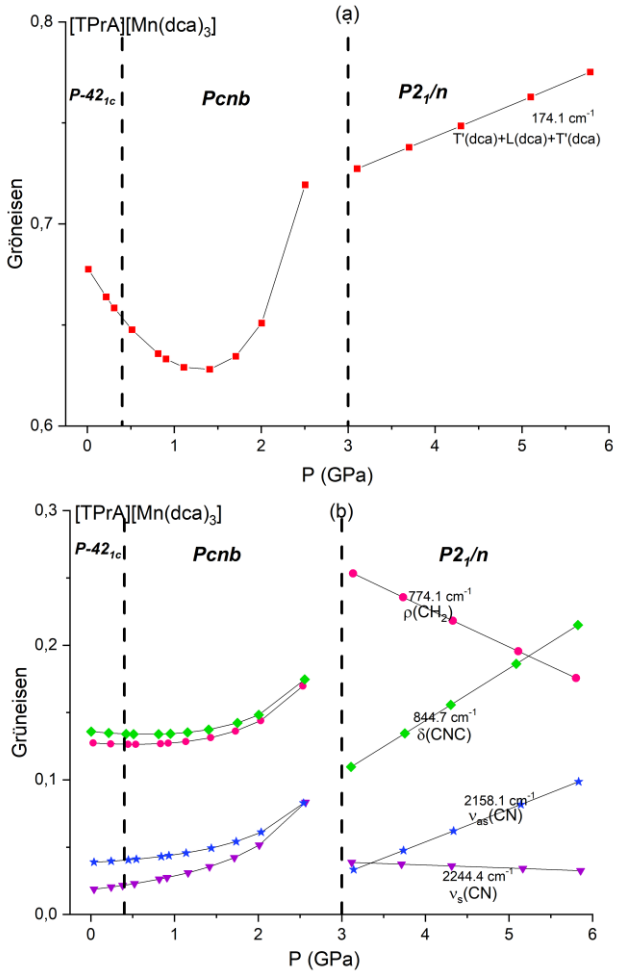

Figure 3. Calculated Isothermal Grüneisen values of ν_s(C≡N), ν_{as}(C≡N), δ(CNC), ϱ(CH$_2$) and T(dca)+L(dca)+T(Mn) for P-42$_1$c, Pcnb and P2$_1$/n phases in [TPrA][Mn(dca)$_3$].

The compressibility of a material defines the rate at which its volume alters in reaction to a change in pressure and is also crucial in the manufacturing of perovskite type solar panel cells, as it is for all solid materials. Perovskite materials with a high compressibility value are preferred in PV production processes because they easily modify the crystal structure with pressure (Kurt, 2022). In this study, the pressure-dependent compressibility for a perovskite-like framework of [TPrA][Mn(dca)$_3$] was also calculated by using Eq. 8 to determine how convenient it would be for the solar panel cell production. As seen

in Figure 4, the compressibility decreased up to 3 GPa but was almost constant after this pressure. However, no jump or discontinuity was seen at 0.3 GPa. This behaviour of isothermal compressibility shows that [TPrA][Mn(dca)$_3$] was in ordered phase up to ~3 GPa, after which a cell distortion to monoclinic symmetry occurred.

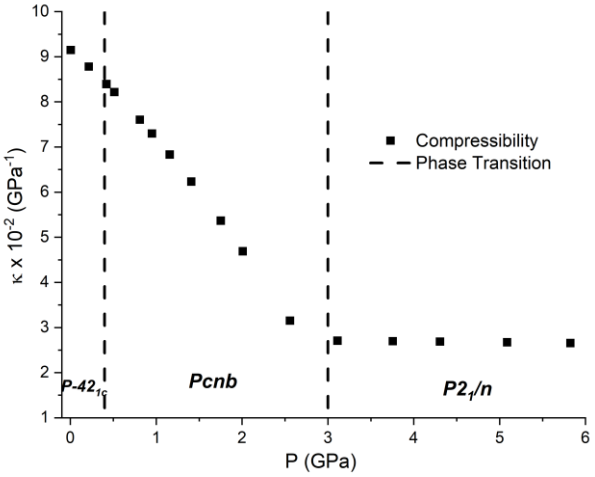

Figure 4. Calculated the isothermal compressibility κ_T by using Eq. (8) for P-42$_1$C, Pcnb and P2$_1$/n phases in [TPrA][Mn(dca)3].

Lastly, the isothermal bulk modulus was calculated depending on pressure through calculated isothermal compressibility for P-42$_1$C, Pcnb and P21/n phases (Figure 5.), also reported in Table 3. Mączka et al. (2019) determined the isothermal bulk modulus by fitting a 2nd order Birch–Murnaghan equation of state (EoS) to the volume–pressure dependence for Pcnb phase in their previous work. Their calculated value for this phase was 8.1 GPa and was almost the same as the calculated value (9.8 GPa) in the current study using Eq. 9 (Table 3). The isothermal bulk modulus was also determined with Eq. 9 for P-42$_1$C phase in [TPrA][Mn(dca)$_3$] and calculated as 36.0 GPa. Although this calculated value is a bit lower than 95 GPa for silicone, which is usually used in solar panel cell production, it is considerably larger than other perovskite materials that are candidates for solar panel cells. Results confirm that the perovskite-like framework of [TPrA][Mn(dca)$_3$] is a good material for new solar panel technology in the future.

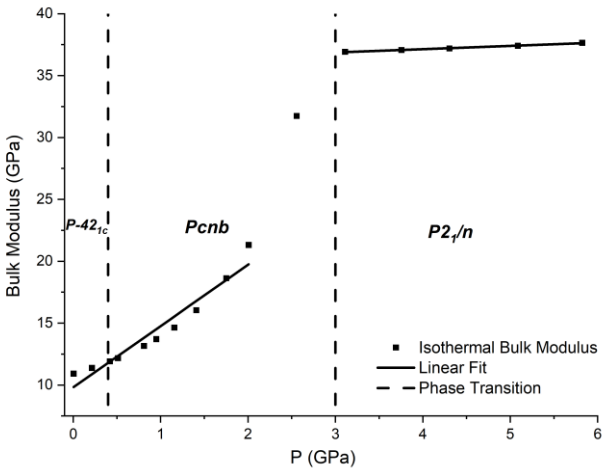

Figure 5. The isothermal Bulk modulus as a function of pressure, calculated by using Eq. (9) using the values of the isothermal compressibility (κ_T) for P-42$_1$C, Pcnb and P2$_1$/n phases in [TPrA][Mn(dca)$_3$]. A linear regression with coefficients (K_0) and (K_0') is shown by a straight line, as presented in Table 3.

CONCLUSION

For this study, we calculated Grüneisen values and isothermal compressibility as a function of pressure for ν_s(C≡N) (2244.4 cm^{-1}), ν_{as}(C≡N) (2158.1 cm^{-1}), δ(CNC) (844.7 cm^{-1}) and ϱ(CH2) (774.1 cm^{-1}) Raman modes in a perovskite-like framework of [TPrA][Mn(dca)$_3$]. We used the observed volume and Raman and IR mode frequency data close to the area where phase transitions occurred (P=0.3 and 3.0 GPa). In addition, we ascertained the Bulk modulus by using calculated isothermal compressibility for this perovskite. The calculated isothermal compressibility and Bulk modulus confirmed potential applications of the perovskite-like framework of [TPrA][Mn(dca)3] in high performance perovskite solar cells, light-emitting diodes, and photonic devices, making it a good candidate material for new solar panel technologies in the future. Our results also suggest that the calculated thermodynamic parameters are similar to those found in other studies, and our method of calculating these parameters can be used for additional perovskite-like frameworks with ferroelectric characteristics.

ACKNOWLEDGEMENTS

This study is part of PhD Thesis of the first author, and supported by Çanakkale Onsekiz Mart University the Scientific Research Coordination Unit, (Project number: FDK-2021-3591). Part of this study was presented at 3rd Global Conference on Engineering Research, 13-16 September 2023, Balıkesir, Türkiye.

Compliance with Ethical Standards

Authors' Contributions

Both authors have contributed equally to the paper. All authors read and approved the final manuscript.

Conflict of Interest

The authors declare that there is no conflict of interest.

Ethical Approval

For this type of study, formal consent is not required.

Data Availability

The data that support the findings of this study are available from the corresponding author upon request.

REFERENCES

Agyei-Tuffour, B., Doumon, N. Y., Rwenyagila, E. R., Asare, J., Oyewole, O. K., Shen, Z., Petoukhoff, C. E., Zebaze Kana, M. G., Ocarroll, D. M., & Soboyejo, W O. (2017). Pressure effects on interfacial surface contacts and performance of organic solar cells. *Journal of Applied Physics, 122*(20), 205501. https://doi.org/10.1063/1.5001765

Agyei-Tuffour, B., Rwenyagila, E. R., Asare, J., Oyewole, O. K., Zebaze Kana, M. G., O'Carroll, D. M., & Soboyejo, W. O. (2016). Influence of pressure on contacts between layers in organic photovoltaic cells. *Advanced Materials Research, 1132*, 204-216. https://doi.org/10.4028/www.scientific.net/AMR.1132.204

Assirey, E. A. R. (2019). Perovskite synthesis, properties and their related biochemical and industrial application. *Saudi Pharmaceutical Journal, 27*(6), 817-829. https://doi.org/10.1016/j.jsps.2019.05.003

Bermúdez-García, J. M., Sánchez-Andújar, M., Yáñez-Vilar, S., Castro-García, S., Artiaga, R., López-Beceiro, J., Botana, L., Alegría, Á., & Señarís-Rodríguez, M. A. (2015). Role of temperature and pressure on the multisensitive multiferroic dicyanamide framework [TPrA][Mn(dca)$_3$] with perovskite-like structure. *Inorganic Chemistry, 54*(24), 11680-11687. https://doi.org/10.1021/acs.inorgchem.5b01652

Bermúdez-García, J. M., Sánchez-Andújar, M., Castro-García, S., López-Beceiro, J., Artiaga, R., & Señarís-Rodríguez, M. A. (2017a). Giant barocaloric effect in the ferroic organic-inorganic hybrid [TPrA][Mn(dca)$_3$] perovskite under easily accessible pressures. *Nature Communications, 8*(1), 15715. https://doi.org/10.1038/ncomms15715

Bermúdez-García, J. M., Sánchez-Andújar, M., & Señarís-Rodríguez, M. A. (2017b). A new playground for organic–inorganic hybrids: Barocaloric materials for pressure-induced solid-state cooling. *The Journal of Physical Chemistry Letters, 8*(18), 4419-4423. https://doi.org/10.1021/acs.jpclett.7b01845

Bermúdez-García, J. M., Yáñez-Vilar, S., García-Fernández, A., Sánchez-Andújar, M., Castro-García, S., López-Beceiro, J., Artiaga, R., Dilshad, M., Moya, X., & Señarís-Rodríguez, M. A. (2018). Giant barocaloric tunability in [($CH_3CH_2CH_2$)$_4$N]Cd[$N(CN)_2$]$_3$ hybrid perovskite. *Journal of Materials Chemistry C, 6*(37), 9867-9874. https://doi.org/10.1039/C7TC03136J

Einstein, A. (1907). Die Plancksche Theorie der Strahlung und die Theorie der spezifischen wärme. *Annalen der Physik, 327*(1), 180-190. https://doi.org/10.1002/andp.19063270110

Grinberg, I., West, D. V., Torres, M., Gou, G., Stein, D. M., Wu, L., Chen, G., Gallo, E. M., Akbashev, A. R., Davies, P. K., Spanier, J. E., & Rappe, A. M. (2013). Perovskite oxides for visible-light-absorbing ferroelectric and photovoltaic materials. *Nature, 503*(7477), 509-512. https://doi.org/10.1038/nature12622

Grüneisen, E. (1912). Theorie des festen Zustandes einatomiger Elemente. *Annalen der Physik, 344*(12), 257-306. https://doi.org/10.1002/andp.19123441202

Huang, J., Yuan, Y., Shao, Y., & Yan, Y. (2017). Understanding the physical properties of hybrid perovskites for photovoltaic applications. *Nature Reviews Materials, 2*(7), 17042. https://doi.org/10.1038/natrevmats.2017.42

Jošt, M., Kohnen, E., Al-Ashouri, A., Bertram, T., Tomšič, Š., Magomedov, A., Kasparavicius, E., Kodalle, T., Lipovšek, B., Getautis, V., Schlatmann, R., Kaufmann, C. A., Albrecht, S., & Topič, M. (2022). Perovskite/CIGS tandem solar cells: from certified 24.2% toward 30% and beyond. *ACS Energy Letters, 7*(4), 1298-1307. https://doi.org/10.1021/acsenergylett.2c00274

Kurt, A. (2020). Pressure dependence of the Raman modes for orthorhombic and monoclinic phases of $CsPbI_3$ at room temperature. *Journal of Applied Physics, 128*(7), 075106. https://doi.org/10.1063/5.0012355

Kurt, A. (2022). Calculation of Gruneisen parameter, compressibility, and bulk modulus as functions of pressure in $(C_6H_5CH_2NH_3)_2PBI_4$. *Çanakkale Onsekiz Mart University Journal of Advanced Research in Natural and Applied Sciences, 8*(1), 63-75. https://doi.org/10.28979/jarnas.1003367

Li, Q., Zhang, L., Chen, Z., & Quan, Z. (2019). Metal halide perovskites under compression. *Journal of Materials Chemistry A, 7*(27), 16089-16108. https://doi.org/10.1039/C9TA04930D

Mączka, M., Collings, I. E., Leite, F. F., & Paraguassu, W. (2019). Raman and single-crystal X-ray diffraction evidence of pressure-induced phase transitions in a perovskite-like framework of $[(C_3H_7)_4N]$ $[Mn(N(CN)_2)_3]$. *Dalton Transactions, 48*(25), 9072-9078. https://doi.org/10.1039/C9DT01648A

Min, H., Lee, D. Y., Kim, J., Kim, G., Lee, K. S., Kim, J., Paik, M. J., Kim, Y. K., Kim, K. S., Kim, M. G., Shin, T. J., & Seok, S. I. (2021). Perovskite solar cells with atomically coherent interlayers on SnO_2 electrodes. *Nature, 598*(7881), 444-450. https://doi.org/10.1038/s41586-021-03964-8

Oyelade, O. V., Oyewole, O. K., Oyewole, D. O., Adeniji, S. A., Ichwani, R., Sanni, D. M., & Soboyejo, W. O. (2020). Pressure-assisted fabrication of perovskite solar cells. *Scientific Reports, 10*(1), 7183. https://doi.org/10.1038/s41598-020-64090-5

Shen, Z., Wang, X., Luo, B., & Li, L. (2015). $BaTiO_3$–$BiYbO_3$ perovskite materials for energy storage applications. *Journal of Materials Chemistry A, 3*(35), 18146-18153. https://doi.org/10.1039/C5TA03614C

Stacey, F. D., & Hodgkinson, J. H. (2019). Thermodynamics with the Grüneisen parameter: Fundamentals and applications to high pressure physics and geophysics. *Physics of the Earth and Planetary Interiors, 286*, 42-68. https://doi.org/10.1016/j.pepi.2018.10.006

Tan, J. C., & Cheetham, A. K. (2011). Mechanical properties of hybrid inorganic–organic framework materials: Establishing fundamental structure–property relationships. *Chemical Society Reviews, 40*(2), 1059-1080. https://doi.org/10.1039/C0CS00163E

Wang, W., Tadé, M. O., & Shao, Z. (2015). Research progress of perovskite materials in photocatalysis-and photovoltaics-related energy conversion and environmental treatment. *Chemical Society Reviews, 44*(15), 5371-5408. https://doi.org/10.1039/C5CS00113G

Xiao, G., Cao, Y., Qi, G., Wang, L., Liu, C., Ma, Z., Yang, X., Sui, Y., Zheng, W., & Zou, B. (2017). Pressure effects on structure and optical properties in cesium lead bromide perovskite nanocrystals. *Journal of the American Chemical Society, 139*(29), 10087-10094. https://doi.org/10.1021/jacs.7b05260

Xiao, G., Zhu, C., Ma, Y., Liu, B., Zou, G., & Zou, B. (2014). Unexpected room-temperature ferromagnetism in nanostructured Bi_2Te_3. *Angewandte Chemie International Edition, 53*(3), 729-733. https://doi.org/10.1002/anie.201309416

Yurtseven, H., & Cebeci, A. (2015). Pressure dependence of the Raman modes related to the phase transitions in cyclohexane. *Acta Physica Polonica A, 127*(3), 744-747. https://doi.org/10.12693/aphyspola.127.744

Yurtseven, H., & Kurt, M. (2011). Pressure dependence of the Raman frequency shifts related to the thermodynamic quantities in phase II of s-triazine. *Indian Journal of Physics, 85*, 615-628. https://doi.org/10.1007/s12648-011-0064-0

Yurtseven, H., & Ünlü, D. (2015). Temperature and pressure effect on the Raman frequencies calculated from the crystal volume in the γ-phase of solid nitrogen. *Journal of Applied Spectroscopy, 82*(4), 700-704. https://doi.org/10.1007/s10812-015-0166-0

Acta Nat. Sci. (2024) 5(1): 11-18
DOI: 10.61326/actanatsci.v5i1.2
e-ISSN: 2718-0638

Original Research Paper
info@actanatsci.com
www.actanatsci.com

ACTA NATURA ET SCIENTIA PRENSİP

The Preventive Effect of N-Acetylcysteine on Liver Tissue Against Doxorubicin-Induced Oxidative Stress in Rats

Suat Cakina[1]✉ • Samil Ozturk[1] • Latife Ceyda Irkin[2]

[1] Çanakkale Onsekiz Mart University, Health Service Vocational College, 17100, Çanakkale, Türkiye, suatcakina@comu.edu.tr, samilozturk16@hotmail.com
[2] Çanakkale Onsekiz Mart University, Canakkale Faculty of Applied Sciences, Department of Fisheries Technology, 17100, Çanakkale, Türkiye, latifeirkin@gmail.com

✉ Corresponding Author: suatcakina@comu.edu.tr

Please cite this paper as follows:
Cakina, S., Ozturk, S., & Irkin, L. C. (2024). Title: The Preventive Effect of N-Acetylcysteine on Liver Tissue Against Doxorubicin-Induced Oxidative Stress in Rats. *Acta Natura et Scientia*, *5*(1), 11-18. https://doi.org/10.61326/actanatsci.v5i1.2

ARTICLE INFO

Article History
Received: 04.12.2023
Revised: 13.02.2024
Accepted: 05.03.2024
Available online: 22.05.2024

Keywords:
Doxorubicin
N-Acetylcysteine
Liver
Oxidative stress

ABSTRACT

Doxorubicin (DOX) is a chemotherapeutic agent and is widely used in cancer treatment. There are some studies suggesting oxidative stress-induced toxic changes in the liver due to DOX administration. The aim of this study was to reveal the oxidative damage of DOX in liver tissue at molecular level and to evaluate the protective effect of N-acetyl cysteine (NAC) against DOX oxidative damage. Twenty four rats weighing 150-200 g were randomly divided into four equal groups; group 1: control, group 2: received a single dose of DOX, group 3: received NAC for 28 days and group 4: received a single dose of DOX, followed by NAC for 28 days. At the end of the experiment, liver tissues were taken from all animals. Total Antioxidant Capacity (TAC), Total Oxidant Capacity (TOC) levels were determined in these samples by spectrophotometric methods. The histopathological changes of liver tissue were observed routinely in histological staining. It was determined that TOC level increased, TAC levels decreased in the group given DOX compared to the control group. In addition, TAC levels increased in the DOX+NAC group. It was showed the occurrence of congestion in portal triad, and pycnotic cells degeneration in DOX group. It was concluded that DOX administration increased oxidative stress and NAC administration could prevent the increased oxidative stress ($p<0.05$). NAC caused modulatory effects on oxidative stress and antioxidant redox system in DOX-induced liver toxicity in the rat.

INTRODUCTION

Doxorubicin (DOX) is an anti-cancer agent used in the treatment of ovarian, breast, liver and lung cancers and solid tumors such as leukemia and lymphoma. In cancer treatment, it is used to block cell division of tumor cells (Aljobaily et al., 2020). However, since it is a highly toxic antineoplastic agent, it causes toxicity on many organs and tissues in the organism. Studies have reported toxic effects on the heart, brain, liver,

kidney, kidney, skin and reproductive organs such as ovaries and testes. It is known that the liver is one of the most vulnerable organs to DOX damage. Although the mechanism of DOX-mediated liver injury is not fully known, it is supported that increased free radical formation and lipid peroxidation as well as decreased antioxidant enzymes may play a role (Moslehi, 2016; Timm et al., 2021; Yu et al., 2020).

Due to its toxicity on organs, studies are carried out with many agents that will eliminate or minimize this effect. One of these is N-acetylcysteine (NAC). NAC is a mucolytic agent that plays a role in the formation of glutathione, an effective antioxidant. NAC has a protective effect against tissue damage caused by free radicals (Saricaoglu et al., 2005; Arakawa & Ito, 2007; Koçkar et al., 2010).

Lipid peroxidation is the reaction in which fatty acids in the membrane are destroyed by free oxygen radicals. Malondialdehyde (MDA), which can be measured with thiobarbituric acid, is formed in the peroxidation of fatty acids formed by the destruction of lipid hydroperoxides. This method is a frequently preferred method for measuring lipid peroxide levels. Lipid peroxidation plays an important role in disease pathogenesis by inducing changes that lead to cell damage (Hjelle & Petersen, 1983; Saleh et al., 2022).

The aim of this study was to reveal the oxidative damage of DOX in liver tissue at molecular level and to evaluate the protective effect of NAC against the oxidative damage of DOX on this tissue.

MATERIAL AND METHODS

Adult male Wistar Albino rats obtained from Çanakkale Onsekiz Mart University Experimental Research and Application Center were used in this study. Animals were maintained under standard environmental conditions and had free access to standard rodent feed and water. Our work was carried out in accordance with the guidelines of the Ethical Committee of Çanakkale Onsekiz Mart University Faculty of Medicine approved the current study (Ethics number: 2022-2200189432). Experiments were conducted in accordance with international guidelines for the ethical use of rats.

Rats were randomly divided in to four experimental groups (6 rats per group) as follows:

- Group 1: Control
- Group 2: DOX (20 mg/kg, intraperitoneal)
- Group 3: NAC (50 mg/kg/day, via gavage) for 28 days
- Group 4: DOX (20 mg/kg Doxorubicin, intraperitoneal) + NAC (50 mg/kg/day, via gavage) for 28 days (from the day of DOX administration)

At the end of the experimental period, the rats were anesthetized by ketamine and xylazine hydrochloride. Then, liver was moved for measuring the oxidative stress markers the rats.

Tissue samples were homogenized in phosphate buffer solution (1:10 w/v, pH: 7.4) using ice-cooled tubes. The homogenate was centrifuged (14,000 rpm, 30 min) and the supernatants were separated for analysis. Protein concentration was estimated by the method of Lowry et al. (1951). Tissue samples, taken for malondialdehyde determination, were homogenized and subjected to procedures as outlined before (Ohkawa et al., 1979). TAC and TOC levels were measured by a spectrophotometric assay using commercially available kits (Rel Assay Diagnostics, Turkey). The OSI was defined as the ratio of the TAC level to TOC level.

Liver tissues fixed with 10% buffered formaldehyde were subjected to routine histologic follow-up. The tissues were embedded in paraffin and then 4 micrometer sections were taken from the blocks with a sliding-microtome and deparaffinized. Rehydrated sections were stained with Mayer hematoxylin and eosin stains. After the procedure, the sections were covered with entellan and evaluated histopathologically under light microscope. Liver histopathologic evaluations were performed according to Gibson-Corley et al. (2013). In the scoring process performed in 10 random fields in the micrographs at 200× magnification obtained from random sections taken from all samples of each group, 0 was determined as none, 1 as mild, 2 as extensive and 3 as severe (Gibson-Corley et al., 2013). In pyknotic nuclei counting performed in liver tissues,

pyknotic nuclei detected in 5 random fields of random sections were counted with the help of ImageJ (NIH, USA, Version 1.53J) program.

Statistical Analysis

Statistical software (IBM SPSS version 19.0, USA) was used to analyze the data obtained. Comparison of multiple groups was determined by analysis of variance (one-way ANOVA) with post hoc Duncan test. Differences were considered significant at P<0.05. All variables were represented as mean ± standard error of the mean (SE).

RESULTS

In group 2 given DOX and group 4 given DOX+NAC; TAC levels decreased compared to the control group (respectively p=0.14; p<0.001) (Table 1 and Figure 1).

Table 1. TAC analysis results

Group	TAC (mmole/L)	P Value
Control	2.16±0.87	
DOX	1.61±0.37	§p:0.14
NAC	2.09±0.07	
DOX+NAC	1.90±0.05	‡p:<0.001

Note: Group comparisons: §p=group 1 and group 2; ¶p=group 1 and group 3; ‡p=group 1 and group 4; ♯p=group 2 and group 4.

Table 2. TOC analysis results

Group	TOC (µmole/L)	P Value
Control	24.58±5.68	
DOX	36.65±2.36	§p:0.002
NAC	23.78±1.39	
DOX+NAC	23.40±4.12	♯p:<0.001

Note: Comparisons: §p=group 1 and group 2; ¶p=group 1 and group 3; ‡p=group 1 and group 4; ♯p=group 2 and group 4.

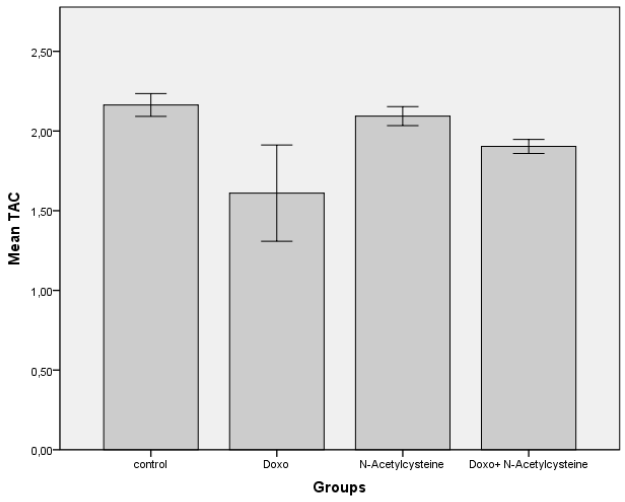

Figure 1. Groups-TAC results

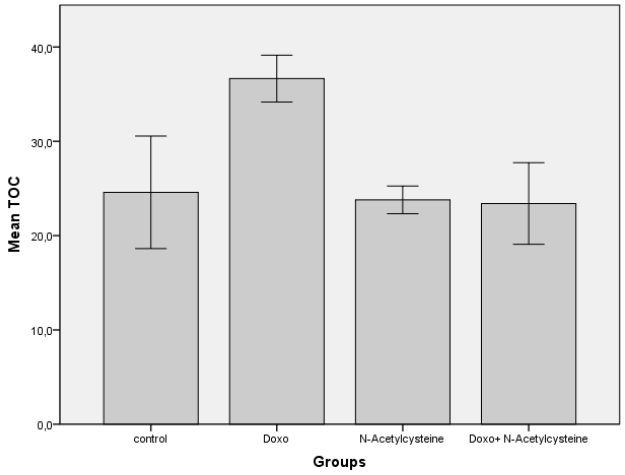

Figure 2. Groups-TOC results

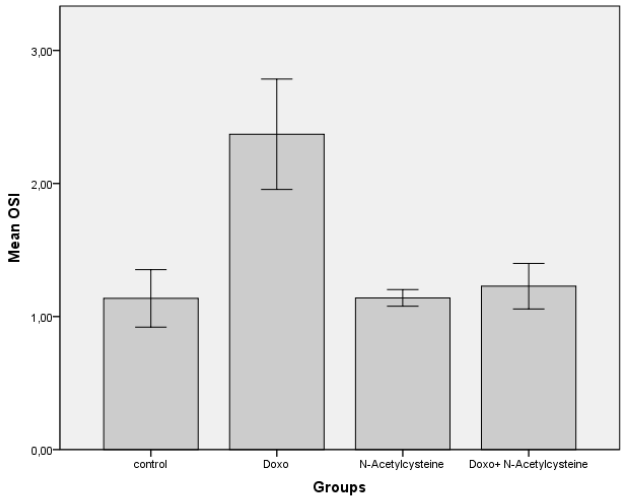

Figure 3. Groups-OSI results

Table 3. OSI analysis results

Group	OSI ratio	P Value
Control	1.14±0.26	
DOX	2.37±0.50	§p:0.001
NAC	1.14±0.07	
DOX+NAC	1.22±0.21	♯p:<0.002

Note: $OSI = \frac{\text{TOC (µmole } H_2O_2 \text{ Equiv./gram protein)}}{\text{TAC (µmole } H_2O_2 \text{ Equiv./gram protein)}} \times 100$

Group Comparisons: §p=group 1 and group 2; ¶p=group 1 and group 3; ‡p=group 1 and group 4; ♯p=group 2 and group 4.

In group 2 given DOX, TAC levels increased compared to the control group (p=0.002). In group 4 given DOX+NAC, TAC levels decreased compared to the group 2 given DOX (p<0.001) (Table 2 and Figure 2).

In group 2 given DOX, OSI ratio increased compared to the control group (p=0.001). In group 4 given DOX+NAC, OSI ratio decreased compared to the group 2 given DOX (p<0.002) (Table 3 and Figure 3).

Inflammatory cell infiltration showing intergroup comparisons was commonly observed in DOX type stroma, while almost none was observed in control types. Congestion and hemorrhagic areas were observed in all groups except the control group (Figure 4A.). Especially hemorrhagic areas were frequently observed in the DOX group. Hemorrhage was observed in the DOX group both in and around the vessel lumen (Figure 4B). Hepatosteatosis and high amounts were scored in DOX and DOX+NAC groups. Steatosis was mostly observed in the connections close to the hepatic triad. The highest amount of pyknotic nuclei was again observed in DOX class, while DOX+NAC class showed loss (Table 4 and Figure 4)

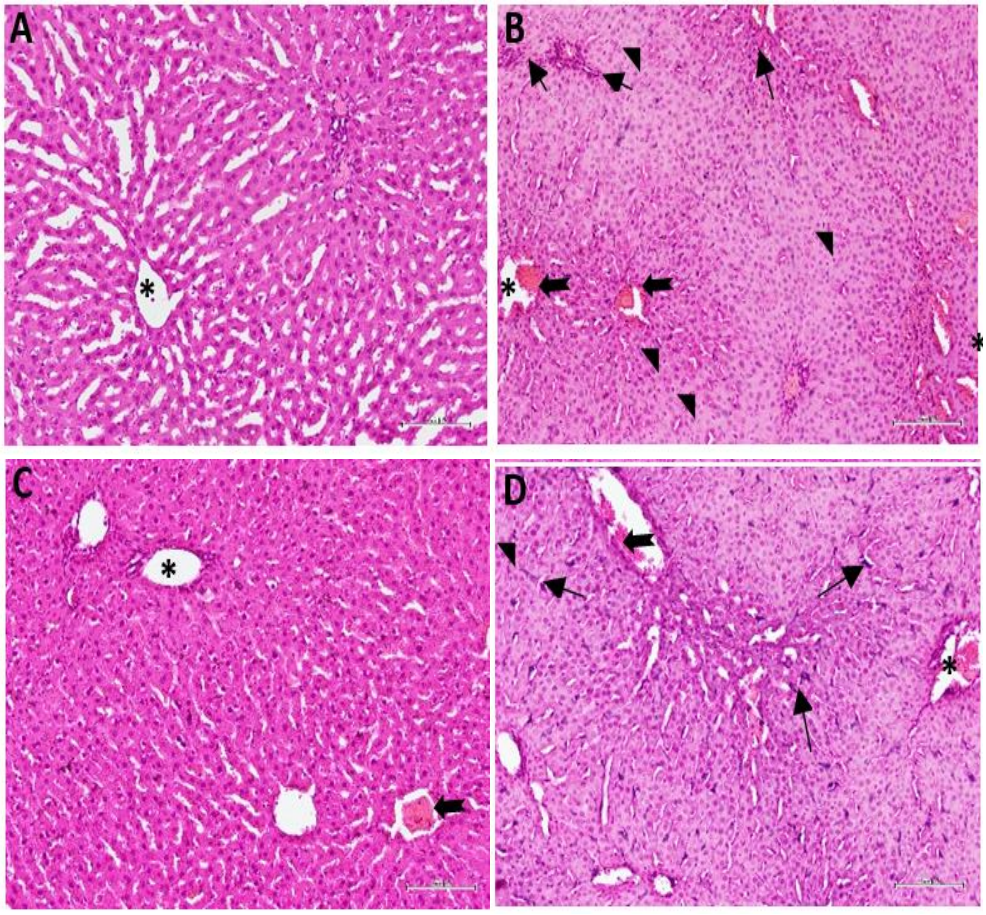

Figure 4. Liver section micrographs of the groups with H-E staining applied (These are micrographs belonging to the groups A: control, B: DOX, C: Nac, D: DOX+Nac. (It belongs to 200× magnification). Asterix indicates central vein, arrowhead indicates steatosis, thick arrows indicate congestion and hemorrhages, and thin arrows indicate inflammatory cell areas)

Table 4. Effects of NAC on some pathological changes in liver tissue of DOX -treated rats

Group	Inflammatory cell infiltration	Number of pyknotic nuclei	Hepatosteatosis	Hemorrhage
Control	0.20±0.08	1.93±0.02	0.20±0.07	0.10±0.04
DOX	2.57±0.02§P	10.13±0.62§P	2.53±0.02§P	2.07±0.02§P
NAC	1.17±0.01¶P	2.53±0.27	0.70±0.02¶P	1.26±0.01¶P
DOX +NAC	1.80±0.09‡P	6.46±0.07‡P, ♯P	1.80±0.17‡P, ♯P	1.86±0.02‡P, ♯P

Note: Group Comparisons: §P=group 1 and group 2; ¶P=group 1 and group 3; ‡P=group 1 and group 4; ♯P=group 2 and group 4.

DISCUSSION

DOX is widely used in the treatment of various malignant diseases, including breast, ovarian, testicular, thyroid, lung and hematologic cancers. However, its use is limited due to its cytotoxic effect on both normal and cancerous cells (Alshabanah et al., 2010; Gibson-Corley et al., 2013; Biller, 2014; Rivankar, 2014). Bilgic & Ozgocmen (2019) showed that single dose doxorubicin administration may cause acute liver injury. In our study, we found that although liver TAC concentrations decreased with DOX administration, TOC levels increased. Therefore, DOX administration in animals is characterized by increased TOC levels and decreased TAC concentrations. Furthermore, liver TOC levels decreased with NAC treatment, but TAC concentrations increased with NAC treatment. Numerous in vivo or in vitro studies on the effects of NAC on the level of oxidative stress have been reported (Saricaoglu et al., 2005; Samuni et al., 2013; Otrubová et al., 2018). To our knowledge, this is the first study to investigate the effects of NAC on the antioxidant system in DOX -induced hepatotoxicity in rats. Our results are consistent with the results of previous studies regarding the increase in oxidative stress in the liver after DOX treatment.

Prasanna et al. (2020) concluded that oxidative stress is the primary cause of DOX -induced liver injury. As a result of DOX-induced oxidative stress, electrons are lost from oxygen, leading to the production of superoxide radicals and reactive oxygen species (ROS). High levels of ROS also lead to an increase in lipid peroxidation. This results in damage to hepatocytes and liver. In our study, it was found that DOX+NAC group increased TAC levels and decreased TOC levels compared to DOX group. Studies have shown that NAC increases intracellular GSH, which directly scavenges oxidants and protects against ROS-related oxidative stress.

In various studies, NAC supplementation was found to reduce increased MDA levels in rat liver. In a similar study, it was reported that expressed as Glutathione Peroxidase (GSH-Px) activity did not change in the liver of DOX+NAC-treated rats, thus liver cell damage was less. NAC is both a potent antioxidant and a precursor of reduced glutathione (GSH) (Saricaoglu et al., 2005; Arakawa & Ito, 2007; Koçkar et al., 2010; Samuni et al., 2013).

Histologic evaluation showed that TAC levels and tissue degeneration decreased with NAC administration. NAC shows antioxidant properties. However, NAC reacts weakly with hydrogen peroxide and superoxide radicals. As a result of our study, we observed the protective effect of NAC on liver antioxidant/oxidant after DOX -induced liver injury. It can be said that NAC plays an active role in reducing superoxide anion and hydroxyl radical release and shows antioxidant properties. We did not examine liver GSH-Px activity in this study because NAC reacts poorly with hydrogen peroxide. However, in this study, liver GSH levels increased with NAC administration because NAC facilitates GSH biosynthesis (Saricaoglu et al., 2005; Bulucu et al., 2009; Koçkar et al., 2010; Li et al., 2016). Similarly, Bulucu et al. (2009) observed that GSH-Px activity was not altered in the liver of rats by DOX and NAC administration. Nagasaki et al. (1998) showed that in a GSH-depleted liver, NAC prevented hepatic injury and improved liver integrity after

ischemia/reperfusion injury by acting directly as a free radical scavenger and not as a substrate for GSH synthesis.

As a result of the examination of liver tissues removed from the subjects in our study, mononuclear cell infiltration, hyperchromatic nuclei in hepatocytes, dilatation in sinusoids and vacuolar degeneration were reported as important structural changes in the DOX group. In many previous studies conducted with DOX, it was determined that the histopathological changes occurring in the liver tissue were structural changes similar to the findings of our study (El-Sayyad et al., 2009; Bilgic & Ozgocmen, 2019; Sikandar et al., 2020).

When we compared the liver tissue of the DOX+NAC group with the group administered DOX alone, a significant decrease in sinusoidal dilatation, inflammation and pyknotic cells was noted. It has been reported that NAC application has beneficial effects similar to these findings in different hepatotoxicity models (Otrubová et al., 2018). The underlying role of NAC in these effects is still debated because its molecular mechanisms are quite complex (Samuni et al., 2013). There are different theories that partially explain the effects of NAC. One of these is the generally accepted classification that it is one of the 'good' antioxidants. Another is that it is associated with 'bad' antioxidants. Its effects on tumor cells are similarly controversial. It was reported by Li et al. (2016), that NAC showed quite opposite effects in tumor cells. They reported that NAC protects telomerase activity in normal cells but inhibits it in cancer cells. Researchers have linked this to opposing effects on telomerase activity. We hypothesize that this situation is due to different intracellular redox homeostasis in normal and tumor cells.

Many *in vivo* and *in vitro* studies have reported that DOX promotes cell death in various tissues by increasing oxidative stress (Yu et al., 2020; Zhang et al., 2020). We also found that DOX significantly increased TAC and TOC in liver tissue and increased the apoptotic index. In the DOX+NAC group, TOC and apoptotic index were found to be significantly reduced in treated animals. Similar to our results, they reported that apoptosis and liver damage decreased after NAC application in the CCl4-induced liver injury model (Otrubová et al., 2018)

CONCLUSION

As a result, NAC shows modulatory effects on oxidative stress and antioxidant redox system in Doxorubicin-induced liver toxicity in the rat. More extensive studies are needed on this subject.

ACKNOWLEDGEMENTS

This work was supported by Çanakkale Onsekiz Mart University, Scientific Research Unit (TSA-2022-4230).

Compliance with Ethical Standards

Authors' Contributions

SC: Conceptualization, Writing – Original draft, Data curation, Formal analysis, Writing – review & editing

SO: Conceptualization, Writing – Original draft, Data curation, Formal analysis

LCI: Conceptualization, Writing – Original draft, Data curation, Formal analysis

All authors read and approved the final manuscript.

Conflict of Interest

The authors declare that there is no conflict of interest.

Ethical Approval

Ethical Committee of Çanakkale Onsekiz Mart University Faculty of Medicine approved the study (Ethics number: 2022-2200189432). All applicable international, national, and/or institutional guidelines for the care and use of animals were followed.

Funding

This work was supported by Çanakkale Onsekiz Mart University, Scientific Research Unit (TSA-2022-4230).

Data Availability

The data that support the findings of this study are available from the corresponding author upon request.

REFERENCES

Aljobaily, N., Viereckl, M. J., Hydock, D. S., Aljobaily, H., Wu, T.-Y., Busekrus, R., & Han, Y. (2020). Creatine alleviates doxorubicin-induced liver damage by inhibiting liver fibrosis, inflammation, oxidative stress, and cellular senescence. *Nutrients*, *13*(1), 41. https://doi.org/10.3390/nu13010041

Alshabanah, O. A., Hafez, M. M., Al-Harbi, M. M., Hassan, Z. K., Al Rejaie, S. S., Asiri, Y. A., & Sayed-Ahmed, M. M. (2010). Doxorubicin toxicity can be ameliorated during antioxidant L-carnitine supplementation. *Oxidative Medicine and Cellular Longevity*, *3*(6), 428-433. https://doi.org/10.4161/oxim.3.6.14416

Arakawa, M., & Ito, Y. (2007). N-acetylcysteine and neurodegenerative diseases: basic and clinical pharmacology. *Cerebellum*, *6*(4), 308-314. https://doi.org/10.1080/14734220601142878

Bilgic, S., & Ozgocmen, M. (2019). The protective effect of misoprostol against doxorubicin induced liver injury. *Biotechnic & Histochemistry*, *94*(8), 583-591. https://doi.org/10.1080/10520295.2019.1605457

Biller, B. (2014). Metronomic chemotherapy in veterinary patients with cancer: rethinking the targets and strategies of chemotherapy. *The Veterinary Clinics of North America. Small Animal Practice*, *44*(5), 817–829. https://doi.org/10.1016/j.cvsm.2014.05.003

Bulucu, F., Ocal, R., Karadurmus, N., Sahin, M., Kenar, L., Aydin, A., & Yaman, H. (2009). Effects of N-acetylcysteine, deferoxamine and selenium on doxorubicin-induced hepatotoxicity. *Biological Trace Element Research*, *132*(1-3), 184-196. https://doi.org/10.1007/s12011-009-8377-y

El-Sayyad, H. I., Ismail, M. F., Shalaby, F. M., Abou-El-Magd, R. F., Gaur, R. L., Fernando, A., Raj, M. H. G., & Ouhtit, A. (2009). Histopathological effects of cisplatin, doxorubicin and 5-flurouracil (5-FU) on the liver of male albino rats. *International Journal of Biological Sciences*, *5*(5), 466-473. https://doi.org/10.7150/ijbs.5.466

Gibson-Corley, K. N., Olivier, A. K., & Meyerholz, D. K. (2013). Principles for valid histopathologic scoring in research. *Veterinary Pathology*, *50*(6), 1007–1015. https://doi.org/10.1177/0300985813485099

Hjelle, J. J., & Petersen, D. R. (1983). Metabolism of malondialdehyde by rat liver aldehyde dehydrogenase. *Toxicology and Applied Pharmacology*, *70*(1), 57-66. https://doi.org/10.1016/0041-008X(83)90179-5

Koçkar, M. C., Nazıroğlu, M., Çelik, Ö., Tola, H. T., Bayram, D., & Koyu, A. (2010). N-acetylcysteine modulates doxorubicin-induced oxidative stress and antioxidant vitamin concentrations in liver of rats. *Cell Biochemistry and Function*, *28*(8), 673-677. https://doi.org/10.1002/cbf.1707

Li, P., Wu, M., Wang, J., Sui, Y., Liu, S., & Shi, D. (2016). NAC selectively inhibit cancer telomerase activity: A higher redox homeostasis threshold exists in cancer cells. *Redox Biology*, *8*, 91-97. https://doi.org/10.1016/j.redox.2015.12.001

Lowry, O. H., Rosebrough, N. J., Farr, A. L., & Randall, R. J. (1951). Protein measurement with the Folin phenol reagent. *Journal of Biological Chemistry*, *193*(1), 265-275. https://doi.org/10.1016/S0021-9258(19)52451-6

Moslehi, J. J. (2016). Cardiovascular toxic effects of targeted cancer therapies. *The New England Journal of Medicine*, *375*(15), 1457-1467. https://doi.org/10.1056/nejmra1100265

Nagasaki, H., Nakano, H., Boudjema, K., Jaeck, D., Alexandre, E., Baek, Y., Kitamura, N., Yamaguchi, M., & Kumada, K. (1998). Efficacy of preconditioning with N-acetylcysteine against reperfusion injury after prolonged cold ischaemia in rats liver in which glutathione had been reduced by buthionine sulphoximine. *European Journal of Surgery*, *164*(2), 139-146. https://doi.org/10.1080/110241598750004805

Ohkawa, H., Ohishi, N., & Yagi, K. (1979). Assay for lipid peroxides in animal tissues by thiobarbituric acid reaction. *Analytical Biochemistry*, *95*(2), 351-358. https://doi.org/10.1016/0003-2697(79)90738-3

Otrubová, O., Turecký, L., Uličná, O., Janega, P., Luha, J., & Muchová, J. (2018). Therapeutic effects of N-acetyl-L-cysteine on liver damage induced by long-term CCl_4 administration. *General Physiology and Biophysics*, *37*(1), 23-31. https://doi.org/10.4149/gpb_2017016

Prasanna, P. L., Renu, K., & Gopalakrishnan, A. V. (2020). New molecular and biochemical insights of doxorubicin-induced hepatotoxicity. *Life Sciences*, *250*, 117599. https://doi.org/10.1016/j.lfs.2020.117599

Rivankar, S. (2014). An overview of doxorubicin formulations in cancer therapy. *Journal of Cancer Research and Therapeutics*, *10*(4), 853–858. https://doi.org/10.4103/0973-1482.139267

Saleh, D. O., Mahmoud, S. S., Hassan, A., & Sanad, E. F. (2022). Doxorubicin-induced hepatic toxicity in rats: Mechanistic protective role of Omega-3 fatty acids through Nrf2/HO-1 activation and PI3K/Akt/GSK-3β axis modulation. *Saudi Journal of Biological Sciences*, *29*(7), 103308. https://doi.org/10.1016/j.sjbs.2022.103308

Samuni, Y., Goldstein, S., Dean, O. M., & Berk, M. (2013). The chemistry and biological activities of N-acetylcysteine. *Biochimica et Biophysica Acta*, *1830*(8), 4117–4129. https://doi.org/10.1016/j.bbagen.2013.04.016

Saricaoglu, F., Dal, D., Salman, A. E., Atay, O. A., Doral, M. N., Salman, M. A., Kilinç, K., & Aypar, U. (2005). Effect of low-dose N-acetyl-cysteine infusion on tourniquet-induced ischaemia-reperfusion injury in arthroscopic knee surgery. *Acta Anaesthesiologica Scandinavica*, *49*(6), 847-851. https://doi.org/10.1111/j.1399-6576.2005.00722.x

Sikandar, A., Farhat, K., Afzal, A., Ajmal, K., Laeeq, M., & Khokhar, A. (2020). Protective effects of trimetazidine against doxorubicin-induced cardiotoxicity and hepatotoxicity in mice. *Journal of Ayub Medical College, Abbottabad: JAMC*, *32*(3), 304-309.

Timm, K. N., Ball, V., Miller, J. J., Savic, D., West, J. A., Griffin, J. L., & Tyler, D. J. (2021). Metabolic effects of doxorubicin on the rat liver assessed with hyperpolarized MRI and metabolomics. *Frontiers in Physiology*, *12*, 782745. https://doi.org/10.3389/fphys.2021.782745

Yu, X., Ruan, Y., Huang, X., Dou, L., Lan, M., Cui, J., & Shen, T. (2020). Dexrazoxane ameliorates doxorubicin-induced cardiotoxicity by inhibiting both apoptosis and necroptosis in cardiomyocytes. *Biochemical and Biophysical Research Communications*, *523*(1), 140–146. https://doi.org/10.1016/j.bbrc.2019.12.027

Zhang, J., Wang, M., Ding, W., Zhao, M., Ye, J., Xu, Y., Wang, Z., Ye, D., Li, D., Liu, J., & Wan, J. (2020). Resolvin E1 protects against doxorubicin-induced cardiotoxicity by inhibiting oxidative stress, autophagy and apoptosis by targeting AKT/mTOR signaling. *Biochemical Pharmacology*, *180*, 114188. https://doi.org/10.1016/j.bcp.2020.114188

Acta Nat. Sci. (2024) 5(1): 19-30
DOI: 10.61326/actanatsci.v5i1.3
e-ISSN: 2718-0638

Original Research Paper
info@actanatsci.com
www.actanatsci.com

ACTA NATURA ET SCIENTIA PRENSİP

Assessment of Some Inspection Properties of Commonly Used Medicinal Excipients Using Statistical Process Control for Monitoring of Manufacturer Quality

Mostafa Essam Eissa[1]✉

[1] Independent Researcher, Pharmaceutical and Healthcare Research Facility, Cairo, Egypt, mostafaessameissa@yahoo.com

✉ Corresponding Author: mostafaessameissa@yahoo.com

Please cite this paper as follows:
Essam Eissa, M. (2024). Assessment of Some Inspection Properties of Commonly Used Medicinal Excipients Using Statistical Process Control for Monitoring of Manufacturer Quality. *Acta Natura et Scientia*, *5*(1), 19-30. https://doi.org/10.61326/actanatsci.v5i1.3

ARTICLE INFO

Article History
Received: 28.12.2023
Revised: 05.03.2024
Accepted: 06.03.2024
Available online: 22.05.2024

Keywords:
Box plot
Bubble plot
Control chart
Contour plot
Corn starch
SPC

ABSTRACT

This study is a component of a larger initiative that involves the assessment and screening of pharmaceutical and chemical factories that produce medical substances, particularly in Asia and export them to poor nations. The present study concentrated on the inactive pharmaceutical ingredients of a frequently used excipient in pharmaceutical products made of amylopectin and amylose, named Amylum Maydis by the International Union of Pure and Applied Chemistry (IUPAC) nomenclature. This compound has the chemical formula $C_6H_{10}O_5$. Manufacturers asserted that all raw ingredients complied with the British Pharmacopoeia (BP), harmonizing requirements and analytical criteria in the process. As a result, every test complied with the official standard procedures described in the raw material testing monograph. The chosen tests included oxidizing agents, sulfated ash, and loss on drying (LOD). Software for statistical process control, or SPC, was used to collect and handle datasets. Preliminary data examination was done using box plots and three variable visualization techniques associated with the correlation matrix. All results showed that improvements of the inspection characteristics records are mandated to show stable variations even if there was no out-of-specification detected. Accordingly, the output of the tests should be investigated to correct for the assignable causes of the variations. It should be noted that the present data did not follow specific distributions, especially with the presence of aberrant values. Furthermore, it was found that there were several out-of-control points even in cases where there was no deviation from the specification, highlighting the need for suitable inquiry and correction for assignable reasons of variances among batches. Government enforcement of industrial SPC regulations is necessary to ensure the safety and quality of produced medical substances.

INTRODUCTION

As pharmaceutical manufacturing moves towards continuous processing with Process Analytical Technology (PAT) tools, it is important to have effective monitoring and control strategies to ensure consistent and high quality of pharmaceutical products (Wierzbicki et al., 2022). Statistical process control (SPC) can be a useful tool for monitoring critical quality attributes (CQAs) and facilitating continuous process verification (Hahn et al., 2023; Sharma et al., 2024). Commonly used pharmaceutical excipients play an important role in determining the quality and performance properties of drug products (You et al., 2022). As such, it is necessary to assess key inspection properties of excipients and ensure they meet manufacturer specifications using appropriate quality control methods such as SPC. This will help in the monitoring of excipient quality and manufacturer performance over time **(**Kim & Choi 2020; Kim et al., 2021**)**. Together, the implementation of PAT and SPC can enable real-time release and reliable continuous monitoring of unit operations as well as excipient quality.

To attain a consistent and acceptable level of quality, the use of statistical process control techniques (SPCs) has become a standard procedure in pharmaceutical firms (Eissa et al., 2016; Mostafa-Eissa, 2018; Eissa, 2021). The Shewhart plot (SPC) is one of the most crucial SPC instruments in the medicinal and healthcare sector (Eissa, 2015). It has a broad variety of applications for process and inspection parameter evaluation and control in several industries and non-industries (Essam-Eissa, 2017; Eissa et al., 2021a, 2021b, 2023; Eissa, 2023a). Pharmaceutical-grade raw chemical manufacturers have spread throughout the globe, enabling its availability through supply chain system and retail marketplaces worldwide (Eissa & Rashed, 2020). However, sustainable quality assurance for the anticipated chemical and physical qualities is crucial to guaranteeing the quality of pharmaceutical goods both now and in the future.

It is anticipated that there will be an increase in chemical production facilities, particularly in economically emerging nations. There is disagreement over how well chemical manufacturing companies adhere to Good Practices (G×P), particularly in the pharmaceutical and healthcare industries (Eissa, 2018; Eissa & Abid, 2018). The caliber of the production process may be reflected in the final product's quality (Eissa, 2016). Therefore, with an efficient strategy of SPC application, an organization with the right quality concept in place throughout the entire firm would generate goods with acceptable, stable, and predictable qualities with a low likelihood of failure.

In an era of severe global economic conditions, there is a good chance that the quality of the goods supplied by manufacturers, suppliers, and market retailers will decline in order to meet consumer demands for low prices at the expense of essential quality control features. In light of the aforementioned difficulties, the goal of this investigation was to assess the quality and purity of a selected excipient that is commonly used in pharmaceutical preparations by chemical manufacturing firms. This investigation will center on a crucial examination that is formally acknowledged as one of the fundamental features of inactive material inspection.

MATERIAL AND METHODS

Subject of the Study and the Tests

The quality of the manufacturing output from a chemical manufacturing facility using pharmaceutical and medical-grade raw materials was evaluated (Eissa & Mahmoud, 2016; Eissa, 2022). Loss-on-drying (LOD), residue on ignition result trend, and oxidizing chemicals were examined in 41 samples of a common and traditional inactive medicinal excipient (Eissa & Mahmoud, 2016; Eissa, 2022). The starch known as Amylum Mayd, which contains amylopectin and amylose, is frequently used to make oral solid dosage forms, including bulk granules, tablets, and capsules, as well as medicinal and cosmetic powders. Conventional dosage forms such as lubricants, diluents, glidants, and binders all use native starch. Every test was conducted following the British Pharmacopoeia (BP) standard procedure (BP, 2023; Maize Starch, 2023).

Statistical Analysis

To ensure data normality for statistical analysis, the Anderson-Darling (AD) test was employed at a 95% confidence interval (CI) and α = 0.05. This step verifies if the data follows a normal distribution, a common assumption for many statistical tests. If the data deviated from normality after attempting normalization techniques like the Johnson family, Box-Cox, or logarithmic transformations, Shewhart control charts with corrections for overdispersion or under dispersion were used to monitor trends (Eissa, 2019; Mostafa-Essam, 2019; Eissa, 2023b). In addition, the data were subjected to additional analysis through box plot visualization to interpret the dispersion pattern, mean, median and the presence of outliers. Process-behavior charts were examined for the out-of-control signs and accordingly, a decision for further search into capability analyses would be determined. Version 17.1.0 of Minitab®, an SPC program, was used for all computations. Adjusting the findings to the appropriate trending charts was done when no particular spreading pattern appeared appropriate for the datasets (Essam-Eissa & Refaat-Rashed, 2021). GraphPad Prism version 6.01 was used for the descriptive statistics, correlation matrix analysis and comprehensive normality tests at α 0.05. SPC software was also used for the preliminary assessment of the three variables under study using a contour plot and bubble graph (Eissa, 2018; Eissa et al., 2021b). The correlation matrix is used for the following: Identifying potential relationships between inspection aspects, assessing the strength and direction of relationships and guiding further investigation and process improvement, in addition to informing future studies.

RESULTS AND DISCUSSION

The goal of the organization-wide evaluation, which includes this research, is to meet the Total Quality Management (TQM) goals of the chemical plant (Eissa, 2023b). The process of identifying, minimizing and getting rid of production errors is something that the total quality management (TQM) approach does continuously (Al-Najjar, 1996). It increases customer satisfaction, ensures the competence of the workers or the manpower and speeds up supply chain coordination (Rashid & Haris Aslam, 2012). To achieve complete quality management, every person involved in the manufacturing process must be held accountable for the overall Caliber of the final product or service. Using SPC approaches is a crucial analytical strategy to accomplish this aim. This study serves the basis as one part of holistic survey research in collaboration with the official governmental industrial agencies to control and monitor the standards of the chemical manufacturing industries.

Inspection Aspects Association, Characteristics and Visualization

The association between the three variables under investigation can be seen in Figure 1. The investigation of the correlation between the quality control aspects is detailed in Table 1 using the non-parametric Spearman or ϱ (rho) test which complements the previous graph. It could be summarized that there was no specific association between the examined characteristics after 41 points. The correlation ranged from very weak to weak. The p-value is the probability that random sampling would produce a correlation coefficient as close to zero as possible in this experiment if there is no connection between the two variables generally (Rice, 1989). Incorporating a correlation matrix would offer a more comprehensive understanding of the relationships between the investigated quality control aspects, potentially leading to improved process control and future research directions.

The study examines three quality control aspects: loss-on-drying (LOD), residue on ignition, and oxidizing substances. While the Spearman correlation coefficient is used to assess individual relationships between these aspects, a correlation matrix allows for a comprehensive overview of all pairwise correlations simultaneously. This can reveal hidden patterns or unexpected relationships that might not be evident from individual tests. The correlation coefficient calculated for each pair of variables indicates the strength and direction of the relationship. A positive coefficient suggests a tendency for both aspects to increase or decrease together, while a negative

coefficient suggests an opposite tendency. The magnitude of the coefficient (closer to 1 or -1) signifies a stronger relationship. By identifying potentially correlated aspects, the study can prioritize further investigation into the underlying reasons behind these relationships. This knowledge can be crucial for optimizing the manufacturing process to achieve better control over multiple quality characteristics simultaneously. Understanding the relationships between these aspects can inform the design of future studies. By focusing on aspects with strong correlations, researchers can gain a deeper understanding of how changes in one aspect might impact the others, leading to more efficient and targeted investigations.

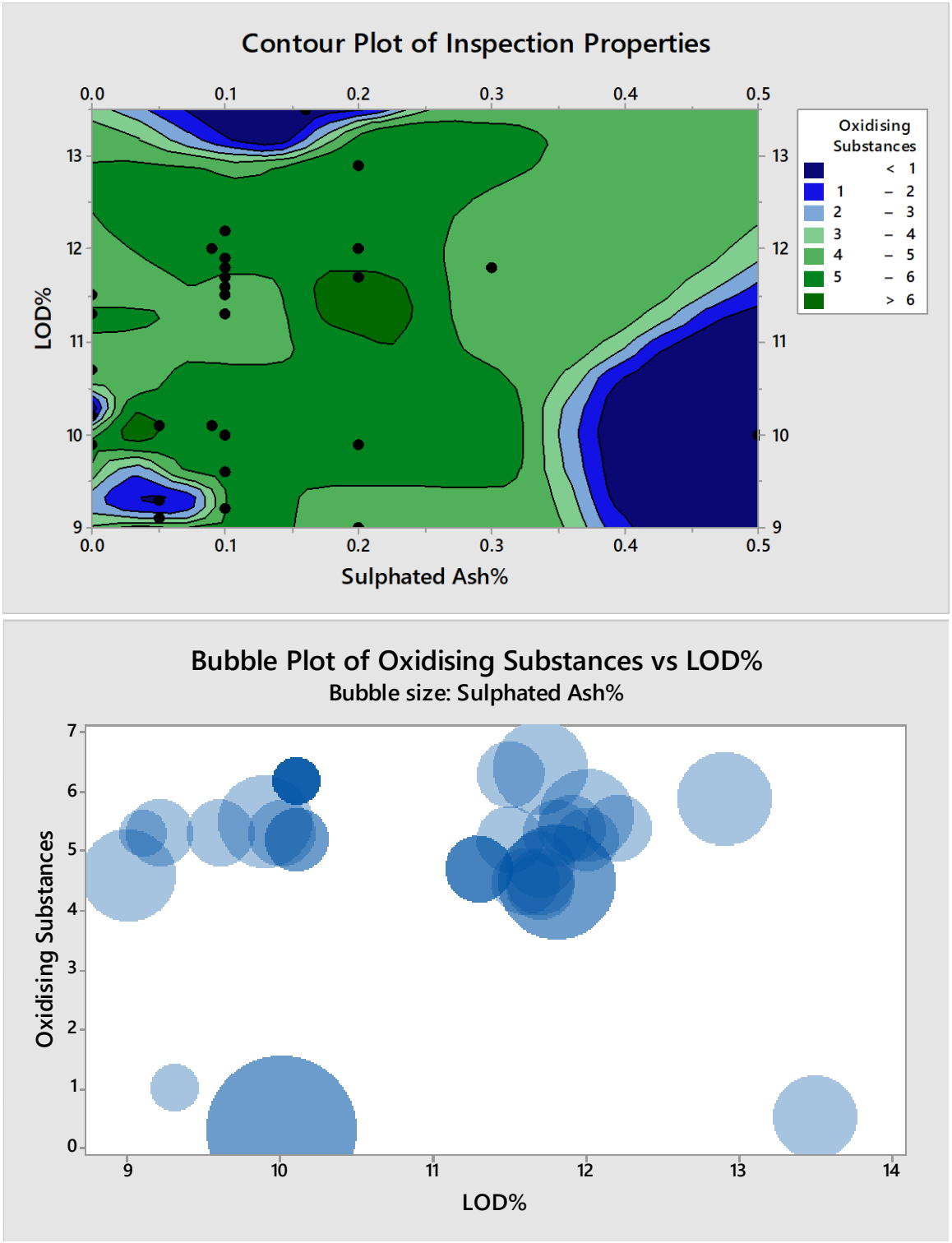

Figure 1. Visualization plots for three variables using contour graph (upper) and bubble chart (lower)

Table 1. Spearman correlation (ϱ) matrix showing (r) and (p) data with criteria range

Oxidizing Substances	**Loss on Drying**	**Sulphated Ash**	**Inspection Characteristics (r)**		
	-0.02	-0.15	**Oxidizing Substances**		
-0.02		0.28	**Loss on Drying**		
-0.15	0.28		**Sulphated Ash**		
Correlation coefficient (r)		Lower	Upper	Lower	Upper
Very weak		0.00	0.19	0.00	-0.19
Weak		0.20	0.39	-0.20	-0.39
Moderate		0.40	0.59	-0.40	-0.59
Strong		0.60	0.79	**-0.60**	**-0.79**
Very Strong		0.80	1.00	-0.80	-1.00
Oxidizing Substances	**Loss on Drying**	**Sulphated Ash**			
	89.7%	35.9%	**Oxidizing Substances**		
89.7%		7.8%	**Loss on Drying**		
35.9%	7.8%		**Sulphated Ash**		
P-value	**P-value %**		**Evidence for rejecting H_0**		
More than 0.1	>	10%	Very weak to none		
Between 0.1 - 0.05	5%	10%	Weak		
Between 0.05 - 0.01	5%	1%	Strong		
Less than 0.01	<	1%	Very strong		

Note: Oxidizing substances, loss on drying and sulphated ash are the tested inspection characteristics of corn flour of medicinal grade.

The coefficient of variations (as a percentage) for oxidizing substances, LOD and sulfated ash was 36.34%, 9.98% and 93.64%, with a total sum of each was 192.4, 445.7 and 4.930, respectively. Results were generated according to the computation done by the statistical software (Motulsky, 2007). D'Agostino and Pearson omnibus, Shapiro-Wilk (SW) and Kolmogorov-Smirnov (KS) normality tests normality test with K2, W and KS statistics, P value, passage of normality test (α=0.05) and P-value summary for oxidizing substances were 21.64, < 0.0001, No, ****, 0.7167, < 0.0001, No, ****, 0.3102, < 0.0001, No, ****, -1.833 and 2.532, LOD were 1.442, 0.4863, Yes, not significant (ns), 0.9327, 0.0177, No, *, 0.2002, 0.0003, No, ***, 0.1753 and -0.6760 and sulphated ash were 29.39, < 0.0001, No, ****, 0.7557, < 0.0001, No, ****, 0.3274, < 0.0001, No, ****, 2.064 and 4.919, respectively. Several tests were shown together for addressing the strengths and weaknesses of each test and to examine potential conflicts of results.

The use of non-parametric statistical tests was sought more convenient for the following reasons:

***Non-normal data distribution*:** The normality tests revealed the data for all three quality control aspects (oxidizing substances, LOD, and sulfated ash) were not normally distributed. The p-values from the normality tests were all less than 0.05, indicating a rejection of the null hypothesis that the data follow a normal distribution.

Rank-based method: The Spearman test is a rank-based correlation test, meaning it analyzes the order or ranking of the data points rather than their actual values. This makes it more reliable than the commonly used Pearson correlation coefficient when dealing with non-normal data. The Pearson correlation coefficient assumes normality and can be misleading if the data is not normally distributed. Therefore, the Spearman test was chosen as a more appropriate statistical method for analyzing the relationship between the quality control aspects due to the non-normality of the data. It utilizes the ranking of the data

points, making it robust against the influence of extreme values or non-normal distributions.

Box and Whisker Plot (Box Plot)

Figure 2 displayed the degree of skewness and the data sets' dispersion pattern (Besseris, 2013). Regarding Figure 2, it can be observed that the datasets exhibited varying degrees of distortion from the regular pattern, which are not as noticeable in the LOD. Additionally, the results of the oxidizing substances and sulfated ash records were further skewed by the existence of outliers. Consequently, the AD test at P = 0.05 was used to test for normality, and all raw data failed. Even after all forms of changes, best-fitting distribution identification could not yield any meaningful spreading since all P values were less than 0.05 with a 95% confidence interval. The AD test is another commonly used statistical test to assess normality, and it was employed here to confirm the previous tests' conclusions and support findings. The AD test confirmed that the data for all three quality control aspects were not normally distributed ($p < 0.05$).

The descriptive statistics of the distribution of datasets as minimum, 25% percentile, median, 75% percentile, maximum, 10% percentile, 90% percentile, mean, standard deviation, standard error of mean, lower 95% CI of mean, upper 95% CI of mean, lower 95% CI of median and upper 95% CI of median (Chang et al., 2019). For oxidizing substances, LOD and sulphated ash, the results were (0.2500, 4.500, 5.200, 5.550, 6.400, 0.6000, 6.200, 4.691, 1.705, 0.2663, 4.153, 5.230, 4.700 and 5.300), (9.000, 10.05, 11.30, 11.70, 13.50, 9.360, 12.00, 10.87, 1.085, 0.1695, 10.53, 11.21,10.10 and 11.60), (0.0, 0.0500, 0.1000, 0.1300, 0.5000, 0.0, 0.2800, 0.1202, 0.1126, 0.01758, 0.08470, 0.1558, 0.0900 and 0.1000), respectively (Table 2).

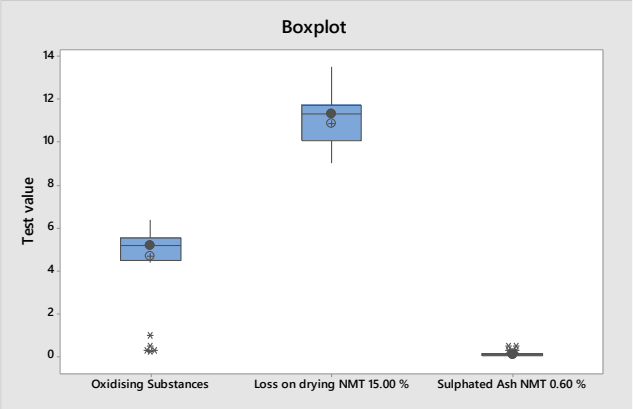

Figure 2. Box plot showing the examined inspection characteristics of corn starch showing data spreading's, means, medians and the presence of outliers

Table 2. Results of descriptive statistics of datasets for oxidizing substances, LOD, and sulphated ash using statistical software

Statistic	Oxidizing Substances	LOD	Sulphated Ash
Minimum	0.2500	9.000	0.0
25% Percentile	4.500	10.05	0.0500
Median	5.200	11.30	0.1000
75% Percentile	5.550	11.70	0.1300
Maximum	6.400	13.50	0.5000
10% Percentile	0.6000	9.360	0.0
90% Percentile	6.200	12.00	0.2800
Mean	4.691	10.87	0.1202
Standard Deviation	1.705	1.085	0.1126
Standard Error of Mean	0.2663	0.1695	0.01758
Lower 95% CI of Mean	4.153	10.53	0.08470
Upper 95% CI of Mean	5.230	11.21	0.1558
Lower 95% CI of Median	4.700	10.10	0.0900
Upper 95% CI of Median	5.300	11.60	0.1000

Control Charts and Examination of the Time-Series Pattern

No out-of-specifications (OOS) could be detected, although out-of-control states would be observed (Yu et al., 2018). The implementation of the trending charts based on the dispersion adjustment concept was used in Figures 3 to 5. The alarms were indicated with red dots and the meaning of each number could be tracked as generated by the program as the following (Pakdil, 2020):

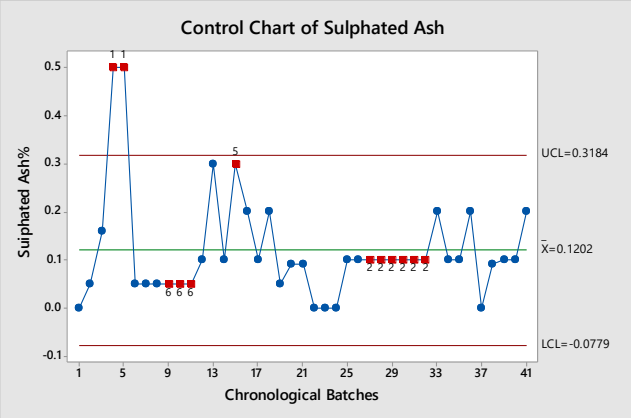

Figure 3. Process-behavior chart showing the common-cause, the assignable-cause variations, average line and the control limits for the sulphated ash test of the maize starch

Test Results for the Process-Behavior Chart of Sulphated Ash With Maximum Specification Limit of 0.60%

TEST 1: One point more than 3.00 standard deviations from center line (CL). Test Failed on points: 4, 5. TEST 2: 9 points in a row on same side of center line. Test Failed at points: 27, 28, 29, 30, 31, 32. TEST 5: 2 out of 3 points more than 2 standard deviations from center line (on one side of CL). Test Failed at points: 5, 15. TEST 6: 4 out of 5 points more than 1 standard deviation from center line (on one side of CL). Test Failed at points: 9, 10, 11. TEST 8. 8 points in a row more than 1 standard deviation from center line (above and below CL). Test Failed at points:11.

Test Results for the Process-Behavior Chart of LOD With Maximum Specification Limit of 15.00%

TEST 1: One point more than 3.00 standard deviations from CL. Test Failed at points: 3. TEST 2: 9 points in a row on same side of center line. Test Failed at points: 41. TEST 6. 4 out of 5 points more than 1 standard deviation from center line (on one side of CL). Test Failed at points: 15, 36, 38, 39.

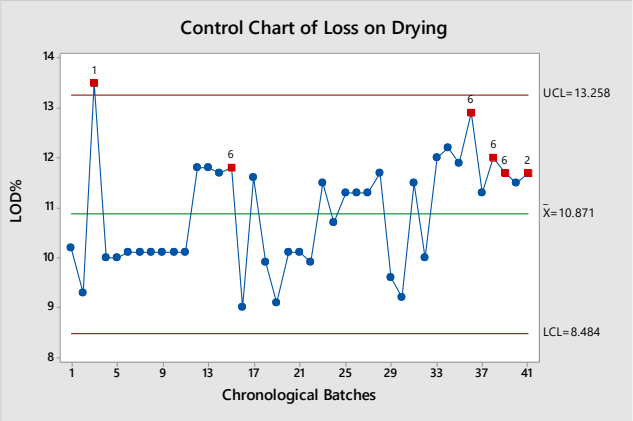

Figure 4. Process-behavior chart showing the common-cause, the assignable-cause variations, average line and the control limits for the loss-on-drying test of the maize starch

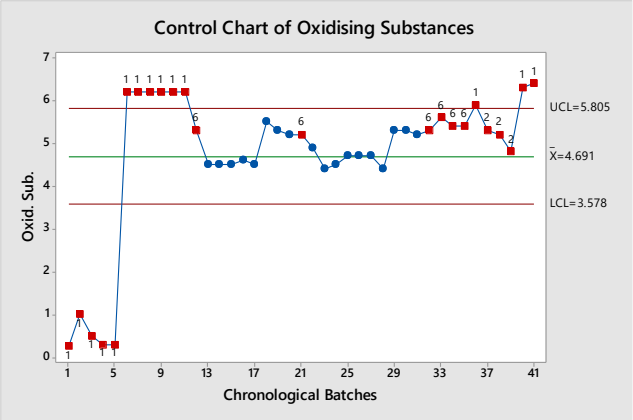

Figure 5. Process-behavior chart showing the common-cause, the assignable-cause variations, average line and the control limits for the oxidizing substances test of the maize starch

Test Results for the Process-Behavior Chart of Oxidizing Substances With Maximum Specification Limit of 20 ppm

TEST 1: One point more than 3.00 standard deviations from CL. Test Failed at points: 1, 2, 3, 4, 5, 6, 7, 8, 9, 10, 11, 36, 40, 41. TEST 2: 9 points in a row on same side of CL. Test Failed at points: 37, 38, 39, 40, 41. TEST 5: 2 out of 3 points more than 2 standard deviations from center line (on one side of CL). Test Failed at points: 2, 3, 4, 5, 7, 8, 9, 10, 11, 41. TEST 6: 4 out of 5 points more than 1 standard deviation from center line (on one side of CL). Test Failed at points: 4, 5, 9, 10, 11, 12, 21, 32, 33, 34, 35, 36, 37, 38, 40, 41. TEST 8: 8 points in a row more than 1 standard deviation from center line (above and below CL). Test Failed at points: 8, 9, 10, 11, 12, 36, 37, 38.

The three variables do not follow a normal distribution. This can be attributed to various factors, including: The inherent nature of the data: Some processes naturally generate non-normal data due to their underlying mechanisms. Outliers: Extreme values in the data can skew the distribution away from normality. Sample size: Smaller sample sizes can be less reliable in representing the true population distribution, and deviations from normality are more likely. Interactions: Complex interactions between variables can lead to non-normal distributions. Nevertheless, non-normality doesn't necessarily invalidate the use of control charts. Prioritization for investigating points that fall outside both the control limits and the specification limits: Points exceeding the specification limits (OOS) indicate a direct violation of the acceptable product quality standards and require immediate attention.

Points exceeding the control limits but falling within the specification limits (OOC) might represent potential process instability but don't necessarily translate to a product quality issue. However, they still warrant investigation to prevent future OOS occurrences. The alarm analysis mentions numerous out-of-control signals for all three control charts despite no "out-of-specification" (OOS) observations. While activating additional tests beyond the standard ±3 sigma limits can increase the chance of false alarms, it's crucial to balance this risk with the potential benefits of identifying true process issues. Justification for the use of additional tests – with caution - could be addressed through the following:

1. Acknowledgement of the increased risk of false alarms: Acknowledging the concern that using additional tests beyond +/- 3 sigma can lead to more false positives due to random chance.

2. The importance of identifying true process issues: The importance of not overlooking potential process problems that might not be captured by the basic ±3 sigma limits should not be underestimated. Early detection and correction of process issues can lead to improved product quality and reduced costs.

3. Justification for the use of specific tests: Clear justifications for each additional test used beyond the standard ones could be addressed through the following:

Test 2 (9 points in a row on one side): This test can be helpful in identifying trends or shifts in the process average, even if the individual points fall within the control limits. It can be particularly useful when dealing with autocorrelation (dependence of data points on previous observations) in the data.

Test 5 (2 out of 3 points beyond 2 sigma on one side): This test can be sensitive to sudden changes in the process variability, even if the individual points don't fall outside the control limits.

Test 6 (4 out of 5 points beyond 1 sigma on one side): This test can be used to detect shifts in the process variability even if the mean remains relatively stable.

Test 8 (8 points in a row above and below 1 sigma): This test can be helpful in identifying cyclical patterns in the data that might not be evident from the other tests.

4. The role of combined interpretation: It's crucial to interpret the results of all tests (both standard and additional) together, considering the specific context and historical data of the process. Relying solely on individual tests without considering the overall picture can lead to misinterpretations.

It is important for the investigator to be able to resolve the difference between "out of specification" (OOS) and "out of statistical control" (OOC) for several reasons:

1. Clarification of Control Limits vs. Set Specifications: OOS focuses on whether a single measurement falls outside the predetermined specification limits. Specifications are pre-defined boundaries that establish the acceptable range for a quality parameter. An OOS result indicates a potential deviation from the desired product quality. OOC deals with the statistical behavior of the data over time. It utilizes control charts, which set upper and lower control limits (UCL and LCL) based on the historical data's variability. An OOC signal occurs when a data point falls outside the control limits, suggesting the process might be experiencing increased variability or instability.

2. Distinguishing between Random Variation and Process Issues: OOS doesn't necessarily imply a problem with the process itself. It could be a random event or an isolated incident. Further investigation is needed to determine the cause of the OOS result. OOC signals a potential issue with the process. The data points falling outside the control limits suggest the process variability might be exceeding acceptable levels, potentially leading to inconsistent product quality.

3. Informs Decision Making: OOS might necessitate immediate action, such as retesting the sample or investigating the production line for potential causes. However, the decision depends on the severity of the deviation and the established quality control procedures. OOC often triggers a more in-depth analysis to identify the root cause of the process instability. This could involve adjustments to the process parameters, equipment maintenance, or implementing corrective actions to bring the process back under control.

Understanding the distinction between OOS and OOC helps to interpret quality control data more effectively, differentiate between random variations and potential process issues and make informed decisions regarding corrective actions and ensuring consistent product quality. An analogy to further illustrate the difference, the specification for manufactured device thickness might be 10mm +/- 1mm (between 9 mm and 11 mm). An OOS scenario would be a single, oddly thick (13 mm) single piece. While concerning, it might be a one-off mistake. However, OOC would occur if several units consistently fall outside the acceptable thickness range, indicating a potential issue with the procedure, manufacturing process or processing conditions.

In summary, some datasets fail to follow any distribution type, including the normal or Gaussian distribution, due to factors such as the inherent nature of the data, the presence of outliers or extreme values, small sample sizes, or complex interactions between variables. Since the monitored processes showed signs of out-of-control at several points, improvements are required to stabilize the inspection properties and control them. There are indicators for abnormal freak batches that exceed the control limits. Also, there are signals of mixed operations, early warning of trend shifts and over-control suggesting the presence of variable operations. Then, capability analyses could be conducted to determine the efficiency of the investigated characteristics. The foreign supplier should seek holistic quality improvement in the organization which would be pooled into the final manufactured raw products otherwise the quality aspects could be impaired in the long run.

CONCLUSION

The study employed various statistical techniques to evaluate the quality control aspects of a chemical compound. However, incorporating a correlation matrix would provide a more holistic understanding of the relationships between these aspects. The observed non-normal data distributions, outliers, and out-of-control signals in the control charts highlight the need for further investigation and process improvements to achieve consistent product quality and meet TQM goals.

The current work focused on three tests that are commonly used in most raw chemical materials. The implementation of SPC is crucial to evaluate the quality of the monitored inspection aspects of the chemical compound. The industrial governmental

agencies must supervise and monitor the flux of chemical goods using this methodology. However, till the enforcement and application of these rules, it is up to the final customers to take this responsibility and mandate the extension of these foundations to the primary source of these products. This is critical in the developing countries, especially when dealing with raw chemicals that are incorporated into healthcare, medicine, food and any products that could impact the health and even life of human beings in the country. If the concern about false alarms is significant, alternative approaches should be considered in the further future studies like using EWMA (Exponentially Weighted Moving Average) charts or CUSUM (Cumulative Sum) charts. These charts can be more sensitive to small shifts in the process mean while reducing the chance of false alarms compared to standard control charts with additional tests.

The present situation showed that despite the absence of any excursions in the inspected characteristics, the presence of several assignable causes of variations highlighted issues that need further investigations concerning the processing and manufacturing of the external manufacturer. This could lead to the necessity of the auditing routine to be implemented regularly to ensure GMP execution in the source company. The aberrant situations ranged from extraneous factors to shift and drift or even early warning for the deviation from the process mean. Moreover, the presence of trends, over-control and mixture patterns cannot be ruled out. This is a critical issue when considering raw components that would be incorporated into final manufactured products that would affect the health of the community, especially the sick and ill populations with their life dependent on the products' efficacy and safety. The study would embrace other inspection quality aspects and other raw chemical compounds in the future.

ACKNOWLEDGEMENTS

There is nothing to declare. All the work was supported by the contributing author.

Compliance with Ethical Standards

Conflict of Interest

The author declares that there is no conflict of interest.

Ethical Approval

For this type of study, formal consent is not required.

Funding

Not applicable.

Data Availability

The author confirms that the data supporting the findings of this study are available within the article.

REFERENCES

Al-Najjar, B. (1996). Total quality maintenance: an approach for continuous reduction in costs of quality products. *Journal of Quality in Maintenance Engineering*, *2*(3), 4-20. https://doi.org/10.1108/13552519610130413

Besseris, G. J. (2013). Robust quality controlling: SPC with box plots and runs test. *The TQM Journal*, *25*(1), 89-102. https://doi.org/10.1108/17542731311286450

British Pharmacopoeia. (2023): *In "Maize Starch"*. Medicines and Healthcare products Regulatory Agency, UK, BP 2023 (Ph. Eur. 11.2 update).

Chang, J., Desai, N., & Gosain, A. (2019). Correlation between altimetric score and citations in pediatric surgery core journals. *Journal of Surgical Research*, *243*, 52-58. https://doi.org/10.1016/j.jss.2019.05.010

Eissa, D., Rashed, E., & Eissa, M. (2023). Measuring public health effect of coronavirus disease 2019: A novel perspective in healthcare in pandemic times. *Batı Karadeniz Tıp Dergisi*, *7*(2), 266-268. https://doi.org/10.29058/mjwbs.1257163

Eissa, M., Mahmoud, A., & Nouby, A. (2016). Evaluation and failure risk of microbiological air quality in production area of pharmaceutical plant. *RGUHS Journal of Pharmaceutical Sciences*, *5*, 155-166.

Eissa, M., & Mahmoud, A. (2016). Evaluation of microbial recovery from raw materials for pharmaceutical use. *Journal of Food and Pharmaceutical Sciences*, *4*(1), 6-11. https://doi.org/10.14499/jfps

Eissa, M., Rashed, E., & Eissa, D. E. (2021a). Study of tellurium-129m (129mTe) ground deposition following Fukushima nuclear disaster: Descriptive analysis of UNSCEAR database using statistical process techniques. *Mugla Journal of Science and Technology*, *7*(2), 67-72. https://doi.org/10.22531/muglajsci.955946

Eissa, M., Rashed, E., & Eissa, D. E. (2021b). Quality improvement in routine inspection and control of healthcare products using statistical intervention of long-term data trend. *Dicle Üniversitesi Fen Bilimleri Enstitüsü Dergisi*, *10*(2), 163-184.

Eissa, M., & Rashed, E. (2020). Inventory digital management using statistical process control analysis in healthcare industry. *Journal of Business in The Digital Age*, *3*(2), 123-128. https://doi.org/10.46238/jobda.688641

Eissa, M. (2016). Study of microbial distribution from different processing stages in purified water production plant of pharmaceutical manufacturing facility. *Research & Reviews: Journal of Microbiology and Virology*, *6*(1), 31-45.

Eissa, M. (2021). Implementation of modified Q-control chart in monitoring of inspection characteristics with finite quantification sensitivity limits: A case study of bioburden enumeration in capsule shell. *El-Cezeri*, *8*(3), 1093-1107. https://doi.org/10.31202/ecjse.871179

Eissa, M. (2022). Validation of microbiological assay design of neomycin sulfate in 30 x 30 cm rectangular antibiotic plate. *Journal of Advanced Biomedical and Pharmaceutical Sciences*, *5*(2), 54-63. https://doi.org/10.21608/jabps.2021.104951.1143

Eissa, M. E. (2023a). Studies on morbidities and mortalities from COVID-19: Novel public health practice during pandemic periods. *Asian Journal of Applied Sciences*, *16*(3), 84-94. https://doi.org/10.3923/ajaps.2023.84.94

Eissa, M. E., & Abid, A. M. (2018). Application of statistical process control for spotting compliance to good pharmaceutical practice. *Brazilian Journal of Pharmaceutical Sciences*, *54*(02), e17499. https://doi.org/10.1590/s2175-97902018000217499

Eissa, M. E. (2015). Shewhart control chart in microbiological quality control of purified water and its use in quantitative risk evaluation. *Pharmaceutical and Biosciences Journal*, *4*(1), 45-51. https://doi.org/10.20510/ukjpb/4/i1/87845

Eissa, M. E. (2018). Adulterated pharmaceutical product detection using statistical process control. *Bangladesh Pharmaceutical Journal*, *21*(1), 7-15.

Eissa, M. E. (2019). Trichinosis outbreak risk analysis in USA from food sources and new prospective analysis using statistical process control tools. *International Journal of Research in Pharmacy and Biosciences*, *6*(7), 4-13.

Eissa, M. E. (2023b). Trending perspective in evaluation of inspection characteristics of pharmaceutical compound: comparative study of control charts. *Universal Journal of Pharmaceutical Research*, *8*(5), 15-21. https://doi.org/10.22270/ujpr.v8i5.1006

Essam-Eissa, M., & Refaat-Rashed, E. (2021). Unique quantitative analysis of tsunami waves using statistical software: A case study of the major recorded Hawaii incidents. *Advanced Materials Proceedings*, *6*(1), 1-6.

Essam-Eissa, M. (2017). Monitoring of *Cryptosporidium* spp. outbreaks using statistical process control tools and quantitative risk analysis based on NORS long-term trending. *Microbiology Journal*, *9*(1), 1-7. https://doi.org/10.3923/mj.2019.1.7

Hahn, V. S., Petucci, C, Kim, M. S., Bedi, K. C., Jr., Wang, H., Mishra, S., Koleini, N., Yoo, E. J., Margulies, K. B., Arany, Z., Kelly, D. P., Kass, D. A., & Sharma, K. (2023). Myocardial metabolomics of human heart failure with preserved ejection fraction. *Circulation*, *147*(15), 1147–1161. https://doi.org/10.1161/CIRCULATIONAHA.122.061846

Kim, E. J., Kim, J. H., Kim, M. S., Jeong, S. H., & Choi, D. H. (2021). Process analytical technology tools for monitoring pharmaceutical unit operations: A control strategy for continuous process verification. *Pharmaceutics*, *13*(6), 919. https://doi.org/10.3390/pharmaceutics13060919

Kim, T. S., & Choi, D. H. (2020). Liver dysfunction in sepsis. *The Korean Journal of Gastroenterology*, *75*(4), 182–187. https://doi.org/10.4166/kjg.2020.75.4.182

Maize Starch. (2023). British Pharmacopoeia Commission (Ed.).

Mostafa-Eissa, M. (2018). Quality criteria establishment for dissolution of ascorbic acid from sustained release pellets. *Novel Techniques in Nutrition & Food Science*, *2*(2), 137-142. https://doi.org/10.31031/ntnf.2018.02.000531

Mostafa-Essam, A. E. (2019). The use failure mode and effects analysis as quantitative risk analysis tool. *Journal of Applied Sciences*, *2019*(02), RD-APS-10009.

Motulsky, H. J. (2007). *GraphPad Prism Version 5.0 Statistics Guide*. GraphPad Software, Inc.

Pakdil, F. (2020). Control charts. F. Pakdil (Ed.), *Six Sigma for Students: A Problem-Solving Methodology* (pp. 333-373). Palgrave Macmillan & Springer.

Rashid, K., & Haris Aslam, M. M. (2012). Business excellence through total supply chain quality management. *Asian Journal on Quality*, *13*(3), 309-324. https://doi.org/10.1108/15982681211287829

Rice, W. R. (1989). Analyzing tables of statistical tests. *Evolution*, *43*(1), 223-225. https://doi.org/10.2307/2409177

Sharma, P., Zhang, X., Ly, K., Kim, J. H., Wan, Q., Kim, J., Lou, M., Kain, L., Teyton, L., & Winau, F. (2024). Hyperglycosylation of prosaposin in tumor dendritic cells drives immune escape. *Science*, *383*(6679), 190–200. https://doi.org/10.1126/science.adg1955

Wierzbicki, A. S., Kim, E. J., Esan, O., & Ramachandran, R. (2022). Hypertriglyceridaemia: An update. *Journal of Clinical Pathology*, *75*(12), 798–806. https://doi.org/10.1136/jclinpath-2021-207719

You, H., Ma, X., Efe, C., Wang, G., Jeong, S. H., Abe, K., Duan, W., Chen, S., Kong, Y., Zhang, D., Wei, L., Wang, F. S., Lin, H. C., Yang, J. M., Tanwandee, T., Gani, R. A., Payawal, D. A., Sharma, B. C., Hou, J., … Jia, J. (2022). APASL clinical practice guidance: the diagnosis and management of patients with primary biliary cholangitis. *Hepatology International*, *16*(1), 1–23. https://doi.org/10.1007/s12072-021-10276-6

Yu, B., Zeng, L., & Yang, H. (2018). A Bayesian Approach to setting the release limits for critical quality attributes. *Statistics in Biopharmaceutical Research*, *10*(3), 158-165. https://doi.org/10.1080/19466315.2018.1482780

Acta Nat. Sci. (2024) 5(1): 31-40
DOI: 10.61326/actanatsci.v5i1.4
e-ISSN: 2718-0638

Original Research Paper
info@actanatsci.com
www.actanatsci.com

ACTA NATURA ET SCIENTIA PRENSİP

Current Perspective in Quality Control Examining and Extended Researching for Certain Aspects of Active Pharmaceutical Ingredient Using Statistical Process Control

Mostafa Essam Eissa[1]✉

[1] Independent Researcher, Pharmaceutical and Healthcare Research Facility, Cairo, Egypt, mostafaessameissa@yahoo.com

✉ Corresponding Author: mostafaessameissa@yahoo.com

Please cite this paper as follows:
Essam Eissa, M. (2024). Current Perspective in Quality Control Examining and Extended Researching for Certain Aspects of Active Pharmaceutical Ingredient Using Statistical Process Control. *Acta Natura et Scientia*, *5*(1), 31-40. https://doi.org/10.61326/actanatsci.v5i1.4

ARTICLE INFO

Article History
Received: 28.12.2023
Revised: 05.03.2024
Accepted: 06.03.2024
Available online: 22.05.2024

Keywords:
Capability plot
Johnson transformation
Individual-Moving Range
Normal probability
Weibull distribution

ABSTRACT

Control charts are an important part of statistical control because they allow the inspection characteristics of manufactured pharmaceutical products to be tracked and controlled. It helps show current processes and status and, if necessary, identifies areas for further development. The investigation and analysis of an initial trend for a few inspection properties of the manufactured chemical 3-O-ethyl 5-O-methyl 2-(2-aminoethoxymethyl)-4-(2-chlorophenyl)-6-methyl-1,4-dihydropyridine-3,5-dicarboxylate benzenesulfonic acid is the main focus of the current work. Using the well-known commercial SPC platform for comprehensive SPC analyses. The datasets of the assay and polarization rotation followed the Weibull pattern. While the results of the overall impurities and particle size test data were adopted for Gaussian spreading the Johnson family transformation was implemented for the latter. An exploratory Individual-Moving Range plot is the method used to trend the datasets and capacity analyses were conducted in accordance with that method. Improvements are required to enhance the quality of inspection properties at the preliminary steps since there are signs of a low capability process in the particle size test and the assay to some extent. In addition, the means of the quality tests should be brought to the center since the preliminary data are not in the middle of the specification range. Thus, some inspection characteristics are lower quality than others and need immediate correction and enhancement at the initial stages of the establishment of the manufacturing process and criteria. This perspective highlights the importance of control charts in the examination of the quality of chemically manufactured materials.

INTRODUCTION

In the highly competitive worlds of healthcare and the pharmaceutical industry, many businesses and organizations compete in the drug and medical product market (Eissa, 2016a, 2017, 2021). However, the patient's health should take precedence and not only quality and efficiency (Eissa, 2018a, 2022; Essam, 2019). The active or inactive medicinal substances inspection properties should serve as the foundation for the standard quality before analyzing the inspection properties of the final medication dosage forms.

Using statistical process control (SPC) techniques to reach a high standard of reliable and acceptable quality has become a common and crucial task for all healthcare businesses (Mostafa Eissa, 2018; Essam, 2023; Eissa & Rashed, 2023). The Shewhart trending plot is among the most crucial SPC methodologies (Eissa, 2015). It is extensively utilized to assess and control processes and inspection aspects in both industrial and non-industrial sectors (Eissa et al., 2021a, 2021b, 2023; Eissa, 2019, 2023a). Manufacturers of medicinal-grade raw materials are increasingly growing around the world, which facilitates easy access for brokers and retail markets globally (Eissa, & Mahmoud, 2016). On the other hand, maintaining constant quality assurance levels of the expected physical and chemical properties is essential to guaranteeing the chemical goods' value both ongoing and in the future.

Chemical production facilities are becoming increasingly prevalent, especially in emerging nations. It is doubtful if they follow ethical guidelines in several fields, such as medicine and healthcare (Eissa, & Abid, 2018; Eissa, 2018b). Good Manufacturing practices (GMP) may be used to forecast the quality of the final product (Eissa, 2016). Consequently, an organization with the right quality concept in mind across the board would create products with acceptable, reliable, and predictable features with a low failure rate.

It is important to have strict industrial holistic monitoring and control systems that follow regulatory official agencies to avoid the comptonization risk of their product's safety and quality at the expense of the financial benefits, especially in the developing nations. Owing to the aforementioned challenges, the following detailed perspective explains and assesses the quality and purity of a particular medicinal element that is often used in pharmaceutical preparations by chemical manufacturing companies. Substantial tests, which are officially recognized as a group of the key components of active material assessment, will be the main focus of the present article to show the importance of SPC in the chemical industry.

MATERIAL AND METHODS

The establishment of the milestone for the quality control and monitoring of the inspection characteristics of the synthesized compounds from the chemical manufacturing firms is of paramount importance not only for the manufacturing firm or the final consumers but also for the controlling regulatory official agencies in the countries. The present commentary is a model overview for a series of conducted connected studies performed on medicinal chemical materials that are manufactured in companies from Asian developing nations and received in the Egyptian market.

Case Selection of Calcium Channel Blocker Antihypertensive Molecule

The drug substance that is used in this representative investigation is 3-O-ethyl 5-O-methyl 2-(2-aminoethoxymethyl)-4-(2-chlorophenyl)-6-methyl-1,4-dihydropyridine-3,5-dicarboxylate benzenesulfonic acid according to the IUPAC nomenclature. This medicinal chemical compound is a calcium channel blocker drug used to treat variant angina (also known as Prinzmetal angina or coronary artery vasospasm, among other names), excessive blood pressure, and coronary artery disease (CAD) (Amlodipine Monogpraph for Professional, 2016; Goldman & Schafer, 2019). It is ingested orally (by mouth) and shows 64–90% bioavailability with 93% protein binding.

Specifications Criteria of the Raw Material and the Standard Reference Analysis Method

Classical medicinal raw materials usually follow official monographs for their standard analysis and the manufacturers claim their obedience to the specifications mentioned in the respective pharmacopeias. From this standing point, the Specification Limit (SL) could be specified for the range. So, there will be an Upper Specification Limit (USL) and a Lower Specification Limit (LSL) or one of them only based on the test criteria. Apart from the particle size analysis which follows an instrumental method with an upper size threshold of 4,189 μm^3, all other tests follow British Pharmacopeia (2022). These tests include the optical rotation, total impurities and the assay (based on an anhydrous substance).

SPC and the Examination of Selected Inspection Properties of the Manufactured Raw Material

To create a suitable SPC trending profile and check the preliminary test data for distribution fitting, Minitab version 17.1.0 was utilized (Eissa et al., 2015, 2016b; Eissa, 2018c, 2018d). Based on the output findings, the control charts might be applied to ascertain the starting level of control. Shewhart basic structuring and drawing for its basic components have been described in detail before. It has been plotted based on the underlying assumption of the distribution pattern of the datasets. With a Confidence Interval (CI) of 95% and a P-value of 0.05, the statistical process profiling of the capability of the examined inspection properties could be evaluated. If the variation of the process in the chronological order is under control. Then the capability plot could be studied to know whether the investigated characteristic is under control state or needs improvements.

Capability Six-Pack flow could be determined through the following steps. While control charts are used to assess process stability over time, a separate analysis is needed to determine the inherent capability of the process. This capability analysis evaluates whether the process can consistently produce outputs within the specified limits (tolerances). Distribution Analysis: Before constructing control charts, it's crucial to understand the underlying distribution of the data. This can be achieved through techniques like: Exploratory data analysis (EDA): Visualizing the data through histograms or boxplots can reveal potential patterns and departures from normality or other assumed distribution from data spreading fitting study. Formal distribution tests: Statistical tests like the Anderson-Darling (AD) test can help determine if the data follows an assumed distribution, which is a common assumption for control chart calculations. Capability Analysis: Once the data distribution is understood, capability analysis tools like capability plots and indices (Cp, Cpk) can be employed. These tools assess how well the process output falls within the specified limits, considering both process variation and centering.

Confidence Intervals and P-values: Confidence intervals (CIs): These provide a range of values within which the true population parameter (e.g., mean) is likely to lie with a certain level of confidence (e.g., 95%). They don't directly assess capability analysis but can be used to estimate the population mean for further calculations. P-values: These indicate the statistical significance of a hypothesis test in distribution study tests. A low P-value (e.g., 0.05) suggests that the data may not follow hypothesized distribution, potentially impacting control chart calculations. Process Evaluation: By establishing control with control charts and capability with capability analysis, we can gain a more comprehensive understanding of the process performance. Control charts: These help identify process shifts or trends over time, indicating potential issues requiring investigation. Capability plots: These assess whether the process variation is centered within the specified limits and whether improvements are necessary to achieve consistent production within tolerances.

RESULTS AND DISCUSSION

The use of control charts is essential in the inspection of the chemical characteristics of raw compounds in the chemical manufacturing industry. The control chart is a statistical tool that helps in monitoring the quality of a manufacturing process over time. It is used to detect any changes or variations

in the process, which could lead to defects or substandard products. The control chart consists of a central line that represents the process average, and two control limits (upper and lower) that represent the acceptable range of variation in the process. The data points are plotted on the chart, and any points that fall outside the control limits indicate that the process is out of control and needs to be investigated and corrected.

The application of control charts in the chemical manufacturing industry ensures that the raw compounds used in the production process meet the required specifications. This is important because the quality of the raw compounds can affect the quality of the final product. For example, if the concentration of a particular chemical in the raw compound is too high or too low, it could affect the chemical reaction during the manufacturing process and result in a substandard product. Using control charts also helps to identify any trends or patterns in the data, which could indicate a problem in the manufacturing process. For example, if there is a consistent increase or decrease in the chemical concentration of the raw compound over time, it could indicate a problem with the equipment or the manufacturing process itself.

In addition, the use of control charts helps to reduce inspection costs by eliminating the need for 100% inspection of the raw compounds. Instead, a sample of the raw compound is taken and tested, and the results are plotted on the control chart. This reduces the time and cost of inspection while still ensuring that the quality of the raw compound meets the required specifications.

Fast and effective interpretation of the results of the official pharmacopeias tests could be accomplished after identification of the best fitting distribution of the monitored datasets to conduct further analysis as capability plot and histogram associated with the process-behavior chart. The chronological time series diagram that was done batch-wise with the available test material was an Individual-Moving Range (I-MR) chart. Any observable pattern could be detected from the last points of observation. When the test is skipped and not performed in the time series, gaps are indicated in the control charts.

The specific statistical techniques used herein focuses on the implementation of SPC as the following: Individual-Moving Range (I-MR) Charts: This variation is particularly useful for smaller datasets, where subgrouping might not be feasible. I charts monitor individual measurements, while MR charts track the moving range between consecutive measurements. They help identify trends, shifts, and potential outliers. Nuanced Interpretation of Control Chart Signals would be important in this context. While the present analysis mentions out-of-control signals, it's crucial to elaborate on their interpretation, considering some factors. Non-normal data: When data doesn't follow a normal distribution, interpreting control chart signals based on standard statistical assumptions can be misleading. It's essential to acknowledge this limitation and consider alternative approaches, such as control charts for non-normal datasets.

These charts are designed to correct for non-normal data and adjust for control limits of raw values. Cautionary interpretation should be approached when using standard control charts with non-normal data, interpretation out-of-control signals cautiously, considering other process knowledge and potential causes of variation. Causes of variation: Out-of-control signals can arise from various sources, including assignable causes which are specific, identifiable factors causing process variations, such as equipment malfunctions or changes in raw materials. Investigating and addressing these causes are crucial for process improvement. Common causes: These are inherent variations present in any process due to factors like random fluctuations. While not directly controllable, understanding and minimizing their impact is essential for achieving process stability.

Clarifying the Purpose of the AD Test: The AD test, mentioned, refers to the Anderson-Darling (AD) test for normality. This is a statistical test used to assess whether a given sample originates from the assumed distributed population. The AD test is used in the context of control chart construction, where the underlying distribution assumption often underpins

the control chart calculations. By performing the AD test, the study assesses whether the data for each analyzed characteristic (e.g., optical rotation) follows the expected distribution from the screening of the best fitting dispersion of datasets. This information can inform the selection of appropriate control chart types and the interpretation of the resulting control chart signals.

It should be noted that the initial exploratory process-behavior charts were done for preliminary evaluation of small firm of chemical manufacturing company at its infancy to evaluate its starting up synthesis of the medicinal chemical compound. Accordingly, there was evidence of incomplete data collection which could occur due to several obstacles embracing:

Equipment malfunctions: If the instruments used for measurement fail during specific batches, data for those batches would be missing.

Human error: Mistakes during data collection or recording can lead to missing values.

Sample loss or damage: Unforeseen circumstances like sample contamination or loss during processing can result in missing data.

Data exclusion: In rare cases, researchers might intentionally exclude data points deemed outliers or suspected of errors. However, this practice should be clearly justified and documented to avoid transparency concerns.

Optical Rotation Test Analysis

The exploratory preliminary chart showed that the initial batches demonstrated optical rotation data with control limits that are confined within the specification range. The construction of the process-behavior chart was based on the Weibull distribution which was the most fitting type of the dispersion of the dataset. Moreover, the inspection characteristic showed an acceptable capability index, but the process is significantly shifted from the center. Thus, better adjustment is needed to correct the shifting and to guard against any drifts that could lead to excursions in the future. This finding could be deduced visually from Figure 1. The output showed a tendency of oscillation with shifting to the upper side of the centerline.

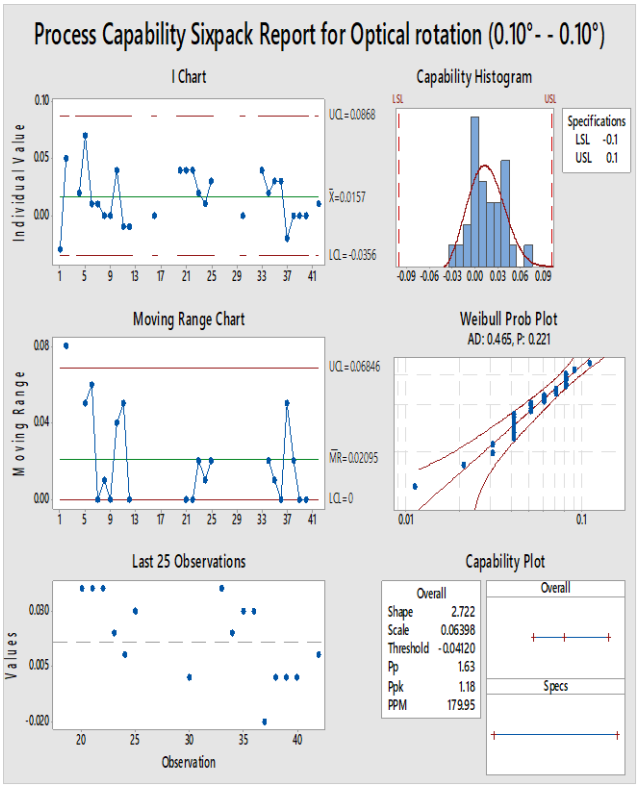

Figure 1. Process capability overview of one of the inspection characteristics of 3-O-ethyl 5-O-methyl 2-(2-aminoethoxymethyl)-4-(2-chlorophenyl)-6-methyl-1,4-dihydropyridine-3,5-dicarboxylate benzenesulfonic acid showing exploratory preliminary trending pattern and process behavior of the optical rotation test

Total Impurities Test Analysis

The early batches displayed the total impurities result with control limits that are contained within the specification range, according to the exploratory preliminary chart. Normal distribution, the most appropriate kind of dataset dispersion, served as the foundation for the creation of the trending chart. Additionally, the inspection feature revealed a competence index that is appropriate, but the process is noticeably shifted from the center. However, since the specification of this test is one-sided with an upper limit only and the drift was toward the zero, then no risk could be encountered in this case. Figure 2 might be used to visually infer this conclusion. The general trend line showed descending pattern.

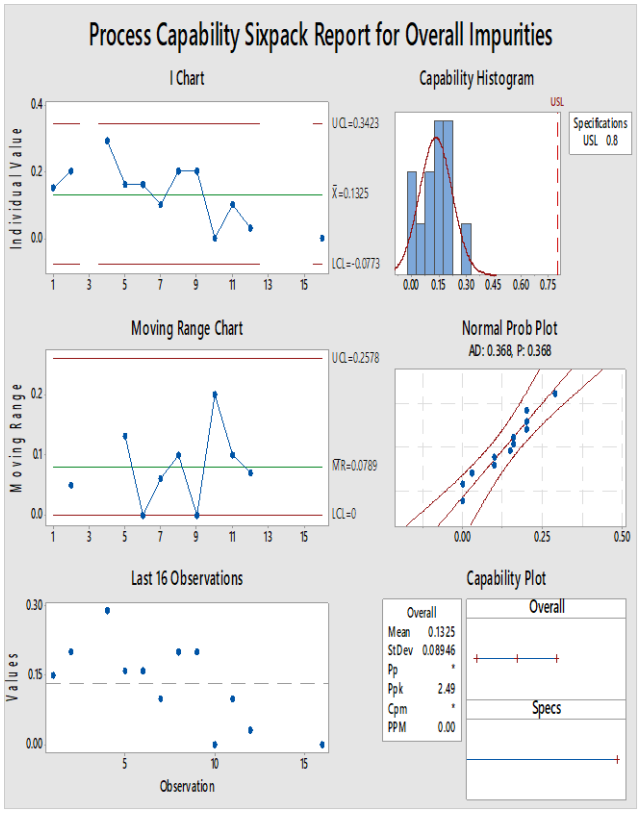

Figure 2. Process capability overview of one of the inspection characteristics of 3-O-ethyl 5-O-methyl 2-(2-aminoethoxymethyl)-4-(2-chlorophenyl)-6-methyl-1,4-dihydropyridine-3,5-dicarboxylate benzenesulfonic acid showing exploratory preliminary trending pattern and process behavior of the total impurities test

Assay Determined Based on Anhydrous Substance

The exploratory preliminary chart shows that the assay of the active material - calculated based on the dried substance - for the early batches was within the specification range with control window contained but shifted to the lower border. The trending chart was created using a Weibull distribution, which is the most acceptable type of dataset dispersion. Furthermore, while the procedure is noticeably shifted from the center, the inspection characteristic displayed an adequate capability index. This could be evident from the difference between P_p and P_{pk}. Therefore, more adjustment is required to make up for the shifting and prevent any drifts that can cause excursions down the road. Figure 3 might be used to visually infer this conclusion. When the output shifted to the lower side of the centerline, it displayed an oscillatory propensity.

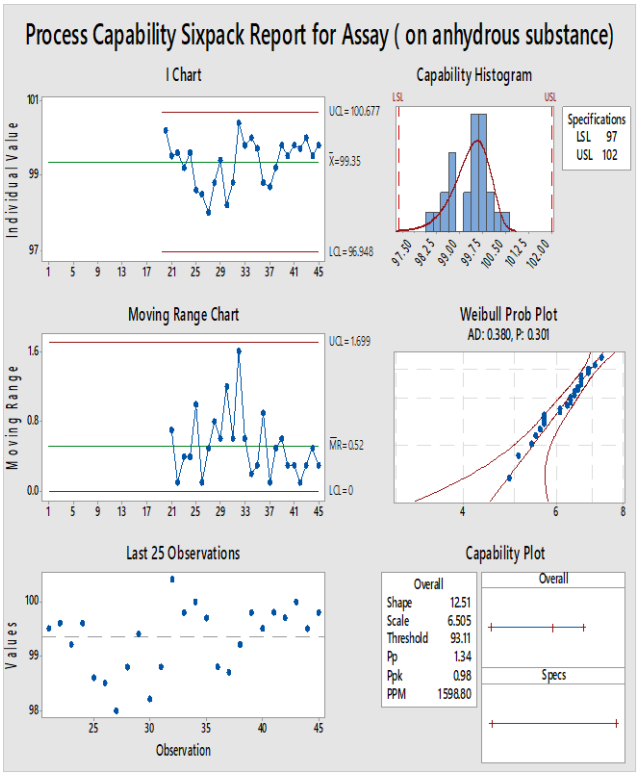

Figure 3. Process capability overview of one of the inspection characteristics of 3-O-ethyl 5-O-methyl 2-(2-aminoethoxymethyl)-4-(2-chlorophenyl)-6-methyl-1,4-dihydropyridine-3,5-dicarboxylate benzenesulfonic acid showing exploratory preliminary trending pattern and process behavior of the assay test (based on anhydrous material)

Particle Size Determination

In contrast to the other previous tests, the examination of this instrumental test showed provisionally a control limit exceeding the specification threshold state that need immediate action to control the particle size distribution. Accordingly, the overall capability plot and histogram showed a control window that exceeded the specification range. The prevalence of the alternating pattern can be seen visually in Figure 4. The best fitting distribution was the Gaussian one but after using the SU distribution type of the Johnson family type of distribution. Minitab's Johnson transformation is a statistical technique used to transform non-normal data into a normal distribution. This transformation allows for the application of control charts and other statistical methods that typically assume normality.

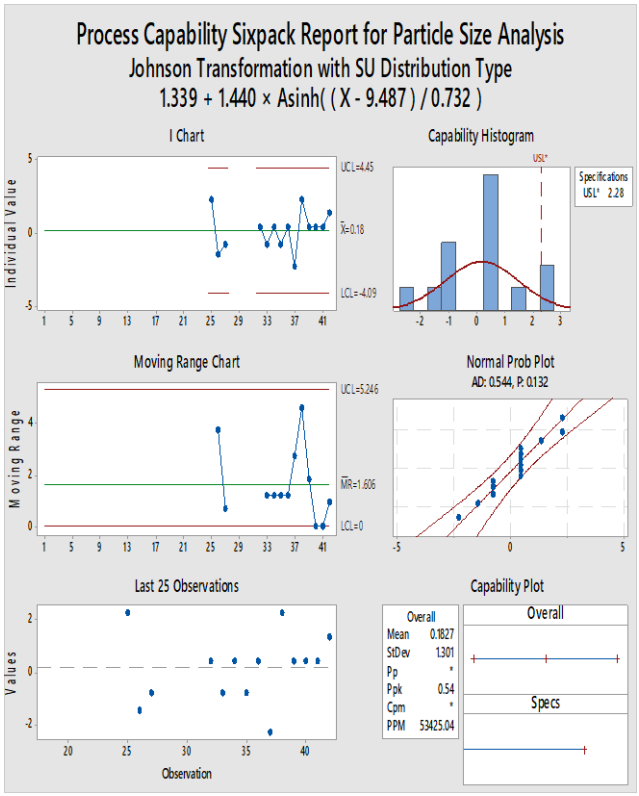

Figure 4. Process capability overview of one of the inspection characteristics of 3-O-ethyl 5-O-methyl 2-(2-aminoethoxymethyl)-4-(2-chlorophenyl)-6-methyl-1,4-dihydropyridine-3,5-dicarboxylate benzenesulfonic acid showing exploratory preliminary trending pattern and process behavior of the particle size analysis test

The Johnson transformation system actually consists of three families of distributions: S_B (bounded), S_L (lognormal), and S_U (unbounded). SU Distribution Type: "SU" in the text refers to the unbounded family of distributions within the Johnson transformation system. Unbounded distributions are suitable for data that can theoretically range from negative infinity to positive infinity, but in practice, may have a lower bound of zero. For example, particle size measurements typically don't have negative values, but they can range from zero upwards. Minitab and SU Distribution: Minitab automatically selects the most appropriate Johnson transformation family (S_B, S_L, or S_U) based on the characteristics of dataset. If the "SU distribution type" is mentioned, it indicates that Minitab identified the unbounded (SU) family as the best fit for the specific dataset being analyzed. This implies the data likely has a lower bound of zero but can theoretically extend infinitely upwards.

Process Versus Customer and Total Quality Management

The Voice of Process (VoP), or the width of the inspection characteristic variation, should be less than the Voice of Customer (VoC) in the capability analysis. The indicator for performance centering is P_{pk} (Advantive, 2023). It measures the extent to which the data is centered within the given parameters. P_p, on the other hand, is the performance indicator (Eissa, 2023b). It calculates the extent to which the data might fall inside the given parameters (USL, LSL) (Eissa, 2023b). However, it makes no difference if it is positioned in the middle of the borders window. The following guidelines would be used to calculate the average and the control window.

Normally, the center line (CL) of an individual (I) chart: Mean of the individual data points. For the I chart, the upper control limit (UCL) is CL + 2.66 x Avg Moving Range (MR). The Lower Control Limit (LCL) for the I chart is equal to CL - 2.66 x Average MR or zero in the event that the MR is negative. The center line (CL) of the MR chart represents the mean of MR [27, 28]. The UCL for the MR chart is 3.27 times the Average Moving Range. LCL for MR charts is zero. The strength of the evidence opposing the null hypothesis is evaluated using a probability known as the p-value (Eissa, 2023b). In an AD test, the predicted distribution of the data is the null hypothesis (Eissa, 2023b). Thus, lower p-values provide greater evidence that the data deviate from the distribution.

Establishing comprehensive SPC methodology implementation is crucial for chemical manufacturing organizations, as it forms an essential component of Total Quality Management (TQM) across the whole enterprise. To enforce safety and quality ideals, however, regulatory monitoring and surveillance in the industrial sector are essential. Until the SPC procedures are properly integrated into the foundations of the legislation governing the chemical sector, the receiver customer should monitor the given lots using appropriate statistical tools to keep a watch

on the goods they get. This is particularly crucial for emerging and economically distressed countries.

CONCLUSION

The current study identifies a significant and distinctive viewpoint in the physical and chemical criterion-based API trending and monitoring. The highly competitive world of pharmaceutical and medical products demands acceptable monitoring and control of the production field's quality. The fundamental components of this concept are the raw ingredients. An important task that, by tracking the trend of the properties of the chemical entities under examination, provides insight into how the inspection characteristics behave with the manufactured batches that are marketed and represents the quality of the final customer's organizations' deliveries. Control charts are essential for time-sequence or serial process monitoring. In order to detect changes in the qualities under examination and ascertain whether these changes are most likely the consequence of common or particular sources of variations, they display the mean and establish limiting thresholds. For the parties concerned and the governing governmental official agencies in the industrial sphere, SPC studies would be beneficial in understanding the trending pattern and the properties (chemical and physical) of the chemical substance that is given as a raw material. Ensuring the production of medical supplies that meet consistent, dependable, and satisfactory quality standards is an essential industrial duty. In conclusion, the application of control charts in the inspection of the chemical characteristics of raw compounds in the chemical manufacturing industry is important for ensuring the quality of the final product, identifying process problems, and reducing inspection costs. It is a valuable tool for ensuring that the manufacturing process is under control and producing high-quality products.

Recommendations

It is recommended that strict governmental rules should be established to monitor and control the indigenously and exported chemical goods by the official agencies. Meanwhile, the final customer firms and companies must keep statistical quality control on the received manufactured chemical to preserve the quality of their final products. Nevertheless, the original manufacturing firms should provide evidence for their SPC implementation on their final manufactured chemical compounds, especially those used in the medicinal, healthcare and pharmaceutical sectors for the sake of human safety and health protection.

ACKNOWLEDGEMENTS

There is nothing to declare. All the work was supported by the contributing author.

Compliance with Ethical Standards

Conflict of Interest

The author declares that there is no conflict of interest.

Ethical Approval

For this type of study, formal consent is not required.

Funding

Not applicable.

Data Availability

The author confirms that the data supporting the findings of this study are available within the article.

REFERENCES

Advantive. (2023). Capability indices: Ppk. Advantive. Retrieved on August 18, 2023, from https://www.advantive.com/solutions/spc-software/quality-advisor/data-analysis-tools/ppk/

Amlodipine Monograph for Professionals. (2016). *amLODIPine (Monograph)*. Retrieved on June 4, 2016, from https://www.drugs.com/monograph/amlodipine.html

British Pharmacopoeia. (2022). *British Pharmacopoeia 2022*. Retrieved on January 1, 2022, from https://www.pharmacopoeia.com/

Eissa, D., Rashed, E., & Eissa, M. (2023). Measuring public health effect of coronavirus disease 2019: A novel perspective in healthcare in pandemic times. *Medical Journal of Western Black Sea*, *7*(2), 266-268. https://doi.org/10.29058/mjwbs.1257163

Eissa, M. (2017). Bioburden control in the biopharmaceutical industry. *BioPharm International*, *30*(9), 24-27.

Eissa, M. (2018c). Evaluation of microbiological purified water trend using two types of control chart. *European Pharmaceutical Review*, *23*(5), 36-38.

Eissa, M. (2021). Implementation of modified Q-control chart in monitoring of inspection characteristics with finite quantification sensitivity limits: A case study of bioburden enumeration in capsule shell. *El-Cezeri*, *8*(3), 1093-1107. https://doi.org/10.31202/ecjse.871179

Eissa, M. (2022). Establishment of biocidal activity evaluation study protocol in healthcare facility for routine monitoring of antibacterial activity of disinfectants. *Journal of Experimental and Clinical Medicine*, *39*(4), 939-947.

Eissa, M. E. (2015). Shewhart control chart in microbiological quality control of purified water and its use in quantitative risk evaluation. *Pharmaceutical and Biosciences Journal*, *4*(1), 45-51. https://doi.org/10.20510/ukjpb/4/i1/87845

Eissa, M. E. (2016 2016a). Novel rapid method in ecological risk assessment of air-borne bacteria in pharmaceutical facility. *Mahidol University Journal of Pharmaceutical Sciences*, *43*(3), 115-126. https://doi.org/10.14456/mujps.2016.14

Eissa, M. E. (2018b). Adulterated pharmaceutical product detection using statistical process control. *Bangladesh Pharmaceutical Journal*, *21*(1), 7-15.

Eissa, M. E. (2018d). Variable and attribute control charts in trend analysis of active pharmaceutical components: Process efficiency monitoring and comparative study. *Experimental Medicine*, *1*(1), 32-44.

Eissa, M. E. (2023a). Studies on morbidities and mortalities from COVID-19: Novel public health practice during pandemic periods. *Asian Journal of Applied Sciences*, *16*(3), 84-94. https://doi.org/10.3923/ajaps.2023.84.94

Eissa, M. E. (2023b). Trending perspective in evaluation of inspection characteristics of pharmaceutical compound: comparative study of control charts. *Universal Journal of Pharmaceutical Research*, *8*(5), 15-21. https://doi.org/10.22270/ujpr.v8i5.1006

Eissa, M. E. A. (2019). Food outbreak: An overview on selected cases over long-term web-based monitoring. *SM Journal of Nutrition and Metabolism*, *5*(1), 1029.

Eissa, M. E. A. M. (2018a). Conventional culture media: an outdated microbiological tool but still useful. *International Journal of Drug Safety and Discovery*, *2*(2), 011.

Eissa, M. E., & Abid, A. M. (2018). Application of statistical process control for spotting compliance to good pharmaceutical practice. Brazilian Journal of Pharmaceutical Sciences, *54*(2), e17499. https://doi.org/10.1590/s2175-97902018000217499

Eissa, M. E., Mahmoud, A. M., & Nouby, A. S. (2016b). Control chart in microbiological cleaning efficacy of pharmaceutical facility. *Dhaka University Journal of Pharmaceutical Sciences*, *14*(2), 133-138.

Eissa, M. E., Seif, M., & Fares, M. (2015). Assessment of purified water quality in pharmaceutical facility using six sigma tools. *International Journal of Pharmaceutical Quality Assurance*, *6*(2), 54-72.

Eissa, M., & Mahmoud, A. (2016). Evaluation of microbial recovery from raw materials for pharmaceutical use. *Journal of Food and Pharmaceutical Sciences*, *4*(1), 6-11. https://doi.org/10.14499/jfps

Eissa, M., & Rashed, E. (2023). Evaluation of microbiological cleanliness of machines/equipment through rinse technique using statistical process control. *EMU Journal of Pharmaceutical Sciences*, *6*(1), 1–12. https://doi.org/10.54994/emujpharmsci.1196909

Eissa, M., Mahmoud, A., & Nouby, A. (2016a). Evaluation and failure risk of microbiological air quality in production area of pharmaceutical plant. *RGUHS Journal of Pharmaceutical Sciences*, *5*, 155-166.

Eissa, M., Rashed, E., & Eissa, D. E. (2021a). Study of tellurium-129m (129mTe) ground deposition following Fukushima nuclear disaster: descriptive analysis of UNSCEAR database using statistical process techniques. *Mugla Journal of Science and Technology*, *7*(2), 67-72. https://doi.org/10.22531/muglajsci.955946

Eissa, M., Rashed, E., & Eissa, D. E. (2021b). Quality improvement in routine inspection and control of healthcare products using statistical intervention of long-term data trend. *Dicle University Journal of the Institute of Natural and Applied Sciences*, *10*(2), 163-184.

Essam, M. (2019). *A novel approach in assessing the antimicrobial efficacy of eye drop products*. European Pharmaceutical Review. Retrieved on January 23, 2019, from https://www.europeanpharmaceuticalreview.com/article/40864/novel-approach-assessing-antimicrobial-efficacy-eye-drop-products/

Essam, M. (2023). *Pharmaceutical component kinetics*. Pharma Focus Asia. Retrieved on July 11, 2023, from https://www.pharmafocusasia.com/articles/pharmaceutical-component-kinetics-inventory-dynamic-control-is-crucial

Goldman, L., & Schafer, A. I. (2019) *Goldman-Cecil Medicine e-book*. Elsevier Health Sciences.

Mostafa Eissa, M. E. A. (2018, May 22). Quality criteria establishment for dissolution of ascorbic acid from sustained release pellets. *Novel Techniques in Nutrition & Food Science*, *2*(2), 137-142. https://doi.org/10.31031/ntnf.2018.02.000531

Acta Nat. Sci. (2024) 5(1): 41-50
DOI: 10.61326/actanatsci.v5i1.5
e-ISSN: 2718-0638

Original Research Paper
info@actanatsci.com
www.actanatsci.com

ACTA NATURA ET SCIENTIA PRENSİP

Doğal Afetin (6 Şubat 2023 Kahramanmaraş Depremleri) Hatay Balıkçılık Sektörüne İlk Etkileri ve Süreç Yönetim Önerileri: Hatay Örneği

Aydın Demirci[1]✉ • Emrah Şimşek[1] • Semih Kale[2] • Sevil Demirci[1]

[1] İskenderun Technical University, Faculty of Marine Sciences and Technology, Department of Marine Technologies, İskenderun, Hatay, Türkiye, aydin.demirci@iste.edu.tr; emrhsimsek@gmail.com; sevil.demirci@iste.edu.tr
[2] Çanakkale Onsekiz Mart University, Faculty of Marine Sciences and Technology, Department of Fishing and Fish Processing Technology, Çanakkale, Türkiye, semihkale@comu.edu.tr

✉ Corresponding Author: aydin.demirci@iste.edu.tr

Please cite this paper as follows:
Demirci, A., Şimşek, E., Kale, S., & Demirci, S. (2024). Doğal Afetin (6 Şubat 2023 Kahramanmaraş Depremleri) Hatay Balıkçılık Sektörüne İlk Etkileri ve Süreç Yönetim Önerileri: Hatay Örneği. *Acta Natura et Scientia*, *5*(1), 41-50. https://doi.org/10.61326/actanatsci.v5i1.5

MAKALE BİLGİSİ

Makale Geçmişi
Geliş: 10.06.2023
Düzeltme: 06.03.2024
Kabul: 06.03.2024
Çevrimiçi Yayınlanma: 22.05.2024

Anahtar Kelimeler:
Deprem
Doğal Afet
Balıkçılık Sektörü
Hatay

ÖZET

Türkiye'de 6 Şubat 2023 tarihinde meydana gelen Kahramanmaraş merkezli depremler ve sonrasındaki sarsıntılar Hatay ilinde de çok büyük yıkımlara neden olmuştur. Doğal olarak balıkçılık sektörü de bu sarsıntılardan direkt ve dolaylı olarak etkilenmiştir. Bölgedeki tüm insanlar gibi birçok balıkçı da can güvenliği nedeni ile balıkçılık faaliyetlerine ara vermek zorunda kalmıştır. Bu çalışmada depremlerin bölgedeki balıkçı barınakları, balıkçı gemileri, perakende ve toptan balık ticareti yapılan işletmeler ve su ürünleri ithalat-ihracat firmalarının üzerindeki etkilerinin belirlenmesi amaçlanmıştır. Bölgedeki tüm insanlar gibi birçok balıkçı da can güvenliği nedeni ile balıkçılık faaliyetlerine ara vermek zorunda kalmıştır. Balıkçılık sektörü depremlerden yaklaşık bir ay sonra diğer sektörlere nazaran çok daha hızlı bir şekilde normalleşme sürecine girmiştir. Bu çalışmada bölge balıkçılığının sürdürülebilir ekosistem kavramı ve denizel kaynaklardan maksimum faydanın sağlanabilmesi için öneriler sunulmuştur. Bu süreçte balıkçılık sektörünün tekrar canlanabilmesi için su ürünleri ticareti yapan işletmelerin (perakende, toptancı ve ihracat) desteklenmesine öncelik verilmesinin büyük önem taşıdığı düşünülmektedir. Çünkü bu işletmelerin faaliyeti doğrudan balıkçılık faaliyetinde bulunan paydaşlara ve özelikle küçük ölçekli balıkçılara yansıyacağı düşünülmektedir. Bu destek kapsamında deprem nedeni ile alınan olağanüstü hal kararları göz önünde bulundurularak fırsatçılığa yol açmamak için denetimlerin daha etkin olması gerekmektedir.

Early Effects of Natural Disaster (February 6, 2023, Kahramanmaraş Earthquakes) on Fishery Sector and Suggestions for Process Management: The Case of Hatay

ARTICLE INFO

Article History
Article History
Received: 10.06.2023
Revised: 06.03.2024
Accepted: 06.03.2024
Available online: 22.05.2024

Keywords:
Earthquake
Natural disaster
Fishery sector
Hatay

ABSTRACT

The Kahramanmaraş-centered earthquakes and subsequent tremors that occurred in Türkiye on February 6, 2023, caused great destruction in Hatay province. Naturally, the fishing industry has been directly and indirectly affected by these shocks. Like all people in the region, many fishermen had to suspend their fishing activities for life safety reasons. In this study, earthquake effects on fishermen's shelters, fishing vessels, retail and wholesale fish trade businesses and aquaculture import-export companies in the region were determined. Like all people in the region, many of the fishing parties had to take a break from their activities due to the safety of life. The fishing sector entered the normalization process much faster than other sectors, about a month after the earthquakes. This paper offers suggestions for the sustainable ecosystem concept of the regional fisheries and for obtaining maximum benefit from marine resources. In this process, it is more realistic to support the fishing trade companies (retail, wholesale and export) for the revival of the sector. Because it is thought that the activities of these enterprises will directly reflect on the stakeholders engaged in fishing activities and especially on small-scale fishermen. Considering the martial law decisions taken due to the earthquake within the scope of this support, the inspections should be more effective in order not to cause opportunism.

GİRİŞ

Balıkçılık endüstrisi, bir ülkenin ekonomik ve sosyal hayatına sağladığı katkıları ile önemli bir sektör olmasının yanında, tüm paydaşlarıyla birlikte yönetilmesi ve sürekliliğin sağlanması açısından zor bir sektördür (Can ve Demirci, 2012). Bununla birlikte balıkçılık bugüne kadar birçok doğal ve çevresel felaket, global ekonomik kriz ve pandemi gibi olumsuz durumlardan etkilenen hassas bir endüstri olarak bilinmektedir (Can vd., 2020; Demirci vd., 2020; Kaya & Can, 2022).

Türkiye'de 6 Şubat 2023 tarihli Kahramanmaraş merkezli Mw 7,7 ve Mw 7,6 şiddetindeki iki büyük deprem sarsıntısının, Türkiye'nin güney kısmında birçok şehirde (Kahramanmaraş, Hatay, Adıyaman, Malatya, Adana, Gaziantep, Elazığ, Diyarbakır, Kilis, Şanlıurfa ve Osmaniye) (Şekil 1) yıkıcı etkisi olmuş ve çevre illerde de hissedilmiştir. Meydana gelen deprem afetleri nedeniyle yaşanan yıkım ve can kayıpları üzerine 11 il ve Sivas ilinin Gürün ilçesi T.C. İçişleri Bakanlığı Afet ve Acil Durum Yönetimi Başkanlığı tarafından "Genel Hayata Etkili Afet Bölgesi" olarak kabul edilmiştir (AFAD, 2023a). Bu yıkıcı depremlerden sonra çok sayıda artçı ve 20 Şubat 2023 tarihinde Antakya merkezli büyük şiddetli (Mw 6,4 ve Mw 5,8) iki deprem daha meydana gelmiştir. Bu depremler Hatay ili genelinde 20 binin üzerinde can kaybına ve şehirde büyük yıkıma neden olmuştur (AFAD, 2023b). Bu depremler şiddet ve kapsadığı alan açısından yakın tarihte eşi benzeri olmayan felaketler olarak nitelendirilmiştir (SBB, 2023). Bu yıkıcı depremler ve yaşanan çok sayıda artçı sarsıntılardan dolayı bölgede sosyal hayat asgari düzeyde bile sürdürülemez hale gelmiştir. Bu bölgede yaşayan binlerce insan Türkiye'de başka bölgelere göç ederken bölgede kalanlarsa binalara giremeyip çadır, konteyner ya da tek katlı binalarda yaşamlarını sürdürmeye devam etmektedirler.

Depremden en çok etkilenen illerde oluşan can ve mal kaybı ile deprem sonrası yapılacak barınma ve bakım, onarım ve inşa maliyetlerinin ekonomik

aktivite, istihdam, fiyat ve finansman başta olmak üzere Türkiye ekonomisi üzerinde ciddi ve uzun vadeli olumsuz etkileri olacağı öngörülmektedir (Aydın Özüdoğru, 2023). Öte yandan, depremden kaynaklanan varlık kaybının da yoksulluğu tetikleyebileceği tahmin edilmektedir. Dolayısıyla, uluslararası kuruluşlarla iş birliği yapılması ile deprem sonrası kalkınma programının etkili ve verimli bir biçimde gerçekleştirilmesi önemli katkılar sağlayacaktır.

Figure 1. Provinces affected by earthquakes on February 6, 2023 in Türkiye

Şekil 1. *Türkiye'de 6 Şubat 2023'teki depremlerde etkilenen iller*

Hatay ilinin İskenderun Körfezi balıkçılık kaynakları ve tür çeşitliliği açısından önemli bir bölgedir (Gökçe 2015, Can vd., 2006, Şimşek vd., 2019; Demirhan vd., 2020). Bununla birlikte bölgede balıkçılığın yanı sıra turizm, lojistik ve ticaret olmak üzere yoğun denizcilik faaliyetleri yürütülmektedir (Demirci, 2003; Demirci & Karagüzel, 2018; Mazlum vd., 2019; Akar vd., 2021, 2022; Yılmaz vd., 2022). Deprem nedeniyle İskenderun Körfezi'nde Hatay balıkçıları tarafından sürdürülen balıkçılık faaliyetlerinin tamamen sekteye uğradığı düşünülmektedir. Dolayısıyla, bu çalışmada depremlerin bölgedeki balıkçı barınakları, balıkçı gemileri, perakende ve toptan balık ticareti yapılan işletmeler ve su ürünleri ithalat-ihracat firmalarının üzerindeki etkilerinin belirlenmesi amaçlanmıştır. Deprem nedeni ile etkilenen bölgedeki balıkçılık sektörü tüm yönleri ile değerlendirilmiş, mevcut durum karşısında sürecin etkin ve verimli bir şekilde yönetilebilmesi için öneriler sunulmuştur.

MATERYAL VE YÖNTEM

Bu çalışmada Türkiye'nin Hatay ilindeki balıkçılık faaliyetlerinin deprem sonrası devamlılığının sağlanabilmesi açısından mevcut durumun değerlendirilmesi yapılmıştır. Bu nedenle Hatay'ın Dörtyol, Payas, İskenderun, Arsuz ve Samandağ ilçelerinde bir saha çalışması gerçekleştirilmiştir. Öncelikle balıkçı barınaklarının mevcut durumları yerinde incelemeler yapılarak tespit edilmiştir. Bölgede balıkçık faaliyetleri gerçekleştiren tüm paydaşlarla yaşanan depremlerden sonra görüşmeler gerçekleştirilmiştir. Depremlerden sonra durumun değerlendirilmesinde balıkçılık sektörünün balıkçı, perakende ve toptancı bileşenleri bölgesel farklılıklar göz önünde bulundurmuştur. Depremden sonra bozulan altyapı da dikkate alınarak mevcut imkanlar çerçevesinde yapılması gerekenlere dair çözüm önerileri sunulmuştur.

Bölgede faaliyet gösteren trol ve gırgır gemilerinin balıkçılık çabasının Tarım ve Orman Bakanlığı'na ait Balıkçı Gemileri İzleme Sistemi (BAGİS) ve Otomatik Tanımlama Sistemi (AIS) verilerini toplayan Marine Traffic (MT) (https://www.marinetraffic.com/) ve Global Fishing Watch (GFW) (https://globalfishingwatch.org/) üzerinden takip edilmesi mümkündür. Bu çalışmada deprem nedeniyle oluşan balıkçılık çabasındaki değişiklikler bu üç veri seti üzerinden temin edilmiştir.

BULGULAR VE TARTIŞMA

Bölgedeki Çevlik Dörtyol ve Konacık balıkçı barınağında depremler nedeniyle yaşanan zararlar kısa sürede telafi edilmekle birlikte İskenderun balıkçı barınağındaki rıhtımın çökmesi nedeniyle tamir edilmesinin daha uzun bir süreyi kapsayacağı düşünülmektedir. Bu sürecin daha net bir şekilde anlaşılabilmesi için depremden hemen sonra 07.02.2023 tarihinde (Şekil 2), 25.02.2023 tarihinde (Şekil 3) ve 06.03.2023 tarihindeki deniz su seviyesinin lodos nedeni ile yükselmesinden sonra (Şekil 4) kaydedilen görüntüler sunulmuştur.

Figure 2. The first images from the Iskenderun Fishing Port after the Kahramanmaraş-epicentered earthquake dated February 7, 2023 (A; The state of the dock at the end of the port, B; The situation of the dock in the middle of the port, C: The collapse of the dock in the middle of the port, D: The collapse at the breakwater level in the middle of the port)

Şekil 2. *Kahramanmaraş merkezli depremlerden sonra İskenderun Balıkçı Barınağından 7 Şubat 2023 tarihli ilk görüntüler (A: Barınağın uç kısmındaki rıhtımın durumu, B: Barınağın orta kısmındaki rıhtımın durumu, C: Barınağın orta kısmındaki rıhtımdaki ortadan çökme, D: Barınağın orta kısmındaki dalgakıran seviyesindeki çökme)*

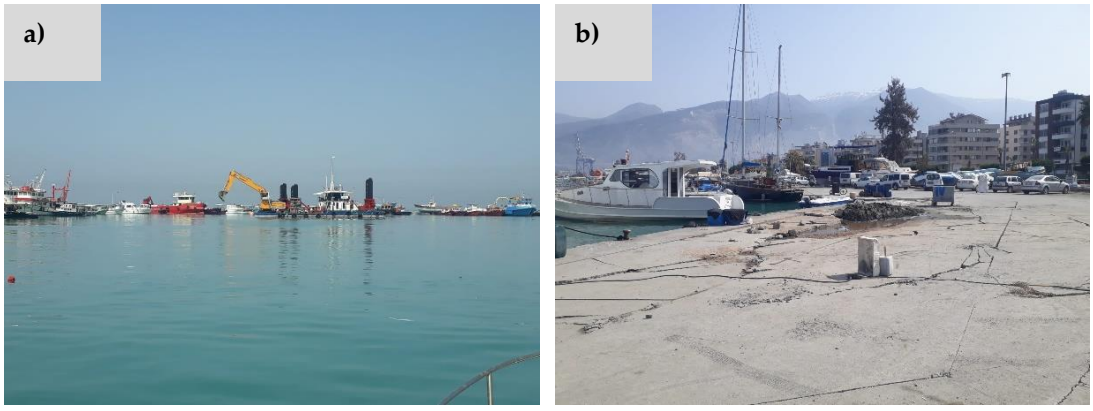

Figure 3. Images from the Iskenderun Fishing Port dated February 25, 2023 (A: Seabed dredging works at the İskenderun Fishing Port, B: The state of the dock at the entrance of the port)

Şekil 3. *İskenderun Balıkçı Barınağından 25 Şubat 2023 tarihli görüntüler (A: İskenderun Balıkçı barınağındaki dip tarama çalışmaları, B; Barınak girişindeki rıhtımın durumu)*

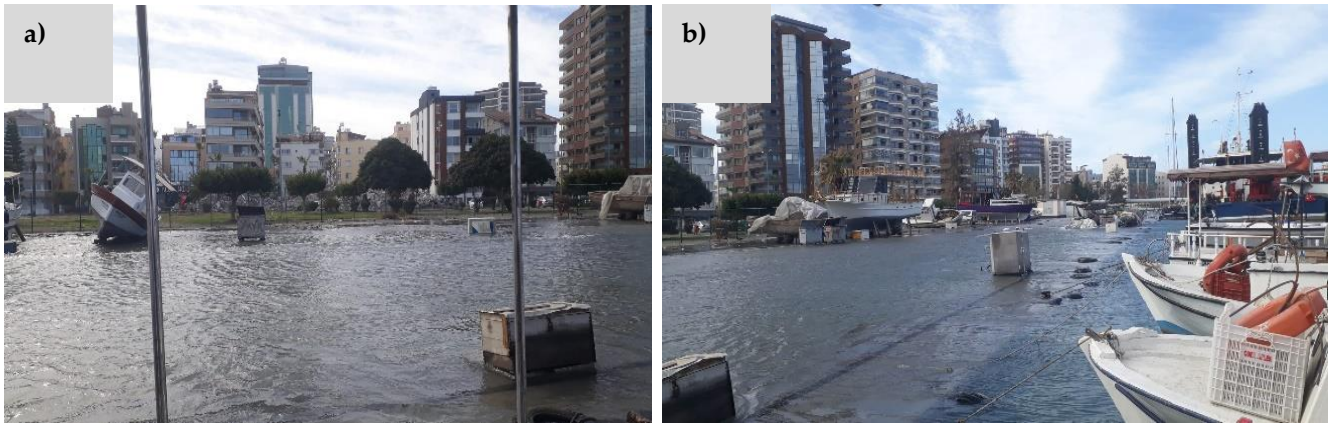

Figure 4. Sea level rising at the İskenderun Fishing Port (March 6, 2023)
Şekil 4. *İskenderun Balıkçı barınağında deniz suyu seviyesinin yükselmesi (6 Mart 2023)*

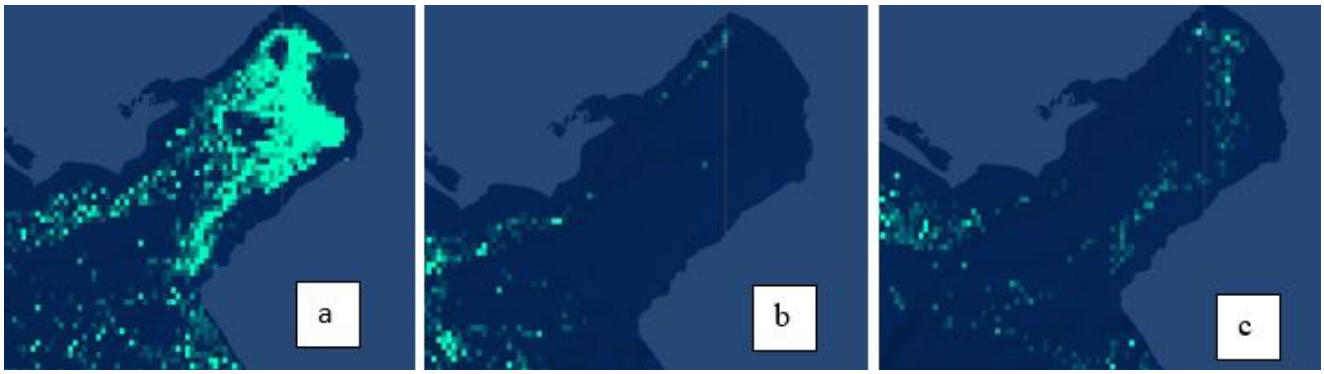

Figure 5. Fishing activities (trawling and purse-seining) for (a) one month before the earthquake, (b) one month after the earthquake, and (c) the 20th day after the earthquake according to Global Fishing Watch (GFW)
Şekil 5. *Global Fishing Watch (GFW) verilerine göre (a) depremden önceki bir ay, (b) depremden sonraki bir ay ve (c) depremden sonraki 20. güne ait balıkçılık aktiviteleri (Trol ve gırgır balıkçılığı)*

Şekil 5'te verilen deprem öncesinde ve sonrasında gerçekleşen balıkçılık faaliyetleri incelendiğinde bölgede bir ay boyunca neredeyse hiç trol ve gırgır balıkçılığı yapılmadığı gözlenmektedir. Bununla birlikte, körfezin batı dış kısmında bazı balıkçılık faaliyetleri görülmektedir. Ancak bu faaliyetler deprem bölgesindeki barınaklardan değil, Karataş ve Yumurtalık balıkçı barınaklarından gerçekleştirilmiştir. Depremden bir ay sonra Dörtyol Konacık ve Çevlik balıkçı barınaklarından balıkçılık faaliyetleri yapılmaya başlamıştır. Bu faaliyetlerin toplam süreleri ve 22 adet trol gemisinin 6 Şubat ile 15 Nisan tarihlerinde 2022 ve 2023 arasındaki ortalama denizde kalma süreleri kıyaslanmıştır. Bu süreler 2022 yılında 155,48 saat (±7,82) olarak belirlenmiştir. Ancak depremden sonra bu süre 51,90 saate (±7,93) düşmüştür. Bu azalmada gemiler arası farklılıklar göze çarpmaktadır. Gemilerin yaklaşık %57'si depremden sonra balıkçılığı dönemsel olarak tamamen terk ederken, kalan gemilerin denizde geçirdikleri sürelerde de %44,16'lık bir azalma meydana gelmiştir. Bununla birlikte trol gemisi sahipleri ile görüşüldüğünde av miktarının da oldukça az olduğu bildirilmiştir. Depremlerin denizel ekosistemdeki balıkçılık kaynakları üzerinde önemli etkileri olabileceği düşünülmektedir. Bu depremler sonrasında balıkçılık kaynaklarının bulunurluğu, göç yolları, yaşam alanları ve yatay/dikey hareketlerinde de ani değişimler gerçekleşmesi beklenmektedir. Dolayısıyla, av miktarının düşük olmasının depremin tetiklediği bu sebeplerden kaynaklanabileceği düşünülmektedir. Nitekim, Tweddle & Crossley (1990) Malawi Gölü'nde özellikle ciklit balığı avcılığında belirgin bir düşüş olduğunu rapor etmiştir. Kodama vd. (2018) 2011 Tōhoku depremi ve tsunamisi sonrasında biyoçeşitlilik açısından önemli bir değişiklik gözlenmemiş olsa da toplam bolluk ve biyokütlenin deprem öncesi ve sonrasında değişkenlik gösterdiğini bildirmiştir. Ayrıca, su sıcaklığındaki ani değişimler, zemindeki kütle

hareketleri, nehirlerden aşırı sediman taşınımı, yer hareketlerinden kaynaklanan habitat değişimleri, bulanıklığın artması ve ışık geçirgenliğinin azalmasının da denizel ekosistemde deprem sonrası balıkçılık üretiminin azalmasına yol açtığı tahmin edilmektedir. Takami vd. (2013) deprem ve tsunamiden 3 ay sonra bile halen deniz tabanında biriken sediman nedeniyle suyun bulanık olduğunu bildirmiştir. Benzer şekilde, Kawamura vd. (2014) deprem ve tsunamiden birkaç ay sonra bile sudaki bulanıklığın ve kıyısal alanlara doğru yoğun bir sediman taşınımının devam ettiğini rapor etmiştir. Bununla birlikte, Takami vd. (2017) deprem ve tsunami sonrasında sualtı görünürlüğünün çok daha düşük olduğunu belirtmiş ve bunun da kayalar arasındaki boşluklarda ve ana kaya yarıklarında ince sediman miktarındaki artıştan kaynaklandığını ifade etmiştir. Gerrity vd. (2020) depremin kültürel ve ticari öneme sahip bir tür olan *Haliotis iris* türünün erken yaşam evreleri için kritik öneme sahip habitatın tahrip edilmesine ve büyük ölüm oranlarına neden olduğunu rapor etmiştir. Benzer şekilde McCowan & Neubauer (2018) depremin kıyı kesimlerde geniş çaplı yükselmeye neden olduğunu, *Haliotis iris* türü için kitlesel ölümlere yol açtığını ve kritik habitatların yok olmasına sebep olduğunu belirtmiştir. Diğer yandan, bölgede uzatma ağlarıyla gerçekleştirilen avcılık faaliyetleri depremden sonra kısa süre içinde Dörtyol'da normale döndüğü tespit edilmiştir. Ancak, İskenderun ve Arsuz balıkçı barınakları için aynı durum söz konusu değildir. Konacık Limanında ise kalamar sezonu olma sebebiyle olta avcılığında balıkçılık faaliyetleri yapılmaktadır.

Türkiye Cumhuriyeti Cumhurbaşkanlığı Strateji ve Bütçe Başkanlığı (SBB, 2023) deprem sonrası değerlendirme raporunda sunulan Ulaştırma ve Altyapı Bakanlığı Altyapı Yatırımları Genel Müdürlüğünün Hatay'daki balıkçı barınaklarında oluşan hasarların tutarına yönelik bilgileri Tablo 1'de verilmiştir. Bu bilgiler dikkate alındığında ekonomik olarak en yüksek hasarın İskenderun balıkçı barınağında meydana geldiği görülmektedir. Hatay'daki barınakların içinde ekonomik olarak en az hasarın ise 94,4 milyon TL ile Çevlik (Samandağ) balıkçı barınağında tahmin edildiği tespit edilmiştir. Balıkçılığın bölgede yeniden başlayabilmesi için yakalanan su ürünlerinin pazar şartlarının oluşması gerekmektedir. Ancak, depremlerin balıkçılık şirketlerinin pazar getirilerini önemli ölçüde etkilediği tahmin edilmektedir. Benzer şekilde, Scholtens & Oueghliss (2020) balıkçılığın afetlere karşı özellikle hassas olduğunu ve depremlerin petrol sızıntılarından daha belirgin etkilere sahip olduğunu ifade etmektedir. Bölgede balık tüketimi talebinin önemli bir kısmını karşılayan Antakya ve İskenderun'da depremden kaynaklanan sosyal hayattaki olumsuzluk bu bölgelerde su ürünleri arzını mümkün kılmamaktadır. Buna rağmen, İskenderun balık-sebze halinde perakende olarak iş yerini açan bazı işletmeler olmuştur. Aynı şekilde, Arsuz ilçesinde de bazı balık marketler perakende ve toptan satışa destek vermektedir. Depremden yaklaşık 15 gün sonra Dörtyol'da balık satışı yapan marketler faaliyetlerini sürdürmeye başlamışlardır. İskenderun'da da az sayıdaki balık toptancısı faaliyetlerini başlatmış durumdadır. Tüm bu paydaşların dışında sektör düşünüldüğünde deprem nedeniyle balıkçılara balıkçılık ve gemi malzemeleri sağlayan işletmelerde de zararlar söz konusudur.

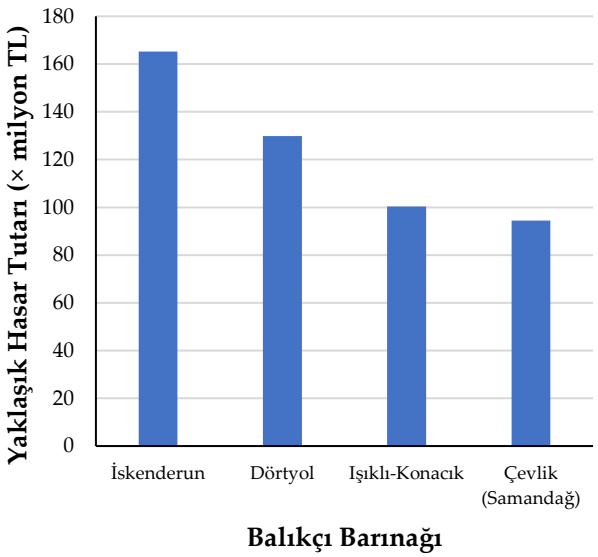

Figure 5. Economic value of damage to fishing port in Hatay (SBB, 2023)

Şekil 6. *Hatay'daki balıkçı barınaklarında oluşan hasarın ekonomik değeri (SBB, 2023)*

Su ürünleri kooperatifleri, balıkçılığın restorasyonu ve yeniden inşasında önemli bir role sahiptir (Okuda & Ohashi, 2012). Mevcut problemlerin çözülebilmesi için birlik ve dayanışma

içinde olarak su ürünleri kooperatifleri çatısı altında toplanan balıkçılar önemli bir güç oluşturabilirler (Kale & Zabun, 2023). Dolayısıyla, depremlerin sonrasında bölgede balıkçılık endüstrilerinin yeniden yapılandırılması açısından kooperatiflerin önemli katkıları olacağı düşünülmektedir. Sorunların çözümü açısından kooperatiflerin çatısı altında ortak bir şekilde hareket edilmesi ihtiyaçların tespit edilmesinde ve hızlıca gerekli eylemlerin gerçekleştirilmesinde faydalı olacaktır. Bu faydaların adil ve eşitlikçi bir şekilde dağıtılmasında su ürünleri kooperatiflerinin sahip olduğu organizasyonel deneyimden yararlanılması büyük kolaylıklar sağlayacaktır.

SONUÇ VE ÖNERİLER

1. Balıkçı barınaklarının mevcut durumu göz önünde bulundurulduğunda bölgede barınakların kısa vadede hizmet verir hale gelmesi önemlidir. Uzun vadede ise barınakların tamamında daha detaylı çalışmalar gerekecektir. Özellikle İskenderun Balıkçı Barınağında gözle görülür bir alçalma ve denize batma/oturma vardır.
2. Bölgedeki ağ kafeslerde balık yetiştiriciliği yapan firmalar İskenderun Balıkçı Barınağını kullanmaktaydı. Bu aşamada firmaların da faaliyetlerini sürdürebilmesi için liman ve barınma ihtiyaçları için bölgedeki kıyı yapılarını kullanmalarının önü açılmalı, altyapı ve üstyapı imkanları açısından uygun olan kıyı yapılarının kullanımına imkan sağlanmalıdır.
3. Tarım ve Orman Bakanlığı tarafından açıklanan çiftçi destekleri kapsamına bölge balıkçılarının da dahil edilmesi gereklidir.
4. Bölgedeki perakende balık ticareti yapan işletmelerin faaliyetlerini başlatması yönünde destek ve yaptırımlar yetkili kurumlarca değerlendirilmelidir.
5. Balıkçıların yakaladıkları balıkları arz edebilecekleri yerel pazarların aktif olmaması sebebiyle, toptan balık ticareti yapan işletmelerin aktif hale gelmeleri öncelikli olmalıdır. Bu bağlamda depremin yıkıcı etkileri de göz önünde bulundurularak bölgede balık ticareti yapan işletmelerin ekonomik olarak desteklenmesi gerekmektedir. Çünkü bu şekilde yapılan destek bölgedeki balıkçılık faaliyetlerinin aktif olarak başlamasını sağlayacaktır ve özelikle de küçük ölçekli balıkçılık faaliyetlerine yansıyacaktır. Bölgedeki uygulanan olağanüstü hal (OHAL) şartları da düşünülerek devlet kurumlarının su ürünleri açısından karar vericileri ve politika uygulayıcıları hızlı kararlar alarak uygulamaya koymalıdır. Küçük ölçekli balıkçıların aleyhine fırsatçılıklar oluşmamalıdır. Bölgedeki balığın arz edildiği Gaziantep, Diyarbakır, Şanlıurfa, Adıyaman, Osmaniye, Kahramanmaraş gibi çevre illerdeki deprem etkileri de göz önüne alınarak bölgede yakalanan balığın Ankara, İstanbul ve İzmir gibi büyük şehirlerde pazarlamasında öncelik ve kolaylık sağlanmalıdır.
6. Su ürünleri ihracatı yapan ve su ürünlerine yönelik soğuk hava hizmeti veren firmaların deprem sonrasında yaşanan elektrik kesintisi nedeniyle karides gibi yüksek ekonomik değere sahip ürünleri zarar görmüştür. Bu firmaların büyük çoğunluğu Suriye'deki savaştan kaynaklanan riskler nedeniyle ürünlerini gerekli şekilde sigorta yaptıramamışlardı. Dolayısıyla, bu durumdaki paydaşların da tespiti yapılıp mümkün olan destekler sağlanmalıdır.
7. Önümüzdeki dönemde karides uzatma ağı balıkçılığı için gerekli olan ağ temininde yerel ölçekte zorluklar yaşanabilir. Çünkü bölgedeki tedarik firmaları depremden zarar görmüş olan ve ticari faaliyetleri sekteye uğrayan firmalardır. Bu bağlamda bu firmalara destek sağlanmalı ve Hatay İl Tarım Müdürlüğü tarafından bölgede balıkçılık yapan kadınlara yönelik bir proje kapsamında eğitim verilerek bu kişilerin ağ bulmasına destek sağlanmalıdır.
8. Bölgede yaz aylarında balıkçı gemilerinin bakımlarının yapılabilmesi için çekek yeri ve gemi bakım malzemesi teminine yönelik destekler planlamalıdır.

9. Mevcutta uygulanan küçük ölçekli balıkçılık destekleri süresinin uzatılması kararı balıkçılar tarafından yerinde bir karar olarak memnuniyetle karşılanmıştır. Bu hususta başvurusunu tamamlayan balıkçılara en kısa sürede ödemelerinin yapılmasında yarar vardır.
10. Bölgedeki kredi borç ödemeleri genel olarak ertelenmiş durumdadır. Bu bölgedeki tüm balıkçılık işletmelerine bu yönde desteklerin artması gerekecektir. Demirci vd. (2020) bölge balıkçılığının COVID-19 sürecinde önemli ölçüde zarar gördüğünü belirtmiştir. Sonrasında da gerçekleşen deprem nedeniyle yaşanan olumsuzluklar sektöre geri dönülmez ve telafisi mümkün olmayan zararlar verebilir. Bu bağlamda özelikle gemi ve balıkçılık ruhsatı satışları yetkililerce izlenmelidir.
11. Deprem nedeni ile illegal balıkçılık faaliyetleri ekosistem ve paydaşlar arasında eşitlik ilkesine zararlar verebilir. Bu bağlamda balıkçılık denetimlerinin de mümkün olduğunca etkin bir şekilde devam ettirilmesi gerekmektedir. Bölgedeki denetim elemanlarının da depremden olumsuz yönde etkilenmiş olmalarından dolayı hem İskenderun Körfezi'ndeki hem de Asi Nehri'ndeki su ürünleri denetimleri için deprem bölgesi dışındaki şehirlerden personel ve araç görevlendirilmesi yapılması faydalı olacaktır.

Etik Standartlara Uygunluk

Yazarların Katkısı

AD: Makalenin tasarımı, Veri toplama, Makale yazımı, Okuma, Düzeltme.
EŞ: Makale yazımı, Taslak kontrolü, Okuma, Düzeltme.
SK: Makale yazımı, Taslak kontrolü, Okuma, Düzeltme.
SD: Makale yazımı, Okuma, Kontrol.
Tüm yazarlar makalenin son halini okumuş ve onaylamıştır.

Çıkar Çatışması

Yazarlar herhangi bir çıkar çatışması olmadığını deklare etmektedir.

Etik Onay

Yazarlar bu çalışma için resmi etik kurul onayının gerekli olmadığını bildirmektedir.

Veri Kullanılabilirliği

Yazarlar, bu çalışmanın bulgularını destekleyen verilerin makale içinde mevcut olduğunu onaylamaktadır.

KAYNAKLAR

AFAD. (2023a). *Genel Hayata Etkili Afet Bölgesi Hk. - Basın Duyurusu*. Erişim tarihi: 08.05.2023, https://www.afad.gov.tr/genel-hayata-etkili-afet-bolgesi-hk

AFAD. (2023b). *Hatay'da Meydana Gelen 6.4 Büyüklüğündeki Deprem Hk. Basın Bülteni-1*. Erişim tarihi: 03.04.2023, https://afad.gov.tr/hatayda-meydana-gelen-64-buyuklugundeki-deprem-hk-basin-bulteni-1

Aydın Özüdoğru, B. (2023). *2023 Yılında Gerçekleşen Kahramanmaraş Merkezli Depremin Etkileri ve Politika Önerileri*. Türkiye Ekonomi Politikaları Araştırma Vakfı Politika Notu, *Mart 2023* (N202306), 35s.

Akar, Ö., Çalışır, V., Demirci, A., & Şimşek, E. (2021). Effects of COVID-19 on fuel gas emissions from marine transportation. *Proceedings of the 4th Global Conference on Innovation in Marine Technology and The Future of Marine Transportation*, Türkiye. pp. 19.

Akar, Ö., Demirci, A., Şimşek, E., Mazlum, Y., & Demirci, S. (2022). Management of Fishing Ports on the Financial Performance of the Türkiye Fishery Sector; A Case of Fishing Ports in Hatay Province. *Journal of Anatolian Environmental and Animal Sciences*, *7*(3), 281-288 https://doi.org/10.35229/jaes.1117772

Can, M. F., & Demirci, A. (2012). Fisheries management in Turkey. *International Journal of Aquaculture*, *2*(8): 48-58.

Can, M. F., Demirci, A., & Demirci, S. (2006). Fisheries in Iskenderun Bay. Report of the ICES-FAO Working Group on Fishing Technology and Fish Behaviour (WGFTFB), pp. 50.

Can, M. F., Şimşek, E., Demirci, A., Demirci, S., & Akar, Ö. (2020). The evaluation of the early impacts of the COVID-19 pandemic on the export of fishery commodities of Turkey. *Marine and Life Sciences*, *2*(1), 18-27.

Demirci, A. (2003). Non-target demersal species inhabiting İskenderun Bay and their Biomass Estimation. [Ph.D. Thesis. Mustafa Kemal University].

Demirci, A., & Karagüzel, M. (2018). The evaluation of fishing vessels fuel consumption and pollutions emissions in the İskenderun Bay. *Fresenius Environmental Bulletin*, *27*(1), 508-514.

Demirci, A., Şimşek, E., Can, M. F., Akar, Ö., & Demirci, S. (2020). Has the pandemic (COVID-19) affected the fishery sector in regional scale? A case study on the fishery sector in Hatay province from Turkey. *Marine and Life Sciences*, *2*(1), 13-17.

Demirhan, S. A., Alkan, A., & Şimşek, E. (2020). Artificial reef application from the Iskenderun Bay, Northeastern Mediterranean, Turkey; an experimental study. *Sakarya University Journal of Science*, *24*(1), 49-54, https://doi.org/10.16984/saufenbilder.527933

Gerrity, S., Alestra, T., Fischman, H. S., & Schiel, D. R. (2020). Earthquake effects on abalone habitats and populations in southern New Zealand. *Marine Ecology Progress Series*, *656*, 153-161. https://doi.org/10.3354/meps13458

Gökçe, G. (2015). Design, deployment and fish assemblages of artificial reefs in Iskenderun Bay, Turkey: initial experiences. *Journal of Applied Ichthyology*, *31*(S3), 35-40. https://doi.org/10.1111/jai.12949

Kale, S., & Zabun, M. (2023). Çanakkale'deki Su Ürünleri Kooperatifleri. U. Özekinci, E. Ş. Çelik & Y. Şen (Eds.), *Çanakkale'de Su Ürünleri, Balıkçılık ve Denizcilik* (ss. 123-139). Nobel Bilimsel Eserler.

Kaya, H. B., & Can, M. F. (2022). Pandemi (COVID-19)'nin dünya su ürünleri sektörü üzerine etkilerinin SWOT analizi yaklaşımı ile değerlendirilmesi. *Marine and Life Sciences*, *4*(1), 35-45. https://doi.org/10.51756/marlife.1072565

Kawamura, T., Takami, H., Hayakawa, J., Won, N. -I., Muraoka, D., & Kurita, Y. (2014). Changes in Abalone and Sea Urchin Populations in Rocky Reef Ecosystems on the Sanriku Coast Damaged by the Massive Tsunami and Other Environmental Changes Associated with the Great East Japan Earthquake in 2011. *Global Environmental Research*, *18*, 47-56.

Kodama, K., Aramaki, T., & Horiguchi, T. (2018). Current status of the megabenthic community in coastal Fukushima Prefecture, Japan, in the wake of the Great East Japan Earthquake. *Marine Environmental Research*, *140*, 358-374. https://doi.org/10.1016/j.marenvres.2018.07.005

Mazlum, Y., Can, M. F., Yılmaz, A. B., Demirci, A., Gürlek, M., Şimşek, E., Şereflişan, M., & Uygur, N. (2019). Removal of abandoned and lost fishing equipment from various seabeds and habitats. *2. Ulusal Denizlerde İzleme ve Değerlendirme Sempozyumu Bildiri Özetleri Kitabı*, Turkey. pp. 173-174

McCowan, T. A., & Neubauer, P. (2018). *Paua biomass estimates and population monitoring in areas affected by the November 2016 Kaikoura earthquake*. New Zealand Fisheries Assessment Report 2018/54. 24 p.

SBB. (2023). *2023 Kahramanmaraş ve Hatay Depremleri Raporu*. Türkiye Cumhuriyeti Strateji ve Bütçe Başkanlığı (SBB) Deprem Sonrası Değerlendirme Raporu. 140s. Erişim tarihi: 12.12.2023 https://www.sbb.gov.tr/wp-content/uploads/2023/03/2023-Kahramanmaras-ve-Hatay-Depremleri-Raporu.pdf

Scholtens, B., & Oueghlissi, R. (2020). Shocks and fish stocks: The effect of disasters and policy announcements on listed fishing companies' market value. *Business Strategy and the Environment*, *29*, 3636-3668. https://doi.org/10.1002/bse.2601

Şimşek, E., Demirci, A., Akar, Ö., & Demirci, S. (2019). Distortions in Eastern Mediterranean deep-sea fishery due to geopolitical instability and fishery pressures. *Proceedings of the 2nd International Congress on Engineering and Life Sciences*, Turkey. pp. 670-672.

Takami H., Won, N. -I., & Kawamura, T. (2013). Impacts of the 2011 mega-earthquake and tsunami on abalone *Haliotis discus hannai* and sea urchin *Strongylocentrotus nudus* populations at Oshika Peninsula, Miyagi, Japan. *Fisheries Oceanography*, *22*(2), 113-120. https://doi.org/10.1111/fog.12008

Takami, H., Kawamura, T., Won, N. -I., Muraoka, D., Hayakawa, J., & Onitsuka, T. (2017). Effects of macroalgal expansion triggered by the 2011 earthquake and tsunami on recruitment density of juvenile abalone *Haliotis discus hannai* at Oshika Peninsula, northeastern Japan. *Fisheries Oceanography*, *26*(2), 141-154. https://doi.org/10.1111/fog.12191

Tweddle, D., & Corssley, R. (1990). Effects of an earthquake on demersal cichlid fishes of southern Lake Malawi. *Journal of Fish Biology*, *38*(2), 305-308. https://doi.org/10.1111/j.1095-8649.1991.tb03116.x

Yılmaz, A. B., Demirci, A., Akar, Ö., Kılıç, E., Uygur, N., Şimşek, E., Yanar, A., & Ayan, O. A. (2022). An assessment of sea surface and seabed macro plastic density in Northeastern Mediterranean Sea. *Pollution*, *8*(2), 543-552. https://doi.org/10.22059/poll.2021.331026.1192

Acta Nat. Sci. (2024) 5(1): 51-56
DOI: 10.61326/actanatsci.v5i1.6
e-ISSN: 2718-0638

Original Research Paper
info@actanatsci.com
www.actanatsci.com

ACTA NATURA ET SCIENTIA PRENSİP

Morphological Investigation of Larval Development in *Maylandia estherae* (Konings, 1995), an Endemic Cichlid Species of Lake Malawi

İhsan Çelik[1] • Pınar Çelik[1]✉

[1] Çanakkale Onsekiz Mart University, Faculty of Marine Sciences and Technology, Department of Aquaculture, 17020 Çanakkale, Türkiye, ihsanceliktr@gmail.com; pinarakaslan@yahoo.com

✉ Corresponding Author: pinarcelik@comu.edu.tr

Please cite this paper as follows:
Çelik, İ., & Çelik, P. (2024). Investigation of the Morphological Investigation of Larval Development in *Maylandia estherae* (Konings, 1995), an Endemic Cichlid Species of Lake Malawi. *Acta Natura et Scientia*, *5*(1), 51-56. https://doi.org/10.61326/actanatsci.v5i1.6

ARTICLE INFO

Article History
Received: 23.03.2024
Revised: 08.05.2024
Accepted: 15.05.2024
Available online: 22.05.2024

Keywords:
Maylandia estherae
Cichlidae
Lake Malawi
Larval development
Morphology

ABSTRACT

This study investigates the morphological aspects of larval development in *Maylandia estherae*, an endemic cichlid species from Lake Malawi. Larvae obtained from mature broodstock were sampled daily from hatching until the juvenile stage, and their morphological development was observed under a microscope. Important morphological features such as mouth opening, exogenous feeding, free swimming, yolk sac, and pigmentation were observed and photographed. The findings indicate that *M. estherae* larvae reached the juvenile stage within approximately 20-25 days. Throughout larval development, it was determined that total length and mouth gape gradually increased, the yolk sac was depleted within 12-13 days, and exogenous feeding commenced alongside the development of free-swimming ability. Additionally, significant changes in fin differentiation and pigmentation were observed in the larvae. The larval development duration and morphological characteristics of *M. estherae* were found to be similar to those of other Malawi cichlid species. The findings of this study contribute to the understanding of the ontogenetic processes of *M. estherae* and have implications for aquaculture practices. Furthermore, the results provide a significant contribution to the literature on the larval development of Malawi cichlids and offer insights for future research.

INTRODUCTION

Cichlid species from Lake Malawi have garnered significant attention in the aquarium industry and hold a substantial market share in recent years (Monticini, 2010). Lake Malawi, located in eastern Africa, is a unique ecosystem considered to be one of the world's largest and deepest lakes. The lake covers an area of approximately 29,600 km² and has a maximum depth exceeding 700 meters (Bootsma & Hecky, 2003). Lake Malawi is renowned for its extraordinary biodiversity, with cichlid fish constituting the vast majority of the lake's species (Snoeks, 2000). Research has revealed that Lake Malawi is home to approximately 1000 endemic cichlid species (Monticini, 2010; Konings, 2016). Many

cichlid species have become popular among aquarium hobbyists due to their color diversity, interesting behaviors, and reproductive strategies. One of the most sought-after and commercially valuable species in the aquarium industry is the *Maylandia estherae* (Konings, 2001).

M. estherae is a cichlid species that inhabits the rocky coastal regions of Lake Malawi (Ribbink et al., 1983). Like many other cichlid species, adult individuals engage in mouth brooding. Mouth brooding is defined as the process in which female individuals carry and protect fertilized eggs in their mouths, ensuring their development (Keenleyside, 1991). This reproductive strategy significantly increases the survival chances of larvae (Barlow, 2000). However, there are limited studies in the literature regarding the larval development of *M. estherae*.

Examining the larval development of fish is of great importance for understanding ontogenetic processes, elucidating reproductive biology, and conducting aquaculture studies (Kendall et al., 1984). The larval stage is a critical phase in the life cycle of fish, characterized by the fastest morphological, physiological, and behavioral changes (Fuiman & Werner, 2009). Therefore, a detailed examination of larval development provides valuable information about the biology, ecology, and evolutionary processes of species. Furthermore, knowledge of larval development is crucial for fish culture and stock management.

M. estherae, being an endemic species of Lake Malawi and its popularity in the aquarium industry, requires further research on its biology and ecology. This study aimed to morphologically investigate the larval development of *M. estherae*. The findings will contribute to understanding the ontogenetic processes of the species and support aquaculture studies. Additionally, the study results will significantly contribute to the knowledge of larval development in Malawi cichlids and provide insights for future research.

MATERIAL AND METHODS

Broodstock Selection and Aquarium Conditions

In this study, *M. estherae* individuals older than one year, having reached reproductive maturity and actively breeding, were selected as broodstock. The broodstock was housed in rectangular glass aquariums measuring 80×40×45 cm with a water capacity of approximately 125-130 liters and a water depth of 40 cm. Each aquarium was stocked with a total of 18 individuals, consisting of 3 males and 15 females. Aquarium aeration was provided only by sponge filters, and no decorative materials were added. Throughout the broodstock maintenance, spawning, and larval development processes, the water temperature was maintained at 29±0.5°C, and the pH was kept between 7.5-8. To ensure a stable water temperature, the room temperature was kept controlled, and no heaters were used in the aquariums.

Egg Collection and Incubation Process

The spawning process lasted for several hours, and fertilized eggs were mouth-brooded by female individuals. The swelling on the ventral side of egg-carrying females was used to detect the presence of eggs. To monitor larval development, eggs were collected from females identified as carrying eggs in their mouths one day after spawning and transferred to an artificial incubation unit. The eggs hatched approximately 4 days after fertilization, and the hatching day was considered as the 1st day of larval age.

Morphological Investigation of Larval Development

To examine larval development, eggs were collected from the mouths of broodstock 1-2 days after spawning was observed, and artificial incubation was performed. The morphological development of larvae was monitored daily from hatching to the juvenile stage. Sampled larvae were kept in an incubation unit at a constant room temperature and a water temperature of 29±0.5°C.

Morphological investigations were performed using an Olympus BX51 research microscope (Tokyo, Japan), and larvae were photographed using a Q Imaging Micropublisher 3.3 RTV camera (Canada) attached to the microscope. After the photography process was completed, live specimens were returned to the incubation unit. The day the larvae hatched from the eggs was defined as Day 1.

RESULTS

The morphological appearance of the larvae between day-1 and day-13 is presented in Figure 1.

1 DAH (1st day after hatching): On the first day, the larva has a yolk sac close to the size of the egg. The head part is distinct. The eye structure has formed, but the eye lenses are indistinct. Development is ongoing. The body is in the form of a primordial fin. The formation of the pelvic fin can be clearly observed. During this period, the larva is completely on the bottom. Occasional short-term tail movements are observed. It is mostly motionless throughout the day.

3 DAH: The yolk sac has slightly decreased in size compared to the first day. However, it still maintains a large volume. The head shape has become slightly more distinct. The eye appears to have a normal eye structure. The primordial fin has started to develop. During these days, the larva can exhibit more rapid tail movements. However, it still cannot exhibit free-swimming behavior.

4-5 DAH: During these days, the yolk sac has slightly decreased in size compared to the first 3 days. It is not small enough in volume for the larva to carry for free swimming. The larva can perform short-term swimming movements. However, it is still mostly on the bottom throughout the day. The mouth is open.

6-8 DAH: The yolk sac has further decreased in size. The larva's short-term free-swimming time has extended. The larva is capable of feeding from external sources. However, even if no food is given to the larva during this period, the yolk sac can provide the energy support for the larva to sustain its life. The dorsal and caudal fins have started to take shape. Pigmentation has intensified on the head and dorsal parts of the body. However, the overall body is still transparent in appearance.

9-11 DAH: The yolk sac has significantly decreased in size. However, it has not been completely consumed. The dorsal fin has taken shape. The anal fin has become distinct. Free-swimming movements have accelerated. During this period, external feeding should be initiated.

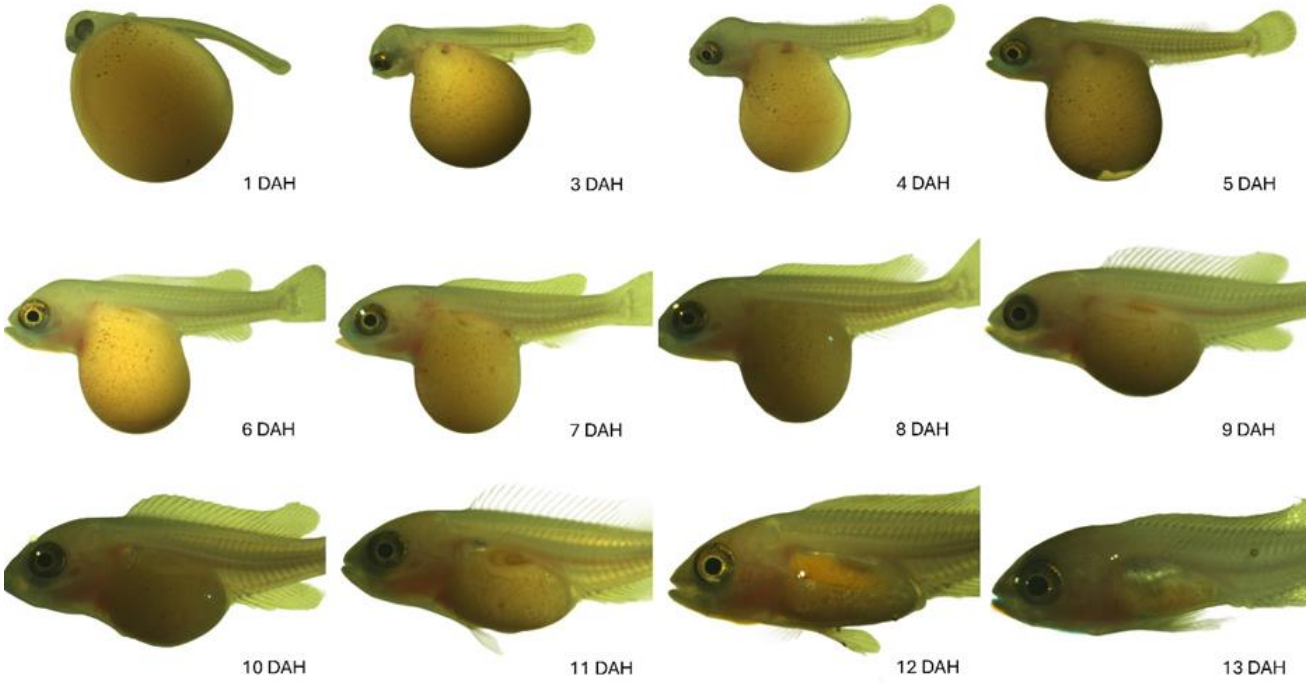

Figure 1. Morphological development of *M. estherae* larvae from the first to 13th days after hatching (DAH: Days After Hatching)

12-13 DAH: The yolk sac has been completely consumed. The shapes of the dorsal, anal, and caudal fins are much more distinct. Pigmentation has spread throughout the body. The transparent appearance of the body is transforming into a colored form. During these days, free-swimming movements have become much more rapid.

13-25 DAH: During this period, the body color of the larva becomes more distinct with each passing day. Gradually, the orange-reddish body color appearance of the parents is forming. Similarly, the rays and shapes of the dorsal, anal, and caudal fins are also transforming into the adult form. The behaviors of external feeding and swimming are like juvenile fish. During this period, the transition from the larval stage to the juvenile stage occurs. The timing of this transition process is directly related to water temperature.

DISCUSSION

In this study, the larval development of *M. estherae* was investigated morphologically and the findings were compared with other Malawi cichlid species. It was determined that *M. estherae* larvae exhibited rapid development from the first day after hatching and reached the juvenile stage in approximately 21 days. Similarly, it has been reported that larval development lasts 21-28 days in other Malawi cichlids such as *Labeotropheus fuelleborni, Pseudotropheus zebra, Cynotilapia afra, and Aulonocara stuartgranti* (Balon, 1977; Holden & Bruton, 1994; Msiska & Costa-Pierce, 1999).

The total lengths and mouth openings of *M. estherae* larvae gradually increased during larval development. Studies on other Malawi cichlids such as *Maylandia zebra, Metriaclima lombardoi, Labidochromis caeruleus* and *Pseudotropheus socolofi* have also reported that larval growth follows a similar course and total length reaches 10-12 mm in 20-25 days (Msiska & Costa-Pierce, 1999; Carleton et al., 2005; Fujimura & Okada, 2007).

Similar results are observed when the larval development of other cichlid species outside Lake Malawi is examined. For instance, it has been reported that larval development lasts approximately 20 days in *Amphilophus citrinellus*, a species living in Central America, and larvae reach an average length of 12 mm at the end of this period (Balon, 1977). Similarly, it has been reported that larval development lasts 25-30 days in *Cichlasoma dimerus*, a species living in South America, and larvae reach a length of 15-20 mm (Meijide & Guerrero, 2000). It has been determined that the larval development duration and growth rates of commercially important cichlid species living in other African lakes, such as *Oreochromis niloticus, Sarotherodon galilaeus,* and *Tilapia zillii*, are similar to those of Malawi cichlids (Fujimura & Okada, 2007).

The morphological changes observed in *M. estherae* larvae are similar to those of other Malawi cichlids. In the first days of larval development, it was observed that larvae carried a yolk sac and their free-swimming ability had not yet developed. It was determined that the yolk sac was completely depleted between the 5th and 7th days and larvae started to feed externally. Similar findings have been reported in *Labeotropheus trewavasae, Metriaclima callainos, Dimidiochromis compressiceps* and *Copadichromis borleyi* (Balon, 1977; Msiska & Costa-Pierce, 1999; Konings, 2001). It is known that the yolk sac is an important food source in the early stages of larval development in other cichlid species and larvae start to feed externally with the development of free-swimming ability. For example, it has been reported that the yolk sac is depleted in 3-4 days and larvae start to feed externally from the 5th day *in Apistogramma cacatuoides*, a species living in South America (Pandolfi et al., 2009). Similarly, it has been reported that the yolk sac is depleted in 6-7 days and larvae start to feed externally from the 8th day in *Amphilophus rostratus*, a species living in Central America (Molina, 2011).

During larval development, important morphological changes such as fin differentiation and pigmentation were observed in *M. estherae* larvae. In the first days after hatching, the caudal fin of larvae was homocercal, while it transformed into a heterocercal structure in the later days of development. Similarly, it was determined that the dorsal and anal fins gradually differentiated during larval development. Pigmentation on the body started to become evident from approximately the 10th day of development and continued to increase until the 21st

day. These findings are consistent with the larval development characteristics observed in other Malawi cichlids, especially in *Pseudotropheus elegans*, *Melanochromis auratus* and *Petrotilapia nigra* (Msiska & Costa-Pierce, 1999; Konings, 2001; Fujimura & Okada, 2007). It is known that fin differentiation and pigmentation are important morphological changes during the larval development process in other cichlid species. For example, it has been reported that during larval development in *Geophagus brasiliensis*, a species living in South America, the caudal fin transforms from a homocercal to a heterocercal structure, dorsal and anal fins differentiate, and body pigmentation increases (Perini et al., 2010). Similarly, it has been reported that similar morphological changes are observed during larval development in *Etroplus suratensis*, a species living in Asia.

CONCLUSION

The larval development of *M. estherae* was examined morphologically and the findings were compared with other Malawi cichlids. It was determined that *M. estherae* larvae show similarities with other Malawi cichlids, especially with species belonging to the genera *Labeotropheus*, *Pseudotropheus*, *Melanochromis*, and *Petrotilapia*, in terms of development duration, growth rate, and morphological characteristics. In addition, similar results were obtained when examining the larval development of other cichlid species outside Lake Malawi. It was observed that the larval development duration varies between 20-30 days among species. Growth rates are similar across the examined species. The yolk sac is depleted in early stages, and external feeding starts with the development of free-swimming ability. Additionally, fin differentiation and pigmentation are important morphological changes during the larval development process. However, it is thought that larval development may show small differences between species and these differences may be related to ecological and evolutionary processes. It is recommended that future studies investigate the causes and consequences of similarities and differences in larval development of different cichlid species in more detail.

ACKNOWLEDGEMENTS

No support or grants were provided by individuals or institutions for the research.

Compliance with Ethical Standards

Authors' Contributions

İÇ: Conceptualization, Data curation, Formal Analysis, Writing – original draft.

PÇ: Conceptualization, Investigation, Methodology, Writing – review & editing.

All authors read and approved the final manuscript.

Conflict of Interest

The authors declare that there is no conflict of interest.

Ethical Approval

For this type of study, formal consent is not required.

Funding

Not applicable.

Data Availability

The data that support the findings of this study are available from the corresponding author upon reasonable request.

REFERENCES

Balon, E. K. (1977). Early ontogeny of Labeotropheus Ahl, 1927 (Mbuna, Cichlidae, Lake Malawi), with a discussion on advanced protective styles in fish reproduction and development. *Environmental Biology of Fishes*, *2*(2), 147-176. https://doi.org/10.1007/BF00005370

Barlow, G. W. (2000). *The cichlid fishes: nature's grand experiment in evolution*. Perseus publishing.

Bootsma, H. A., & Hecky, R. E. (2003). Conservation of the African Great Lakes: A limnological perspective. *Conservation Biology*, *17*(3), 644-656. https://doi.org/10.1046/j.1523-1739.2003.01457.x

Carleton, K. L., Hárosi, F. I., & Kocher, T. D. (2005). Visual pigments of African cichlid fishes: evidence for ultraviolet vision from microspectrophotometry and DNA sequences. *Vision Research*, *45*(1), 75-87. https://doi.org/10.1016/j.visres.2004.07.023

Fuiman, L. A., & Werner, R. G. (Eds.). (2009). *Fishery science: the unique contributions of early life stages*. John Wiley & Sons.

Fujimura, K., & Okada, N. (2007). Development of the embryo, larva and early juvenile of Nile tilapia *Oreochromis niloticus* (Pisces: Cichlidae). Developmental staging system. *Development, Growth & Differentiation*, *49*(4), 301-324. https://doi.org/10.1111/j.1440-169X.2007.00926.x

Holden, K. K., & Bruton, M. N. (1994). The early ontogeny of the southern mouthbrooder, *Pseudocrenilabrus philander* (Pisces, Cichlidae). *Environmental Biology of Fishes*, *41*(1), 311-329. https://doi.org/10.1007/BF02197853

Keenleyside, M. H. (1991). *Cichlid fishes: behaviour, ecology and evolution* (Volume 2). Springer Science & Business Media.

Kendall, A. W., Ahlstrom, E. H., & Moser, H. G. (1984). Early life history stages of fishes and their characters. *Ontogeny and Systematics of Fishes*, *1*, 11-22.

Konings, A. (2001). *Malawi cichlids in their natural habitat*. Cichlid Press.

Konings, A. (2016). *Malawi cichlids in their natural habitat*. Cichlid Press.

Meijide, F. J., & Guerrero, G. A. (2000). Embryonic and larval development of a substrate-brooding cichlid *Cichlasoma dimerus* (Heckel, 1840) under laboratory conditions. *Journal of Zoology*, *252*(4), 481-493. https://doi.org/10.1111/j.1469-7998.2000.tb01231.x

Molina, W. F. (2011). Chromosomal changes and stasis in marine fish groups. In E. Pisano (Ed.), *Fish Cytogenetics*, (pp. 69-110). CRC Press.

Monticini, P. (2010). *The ornamental fish trade. Production and commerce of ornamental fish: technical-managerial and legislative aspects*. FAO.

Msiska, O. V., & Costa-Pierce, B. A. (1999). Growth performance and survival of *Oreochromis lidole*, *Oreochromis squamipinnis* and *Oreochromis shiranus* in fertilized earthen ponds. *Aquaculture Research*, *30*(3), 179-186. https://doi.org/10.1046/j.1365-2109.1999.00315.x

Pandolfi, M., Cánepa, M. M., Meijide, F. J., Alonso, F., Rey Vázquez, G., Maggese, M. C., & Vissio, P. G. (2009). Studies on the reproductive and developmental biology of *Cichlasoma dimerus* (Percifomes, Cichlidae). *Biocell*, *33*(1), 1-18.

Perini, V. R., Sato, Y., Rizzo, E., & Bazzoli, N. (2010). Biology of eggs, embryos and larvae of *Rhinelepis aspera* (Spix & Agassiz, 1829) (Pisces: Siluriformes). *Zygote*, *18*(2), 159-171. https://doi.org/10.1017/S0967199409990165

Ribbink, A. J., Marsh, B. A., Marsh, A. C., Ribbink, A. C., & Sharp, B. J. (1983). A preliminary survey of the cichlid fishes of rocky habitats in Lake Malawi. *South African Journal of Zoology*, *18*(3), 149-310. https://doi.org/10.1080/02541858.1983.11447831

Snoeks, J. (2000). How well known is the ichthyodiversity of the large East African lakes?. *Advances in Ecological Research*, *31*, 17-38. https://doi.org/10.1016/S0065-2504(00)31005-4

Acta Nat. Sci. (2024) 5(1): 57-68
DOI: 10.61326/actanatsci.v5i1.7
e-ISSN: 2718-0638

Original Research Paper
info@actanatsci.com
www.actanatsci.com

ACTA NATURA ET SCIENTIA PRENSİP

Investigation of the Chemical Composition of the Shell Structure of *Mytilus galloprovincialis* Mussel From Kefken, Türkiye

Bayram Kızılkaya[1]✉ • Harun Yıldız[1] • Sefa Acarlı[1] • Pervin Vural[2]

[1] Çanakkale Onsekiz Mart University, Faculty of Marine Sciences and Technology, Department of Aquaculture, Çanakkale, Türkiye, bayram342001@yahoo.com; harunyildiz@comu.edu.tr; sefaacarli@comu.edu.tr
[2] Çanakkale Onsekiz Mart University, Bayramiç Vocational School, Department of Aquaculture, 17700, Çanakkale, Türkiye, pervinvural@comu.edu.tr

✉ Corresponding Author: bayram342001@yahoo.com

Please cite this paper as follows:
Kızılkaya, B., Yıldız, H., Acarlı, S., & Vural, P. (2024). Investigation of the Chemical Composition of the Shell Structure of *Mytilus galloprovincialis* Mussel From Kefken, Türkiye. *Acta Natura et Scientia*, *5*(1), 57-68. https://doi.org/10.61326/actanatsci.v5i1.7

ARTICLE INFO

Article History
Received: 27.02.2024
Revised: 04.05.2024
Accepted: 15.05.2024
Available online: 22.05.2024

Keywords:
Mytilus galloprovincialis
Bivalve shells
Calcium carbonate
The zero charge points

ABSTRACT

In this study, the chemical composition of *Mytilus galloprovincialis* shells was examined. As known, the main component of shell composition in bivalves is calcium carbonate, which constitutes approximately 94% of the shell. The zero charge points (Pzc) of the shells were determined in the study. The Pzc value indicates the surface charge state of the shells. The Pzc value of the shells was determined to be 8.39. The Pzc value of the shells provides important information for the characterization and potential applications of the shells. SEM images and EDS analyzes of the shells were made. According to the EDS results, calcium, carbon, and oxygen atoms belonging to the main structure of calcium carbonate ($CaCO_3$) appeared in the highest proportions. FT-IR analysis was supported to the calcium carbonate ($CaCO_3$) structure. XRD analyses were performed within the scope of the study, and it was determined that the shell structures mainly consist of a mixture of calcium carbonate and aragonite. In conclusion, this study on the chemical composition of *M. galloprovincialis* shells provides a detailed analysis of shell composition. The analyses conducted provide important information about the chemical composition, structural properties, and potential applications of the shells. This study contributes to research on the biological and chemical properties of marine organisms and is considered to form the basis for future studies.

INTRODUCTION

Mollusk shells (bivalves, gastropods, and monoplacophorans) evolved during the earliest Cambrian period (starting around 541 million years ago) to protect their soft tissues from abiotic and biotic stresses. These shells belong to the Mollusca class, which is a diverse group of invertebrates found worldwide and forms an important part of marine life. Mollusk shells not only protect the soft tissues of mollusks from external factors but also serve as food sources and help them defend against predators (Qian

& Bengtson, 1989; Qian, 1999; Li et al., 2017). All mussels (Mollusca: Bivalvia) share unique morphological features, namely the presence of two symmetric calcareous valves that are connected by a calcified structure, forming their shells. This underscores the significance of these organisms as important components of the natural world. Mussels play a critical role in maintaining the ecological balance of oceans, seas, and even freshwater sources. Moreover, the economic importance of mussels cannot be overlooked. Therefore, research on the morphological features and shell structure of mussels holds great importance both scientifically and economically (Bogan, 2007; Graf, 2013; Chakraborty et al., 2020). Mollusk shells evolution is a result of the adaptation process to various environmental pressures during the early stages of life. These shells help protect the internal organs of the organism, aiding in their defense against predators and other threats (Li et al., 2017). Mussels belong to the subclass Bivalvia of the mollusk class Mollusca, which are recognized by their shells. These organisms are protected by two symmetric calcareous valves that make up their shells. These shells not only protect the bodies of mussels from external factors but also provide them with the ability to move and feed. Additionally, mussel shells help balance the chemical composition of the surrounding water, thus contributing to the healthy continuation of the ecosystem (Chakraborty et al., 2020). In bivalves, shells represent a significant portion, typically ranging from 56-61% by weight. The main component of shell composition is calcium carbonate (approximately 94%). Shells serve as the hard outer structures used by marine organisms for protection and structural support. They are produced and utilized by many organisms such as bivalves, gastropods, and other marine invertebrates. These shells are formed by the aggregation of calcium carbonate crystals and are usually covered by a thin organic membrane (Hamester et al., 2012; Ituen, 2015; Mititelu et al., 2022). The main component of shells is typically calcium carbonate, but small inorganic trace elements are also present in different bivalve species. These trace elements can influence the physical properties of shells and play an important role in the life of shelled organisms (Chakraborty et al., 2020). Shells dominant chemical component, calcium carbonate, is typically found in the form of calcite or aragonite crystals. These crystals provide the hardness and durability of the shell. However, other trace elements present in the shells also play a significant role. For example, elements like magnesium, manganese, iron, copper, and zinc can contribute to the coloration and pattern formation of shells. Additionally, these elements can enhance the durability of the shells and help shelled organisms defend against predators (Carroll & Romanek, 2008; Spann et al., 2010; Nakamura et al., 2014; Agbaje et al., 2017, 2018a, 2018b; Chakraborty et al., 2020). This study was conducted to obtain information about the chemical structure and contents of *Mytilus galloprovincialis* mussels shells. Mussel shells consist of a combination of calcium carbonate and organic matrix, and this structure provides the strength and durability of mussel shells. The study determined how the chemical composition of mussel shells is affected by environmental factors such as seawater temperature, pH level and nutrients. These findings may help us understand how mussel shells respond to environmental changes.

MATERIAL AND METHODS

Sampling Stations and Time

In this study, 100 samples of *M.galloprovincialis* were obtained from the Kefken station. The obtained shells were first passed through pure water. After that, these shells were homogenized by grinding.

Determination of Zero Charge Point (P_{ZC}) in Shells

The zero point of charge (P_{ZC}) was determined based on pH measurements of homogenized and ground shell samples (Mahmood et al., 2011). To determine the pH_{PZC}, 100 ml of 0.01 M KNO_3 solutions were first prepared in an Erlenmeyer flask. The initial pH values (pH_I) of these solutions were adjusted between pH 4 and 10 using 0.1 M HCl and NaOH. Then, the modified samples were added to these solutions. Subsequently, the solution was stirred at a constant temperature using a magnetic stirrer for 48 hours. After 48 hours, the final pH (pH_F) of the

solution was measured and recorded. The difference between the initial pH and final pH ($\Delta pH = pH_I - pH_F$) was plotted against the initial pH (pH_I). The point at which the curve intersects the x-axis was determined as the P_{ZC}.

Chemical Structure Analyzes in Shells

SEM-EDS (Scanning Electron Microscope-Energy Dispersive X-Ray Spectroscopy, model JEOL JSM-7100F) analyses were conducted at the Central Laboratory of Çanakkale Onsekiz Mart University. The device has a magnification capacity ranging from ×40 to 300,000 and an accelerating voltage between 0.2 and 30 kV. To enhance the conductivity properties of the samples, a vacuum of 8x10-1mbar/Pa was first applied using a Quorum coating device, followed by a gold-palladium (80-20%) coating process with a voltage of 10 mA (The coating thickness is approximately 2-3 nm). SEM images were captured using a voltage of kV (the applied voltage is indicated in the lower right corner of the images). Images in the SEM device were acquired using secondary electrons. Surface characteristics of the ground shells were examined using a Scanning Electron Microscope (SEM), and differences were identified. Additionally, EDS analysis of the shells was performed to analyze carbon, oxygen, nitrogen, calcium, and sulfur content.

FT-IR spectra were measured in the range of 650-4000 cm^{-1} using the ATR technique on a Perkin-Elmer Spectrum One device. FT-IR analyses of ground and homogenized *M. galloprovincialis* shells were performed to determine the chemical bonding properties. Thus, changes in chemical bonding properties and bond strengths of shell structures were investigated concerning species, time, and area dependencies.

Additionally, XRD analyses were conducted to obtain information about the chemical structures and compositions. The analyses were performed using the PANalytical Empyrean X-RD device located at the Central Laboratory of Çanakkale Onsekiz Mart University.

RESULTS AND DISCUSSION

M galloprovincialis is an economically important species as it is commercially cultivated and consumed in the seafood industry. They are also known for their filter-feeding behavior in ecosystems, where they filter nutrients from the water, contributing to the improvement of water quality. These mussels are typically identified by their blue-purple colored shells and usually measure between 5 to 8 cm in length. Their hard shells provide protection against waves and predators. Additionally, it is important to recognize the ecological impact of this species as they can regulate water quality through their filter-feeding behavior, thereby influencing ecological balance (Yildiz & Berber, 2010; Yıldız et al., 2013; Acarli et al., 2011, 2015; Acarlı et al., 2018, 2023).

The zero point of charge (P_{ZC}) is a parameter in physicochemistry related to the adsorption phenomenon, defining the condition when the electrical charge on a surface is zero. In other words, P_{ZC} is typically the pH value at which the net electrical charge on the surface of a solid immersed in an electrolyte solution is zero. This concept not only defines a specific condition where the surface charge is zero but is also closely associated with adsorption phenomena. P_{ZC} is generally defined as the pH value at which the net electrical charge on the surface of a solid in contact with an electrolyte is zero (Somasundaran & Agar, 1967; Sverjensky, 1994; Babić et al., 1999; Hou et al., 2001; Kosmulski, 2002; Fiol & Villaescusa, 2008; Mahmood et al., 2011). To understand the meaning of this definition, it is important to first grasp what adsorption is. Adsorption is the process by which one substance is held onto the surface of another substance. This process typically occurs between solid and liquid or gas phases, and the electrical charge on the surface plays a significant role in the occurrence of adsorption. In many fields where adsorption phenomena are studied, determining and understanding the P_{ZC} is crucial (Fiol & Villaescusa, 2008; Mahmood et al., 2011). This concept is used to determine at which pH values a surface is electrically neutral, which is a critical step in understanding how adsorption occurs. The determination of P_{ZC} is typically carried out

experimentally, and different pH values can be obtained for different surfaces. This can vary depending on the chemical composition, structure, and other properties of the surface. Therefore, determining and understanding PZC is a fundamental step in understanding the adsorption properties of a surface. Understanding PZC is important not only in physical chemistry but also in various industrial applications. Particularly, in materials science, colloid chemistry, environmental engineering, and other fields where surface chemistry and adsorption phenomena are studied, determining and understanding PZC plays a critical role in the design and application of materials. Consequently, PZC is an important parameter in physical chemistry related to adsorption phenomena, defining the condition when the electrical charge on a surface is zero. PZC is typically the pH value at which the net electrical charge on a surface immersed in an electrolyte solution is zero.

PZC of *M. galloprovincialis* shell particles was determined based on the surface characteristics. The PZC value of the shells was found to be 8.39 (Figure 1). Depending on the surface characteristics of the shells, the PZC value can vary according to the ability of groups on the molecule to gain or lose hydrogen or electrons. When the ambient pH is lower than the PZC value, the system is said to be "below PZC." In this case, acidic water attracts more protons from hydroxyl groups, resulting in a positively charged adsorbent surface, and negative ions are adsorbed. Conversely, when the pH is greater than the PZC value, the system is said to be "above PZC," and the surface becomes negatively charged, with positively charged groups adsorbing. Therefore, it was determined that in environments where the pH of the shells is greater than 8.0, positively charged shells will be significant adsorbents for the adsorption of negatively charged groups, or anionic species. Figure 1 shows the curves of initial pH (pH_I) versus ΔpH for the shells. The experimental PZC values obtained at the end of the study are also shown along with the values obtained by linear regression.

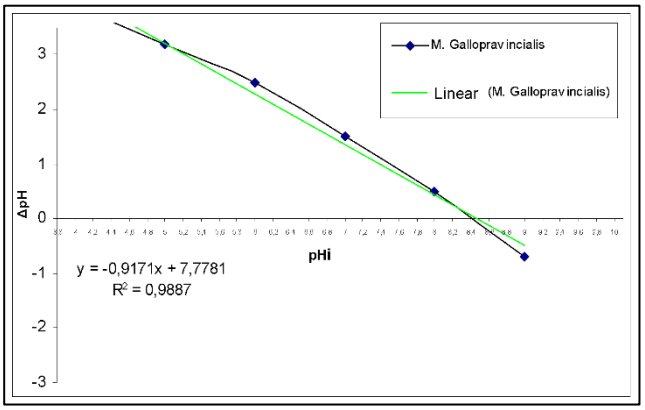

Figure 1. Zero charge point of *Mytilus galloprovincialis* shell particles

SEM-EDS is a microscopy technique used for surface imaging and elemental analysis. This technique allows the electron beam to scan the sample surface to visualize surface topography and simultaneously determine the chemical composition of elements in the sample. SEM-EDS is a widely used analysis method in many industrial and scientific applications. The broad application of SEM-EDS stems from its effectiveness in examining the surface properties and chemical composition of samples. Another significant feature of SEM-EDS is its capability for high-resolution surface imaging. This allows for the examination of surface morphology and observation of microstructures on the surface of the sample. Additionally, regional elemental analysis can be performed to obtain information about the chemical composition of the sample surface, providing detailed insights into the surface properties of the sample. The SEM images of the shells are shown in Figure 2. The SEM image illustrates the microscopic structure of the ground mussel shell. As can be seen from the image, the main component of the mussel shell consists of calcium carbonate crystals. The majority of the image is composed of irregularly shaped and sized plates of calcium carbonate ($CaCO_3$) crystals, which are the main component of the mussel shell. The small particles on the plates may consist of organic matter or other elements. This image provides valuable information about the microscopic structure of the mussel shell, which can be utilized to understand its mechanical properties, chemical composition, and biological activity.

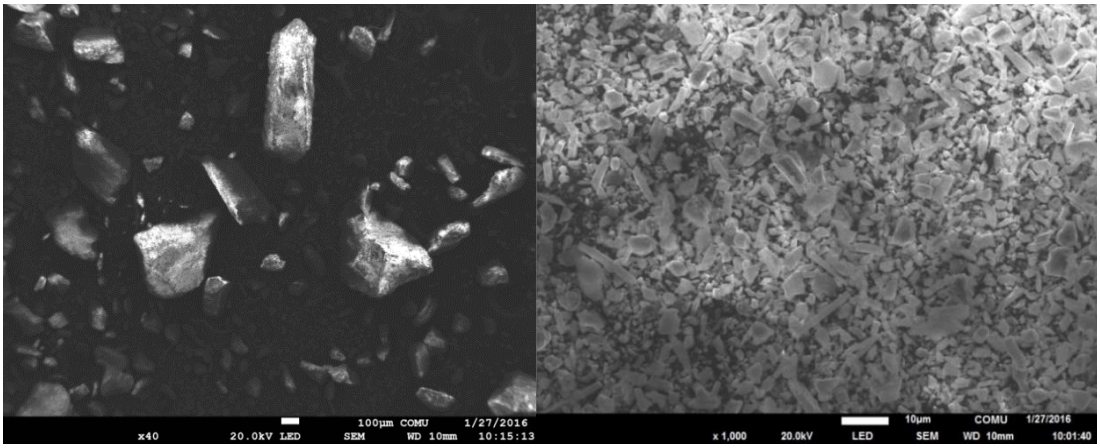

Figure 2. SEM images of *Mytilus galloprovincialis* shells

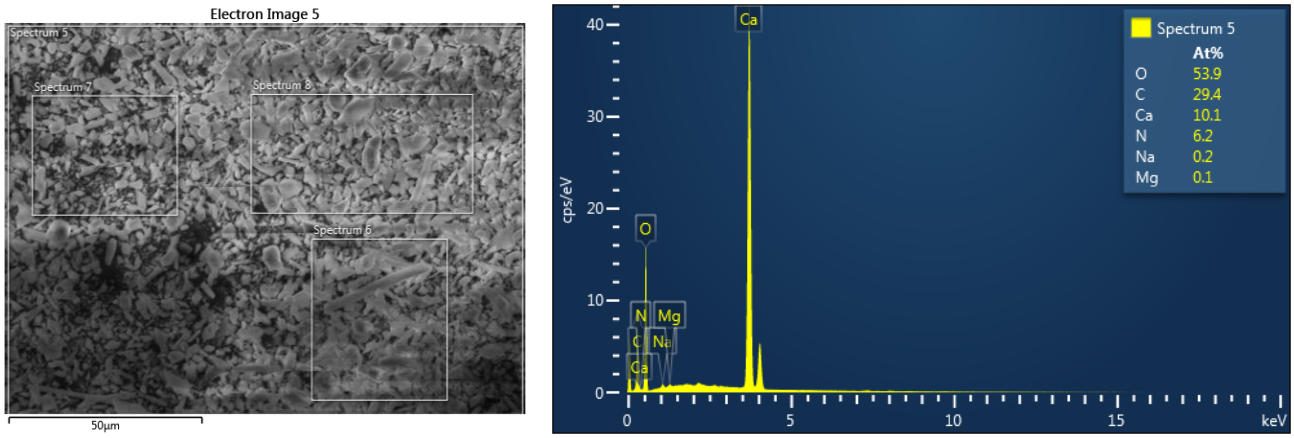

Figure 3. EDS spectrum of *Mytilus galloprovincialis* shell

Figure 3 shows the EDS analysis result of the *M. galloprovincialis* shell. EDS (Energy Dispersive X-ray Spectroscopy) analysis is a technique used to determine the chemical composition of a material. In the spectrum, elements such as C (Carbon), O (Oxygen), Ca (Calcium), Mg (Magnesium), Na (Sodium), and N (Nitrogen) are evident. In the spectrum, it can be observed that calcium (Ca), carbon (C), and oxygen (O) are the predominant and fundamental elements, which constitute the main structural elements of $CaCO_3$. Carbon indicates the presence of calcium carbonate, the main component of the mussel, as well as organic matter. Mussel shells contain proteins and other organic molecules. Oxygen originates from the oxygen atoms in calcium carbonate, the compound present in the mussel shell. Calcium, on the other hand, comes from calcium carbonate, which is the main component of the mussel shell. Magnesium is thought to come from magnesium carbonate, which is present in small amounts in the mussel shell. Sodium can be attributed to sodium chloride in seawater. Nitrogen is generally a significant component of proteins and other organic molecules. Therefore, the presence of nitrogen in the mussel shell indicates the presence of proteins or other organic molecules. It is observed that nitrogen is present in the shell at a rate of 6.8 %. The relatively high concentration of nitrogen compared to other elements in the mussel shell indicates that the shell is rich in proteins or other organic molecules. Possible sources of nitrogen in the mussel shell include proteins from the mussel's diet, proteins secreted by the mussel itself, and bacteria or other microorganisms adhering to the mussel shell. This spectrum provides valuable information about the chemical composition of the mussel shell. This information can be used to determine whether the mussel shell is pure, what elements it contains, and what impurities it may contain. The source of trace elements in shells generally comes from seawater. Seawater contains various minerals and elements, which shell-bearing organisms can utilize in the

formation of their shells. The presence of these elements in shells can affect their chemical composition and physical properties. For example, the integration of magnesium into calcium carbonate crystals can make the shells more durable and flexible. The importance of the elements obtained from seawater by shell-bearing organisms in forming their shells is significant. Seawater contains calcium, magnesium, carbonate, phosphate, and other minerals. These elements are the materials shell-bearing organisms use to form their shells. Especially calcium carbonate is the main component of shell-bearing organisms shells, and shells are formed with calcium and carbonate ions taken from seawater. The chemical composition of shells can vary depending on the ratio of the elements they contain. For example, calcium carbonate crystals can become more durable and flexible with the integration of magnesium. This allows the shells of shell-bearing organisms to be more resistant to environmental impacts. Additionally, it is believed that other elements can also influence the color and texture properties of the shells (Carroll & Romanek, 2008; Nakamura et al., 2014; Chakraborty et al., 2020). The elemental content of the shells of shell-bearing organisms can carry traces of geological and climatic changes. For example, changes in the elemental ratios in seawater can lead to differences in the formation and composition of shells. Therefore, the shells of shell-bearing organisms can be an important source for understanding the history of geological and climatic changes. The source of elements in shells and the processes of shell formation are important research topics for scientists. Understanding how elements taken from seawater are used in shell formation provides information about the evolutionary processes of shell-bearing organisms. Additionally, the elemental content of shells can serve as an indicator for understanding the effects of environmental changes (Carroll & Romanek, 2008; Nakamura et al., 2014; Agbaje et al., 2017, 2018a; Chakraborty et al., 2020). Consequently, trace elements in shells generally originate from seawater and play a significant role in the formation of shell-bearing organisms shells. The presence of elements in shells can affect their chemical composition and physical properties. This situation can provide important insights into the evolutionary processes of shell-bearing organisms and their adaptation to environmental changes. This topic is an important area of research for scientists, and the shells of shell-bearing organisms can serve as a valuable resource for understanding the history of geological and climatic changes.

Fourier Transform Infrared Spectroscopy (FT-IR) is a spectroscopic technique used to determine the bond structures of molecules. Infrared light is directed onto a sample and absorbed by the molecules of the sample. The amount of absorbed light depends on the wavelength of the light. By measuring the absorption of light at different wavelengths, information about the chemical composition of a sample can be obtained. It is a highly effective tool for determining the chemical bonds, functional groups, and molecular structures of the substance under investigation. This analysis method is widely used in various industries, biological research, drug development processes, food analysis, and materials science. FT-IR spectroscopy is a powerful and versatile technique because it provides information at the molecular level. Therefore, the aim of the conducted (FT-IR) analysis is to determine the structure of the main component of the shells. Below, in Figure 4A, the FT-IR spectra of Aragonite, namely $CaCO_3$ mineral crystal, from spectral data characterized within the RRUFF Project are provided (Lafuente et al., 2015). In the spectrum in Figure 4A, the peaks at 1420 cm^{-1} represent the C-O stretching, at 870 cm^{-1} represent the C-O stretching, and at 710 cm^{-1} represent the C-O stretching of the carbonate molecule. The FT-IR spectra of *M. galloprovincialis* shells are provided in Figure 4B. When examining the FT-IR data of the shells, it was determined that there are vibration bands of CO_3^{-2} at 1420 cm^{-1}. The moderately intense in-plane bending band at 710 cm^{-1} emerges as an in-plane bending band (V4) of the carbonate ($-CO_3^{-2}$) molecule, which constitutes the shell's main chemical structure. This band is attributed to carbonate, clearly indicating that the main chemical structure of the shells is carbonate. Generally, in the spectrum of the sample, the peaks are observed at 1420 cm^{-1}: C-O stretching (carbonate), 870 cm^{-1}: C-O stretching (carbonate), 710 cm^{-1}: C-O stretching (carbonate), 3400 cm^{-1}: N-H stretching

(amides), 1650 cm^{-1}: C=O stretching (amides), and 1540 cm^{-1}: N-H bending (amides). Based on the peak positions in the spectrum, we can conclude that the mussel shell consists of calcium carbonate and also contains proteins. This spectrum provides valuable information about the chemical composition of calcium carbonate structure. This information can be used to determine whether the calcium carbonate structure is pure, what crystal form it is in, and what impurities it contains. The basic Raman peaks of carbonate (-CO_3^{-2}) that constitute the main structure of *M. galloprovincialis* shells in this study and aragonite, analyzed by FT-IR under the RRUFF Project, complement each other.

The shells of *M. galloprovincialis* were analyzed using X-Ray Diffraction (XRD) technique and compared with the crystal structures of calcium carbonate and aragonite ($CaCO_3$). This analysis, which examines the atomic and molecular structures of the shells, relies on the characteristic pattern of X-rays scattered by the crystalline phase of the structure, which is unique to each crystal. The crystal structures of calcium carbonate that make up these shells are formed through biomineralization processes influenced by various factors such as species characteristics, growth conditions, and the environment. To understand the changes in the molecular structures of shells depending on the formation of crystals, it is necessary to develop these techniques. Therefore, it is important to understand how the interaction between organic tissue and mineral phase is carried out within tissues (Pokroy et al., 2007). In this study, calcium carbonate and aragonite, which are composed of the same chemical molecules but have different crystal structures, were used as references. Aragonite, with a crystal lattice structure different from calcite (calcium carbonate), is actually a carbonate mineral that typically forms biologically in marine or freshwater environments. Therefore, the crystal structures of the shells within the scope of the study were examined to investigate which structure is more suitable for the shells (Figure 5). Figure 5A shows the XRD spectrum of a mixture of calcite (C) and aragonite (A) produced by the US Geological Survey (USGS, 2001). This spectrum is suitable data for comparing the XRD results of the shells. Calcite and aragonite are two different crystal forms of calcium carbonate ($CaCO_3$) mineral. Both belong to the trigonal crystal system but have different geometric structures. The most intense peak in the image is the calcite peak. Each peak in the image corresponds to the diffraction of X-rays by a specific atomic plane in the crystal structure of a mineral. The intensity of the peak indicates the number of diffracted X-rays. The angle of the peak indicates the angle of the diffracted X-rays. Because calcite and aragonite have different crystal structures, they have different peak positions. From this image, we can see how the chemical composition and crystal structure of a mineral can be determined using X-ray diffraction. Upon examining the spectra in Figure 5A, it was determined that the shell structures of *M. galloprovincialis* predominantly consist of calcium carbonate and aragonite. The blue part of the spectrum represents the samples, the red part represents calcite, and the green part represents aragonite. Thus, it was easier to identify the calcium and aragonite structures in the composition. X-ray diffraction is a powerful tool used to identify minerals and examine the structure of crystals.

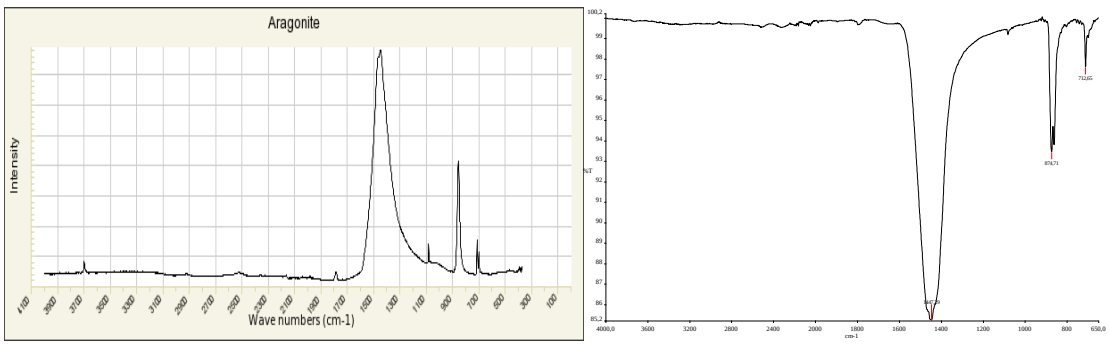

Figure 4. FT-IR spectra of **A)** Aragonite ($CaCO_3$) mineral crystal characterized within the scope of the RRUFF Project (Lafuente et al., 2015) and **B)** *M. galloprovincialis* shells

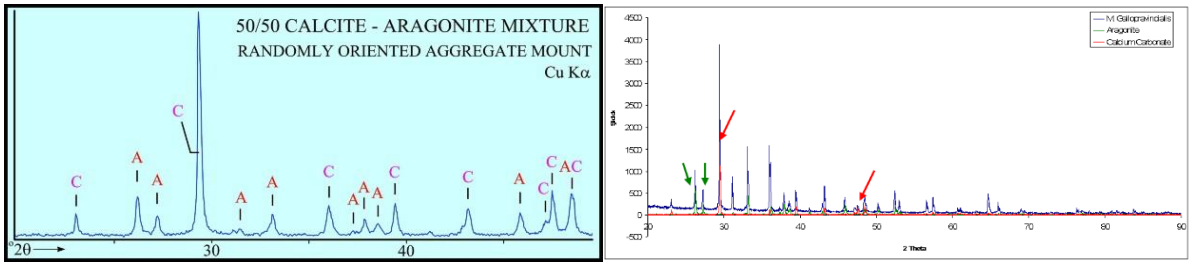

Figure 5. A) X-RD spectrum of the mixture consisting of calcite and aragonite given by the US Geological Survey (USGS) (USGS, 2001): Aragonite (*A*), Calcite (*C*); B) X-Ray Diffraction (XRD) spectrum of *M. galloprovincialis* shell

The shells of shelled organisms are structures formed by the accumulation of minerals such as calcium carbonate. These shells not only protect the organism's body but are also influenced by environmental factors. It is known that trace elements in the shells are affected by environmental factors. For example, the temperature, acidity, and salinity level of seawater can affect the chemical composition and trace element content of the shells. Therefore, environmental changes can affect the composition and properties of shells in shelled organisms (Carroll & Romanek, 2008; Spann et al., 2010; Nakamura et al., 2014; Agbaje et al., 2017, 2018a; Chakraborty et al., 2020). The temperature, acidity, and salinity level of seawater can directly affect the life of shelled organisms. These factors can also influence the growth and composition of their shells. For example, as the acidity of seawater increases, the utilization of calcium carbonate in the formation of shells by shelled organisms may decrease, resulting in thinner and more fragile shells. Similarly, the salinity level of seawater can also affect the composition of the shells. High salinity levels can alter the mineral content of the shells and reduce their durability. The influence of environmental factors on the shells of shelled organisms can also affect the trace element content. Trace elements in seawater play a significant role in the composition of shells. For instance, elements like iron, magnesium, and strontium can be influential in the formation of shells. The levels of these elements can vary depending on environmental changes, thereby impacting the composition of the shells. The effect of environmental factors on the trace elements in the shells of shelled organisms has been a focus of scientific research. Researchers examine the chemical composition of seawater and the effects of environmental changes on the composition of shells, uncovering new findings in this area. The results of these studies can help us understand the life and evolutionary processes of shelled organisms (Spann et al., 2010; Nakamura et al., 2014; Agbaje et al., 2017, 2018b; Chakraborty et al., 2020). Consequently, the shells of shelled organisms are influenced by environmental factors. The temperature, acidity, and salinity level of seawater can affect the chemical composition and trace element content of the shells. Therefore, environmental changes can impact the composition and properties of the shells of shelled organisms. This topic continues to be the focus of scientific research and can have significant implications for the evolutionary processes of shelled organisms.

CONCLUSION

Bivalves are a group of shelled organisms that inhabit both marine and freshwater environments. The growth of these organisms is influenced by various factors, including environmental conditions, nutrition, water temperature, water quality, light, and the presence of other organisms. The effects of these factors on the growth of bivalves are significant, and research on this topic provides important insights into the life cycle and population dynamics of bivalves. Environmental factors play a crucial role in the growth of bivalves. Factors such as seawater temperature, salinity level, oxygen levels, and acidity directly influence the growth of bivalves. For example, some species may grow faster within specific temperature ranges, while others may thrive under different temperature conditions. Similarly, the salinity level of the water also affects the growth of bivalves. Therefore, studying environmental factors provides important information about the habitats and populations of bivalves. Nutrition is also a significant

factor in the growth of bivalves. The availability of plankton and other organisms that bivalves feed on affects their growth rate. Additionally, water quality also influences nutrition. Pollution and other factors can adversely affect the food sources of bivalves, thereby negatively impacting their growth. Calcium carbonate, the main component of shells, allows marine organisms to build their shells using dissolved minerals from the water. These minerals are excreted from the organisms' bodies and used to form shells. Calcium carbonate crystals provide the shell with strength and hardness, helping organisms to protect themselves from predators and survive in the marine environment. The calcium carbonate content in shells is part of the calcium cycle in marine ecosystems. Marine organisms use calcium and carbonate ions from the water to build their shells. These ions play a crucial role in the chemical composition of seawater and are released back into the water after being utilized by marine organisms to form shells. This process helps maintain the chemical balance of seawater and contributes to the overall health of marine ecosystems. The source of trace elements in shells is generally seawater. Seawater contains various minerals and elements that shell-bearing organisms can use in the formation of their shells. The presence of these elements in shells can influence their chemical composition and physical properties. For example, the integration of magnesium into calcium carbonate crystals can make shells more durable and flexible. Additionally, it is known that trace elements in shells are influenced by environmental factors. For instance, factors such as seawater temperature, acidity, and salinity can affect the chemical composition and trace element content of shells. Therefore, environmental changes can impact the composition and properties of shells in shell-bearing organisms. This study provides a detailed examination of the chemical composition of shells belonging to *M. galloprovincialis* mussels. Calcium carbonate, which constitutes a significant portion of the shell composition in bivalves, accounts for 94% of the shells. The study analyzed the surface charge status of the shells by determining their zero charge points (P_{ZC}). The findings revealed that the P_{ZC} value of the shells is 8.39, providing valuable insights into the characterization of the shells and their potential applications. Additionally, scanning electron microscopy (SEM) images and energy-dispersive X-ray spectroscopy (EDS) analyses of the shells were conducted. According to the EDS results, calcium, carbon, and oxygen atoms, which are characteristic of calcium carbonate ($CaCO_3$) structures, were found in the highest proportions, indicating the main structure of the shells. These findings contribute to a more detailed understanding of the chemical composition of the shells. Furthermore, Fourier-transform infrared (FT-IR) analysis supported the presence of calcium carbonate ($CaCO_3$) structures. Within the scope of the study, X-ray diffraction (XRD) analyses were also conducted, and the results indicated that the shell structures mainly consist of a mixture of calcium carbonate and aragonite. These analyses provide important information about the structural properties of the shells. While the predominant chemical component of the shells is calcium carbonate, it is known that small inorganic trace elements are commonly found in different bivalve species. These trace elements can affect the physical properties of the shells, determine their colors and patterns, and play a significant role in the lives of bivalve organisms. Therefore, the conservation of bivalve habitats and the investigation of the effects of environmental changes can help understand the effects on the composition and properties of the shells. Research in this area is considered to be an important step for the conservation of bivalve organisms and the sustainability of marine ecosystems.

ACKNOWLEDGEMENTS

This study was funded by TUBİTAK, Project number: 113O381.

Compliance with Ethical Standards

Authors' Contributions

BK: Conceptualization, Writing – original draft, Data curation, Formal Analysis, Visualization, Writing – review & editing

HY: Conceptualization, Investigation, Methodology, Writing – review & editing, Supervision, Funding acquisition, Project administration

SA: Conceptualization, Methodology, Investigation

PV: Investigation, Methodology, Data curation

All authors read and approved the final manuscript.

Conflict of Interest

The authors declare that there is no conflict of interest.

Ethical Approval

For this type of study, formal consent is not required.

Funding

Not applicable.

Data Availability

The data that support the findings of this study are available from the corresponding author upon reasonable request.

REFERENCES

Acarlı, S., Lok, A., Acarlı, D., & Kucukdermenci, A. (2018). Gamogenetic cycle, condition index and meat yield of the Noah's Ark shell (Arca noae Linnaeus, 1758) from Gerence Bay, Aegean Sea Turkey. *Ege Journal of Fisheries and Aquatic Sciences*, *35*, 141-149. https://doi.org/10.12714/egejfas.2018.35.2.06

Acarli, S., Lök, A., Kirtik, A., Acarli, D., Serdar, S., Kucukdermenci, A., & Saltan, A.N. (2015). Seasonal variation in reproductive activity and biochemical composition of flat oyster (*Ostrea edulis*) in the Homa Lagoon, Izmir Bay, Turkey. *Scientia Marina*, *79*(4), 487-495. https://doi.org/10.3989/scimar.04202.16a

Acarli, S., Lok, A., Kücükdermenci, A., Yildiz, H., & Serdar, S. (2011). Comparative growth, survival and condition index of flat oyster, *Ostrea edulis* (Linnaeus 1758) in Mersin Bay, Aegean Sea, Turkey. *Kafkas Universitesitesi Veterinerlik Fakültesi Dergisi*, *17*(2), 203-210.

Acarlı, S., Vural, P., & Yıldız, H. (2023). An assessment of the cultivation potential and suitability for human consumption of Mediterranean mussels (*Mytilus galloprovincialis* Lamarck, 1819) from the Yalova coast of the Marmara Sea. *Menba Kastamonu Üniversitesi Su Ürünleri Fakültesi Dergisi*, *9*(1), 12-24. https://doi.org/10.58626/menba.1282775

Agbaje, O. B. A., Shir, I. B., Zax, D. B., Schmidt, A., & Jacob, D. E. (2018a). Biomacromolecules within bivalve shells: Is chitin abundant? *Acta Biomaterialia*, *80*, 176–187. https://doi.org/10.1016/j.actbio.2018.09.009

Agbaje, O. B. A., Thomas, D., Dominguez, J. G., Mclnerney, B. V., Kosnik, M. A., & Jacob, D. E. (2018b). Biomacromolecules in bivalve shells with crossed lamellar architecture. *Journal of Materials Science*, *54*(6), 4952-4969. https://doi.org/10.1007/s10853-018-3165-8

Agbaje, O. B. A., Wirth, R., Morales, L. F. G., Shirai, K., Kosnik, M. A., Watanabe, T., & Jacob, D. E. (2017). Architecture of crossed-lamellar bivalve shells: the southern giant clam (*Tridacna derasa*, Röding, 1798). *Royal Society Open Science*, *4*(9), 170622. https://doi.org/10.1098/rsos.170622

Babić, B., Milonjić, S. K., Polovina, M., & Kaludierović, B. (1999). Point of zero charge and intrinsic equilibrium constants of activated carbon cloth. *Carbon*, *37*(3), 477-481. https://doi.org/10.1016/s0008-6223(98)00216-4

Bogan, A. E. (2007). Global diversity of freshwater mussels (Mollusca, Bivalvia) in freshwater. *Hydrobiologia*, *595*(1), 139–147. https://doi.org/10.1007/s10750-007-9011-7

Carroll, M., & Romanek, C. S. (2008). Shell layer variation in trace element concentration for the freshwater bivalve *Elliptio complanata*. *Geo-Marine Letters*, *28*(5-6), 369-381. https://doi.org/10.1007/s00367-008-0117-3

Chakraborty, A., Parveen, S., Chanda, D. K., & Aditya, G. (2020). An insight into the structure, composition and hardness of a biological material: the shell of freshwater mussels. *RSC Advances*, *10*(49), 29543-29554. https://doi.org/10.1039/d0ra04271d

Fiol, N., & Villaescusa, I. (2008). Determination of sorbent point zero charge: Usefulness in sorption studies. *Environmental Chemistry Letters*, *7*(1), 79-84. https://doi.org/10.1007/s10311-008-0139-0

Graf, D. (2013). Patterns of freshwater bivalve global diversity and the state of phylogenetic studies on the Unionoida, Sphaeriidae, and Cyrenidae. *American Malacological Bulletin*, *31*(1), 135–153. https://doi.org/10.4003/006.031.0106

Hamester, M. R. R., Balzer, P. S., & Becker, D. (2012). Characterization of calcium carbonate obtained from oyster and mussel shells and incorporation in polypropylene. *Materials Research*, *15*(2), 204-208. https://doi.org/10.1590/S1516-14392012005000014

Hou, W., Yan-Lei, S., D, S., & Zhang, C. (2001). Studies on zero point of charge and permanent charge density of MG-FE hydrotalcite-like compounds. *Langmuir*, *17*(6), 1885–1888. https://doi.org/10.1021/la0008838

Ituen, E. U. (2015). Mechanical and chemical properties of selected mullusc shells in Nigeria. *International Journal of Agricultural Policy and Research*, *3*(1), 53-59. https://doi.org/10.15739/IJAPR.026

Kosmulski, M. (2002). The significance of the difference in the point of zero charge between rutile and anatase. *Advances in Colloid and Interface Science*, *99*(3), 255–264. https://doi.org/10.1016/s0001-8686(02)00080-5

Lafuente, B., Downs, R. T., Yang, H., & Stone, N. (2015) The power of databases: the RRUFF project. In T. Armbruster & R. M. Danisi (Eds.), *Highlights in mineralogical crystallography* (pp 1-30). De Gruyter. https://doi.org/10.1515/9783110417104-003

Li, L., Zhang, X., Yun, H., & Li, G. (2017). Complex hierarchical microstructures of Cambrian mollusk *Pelagiella*: Insight into early biomineralization and evolution. *Scientific Reports*, *7*, 1935. https://doi.org/10.1038/s41598-017-02235-9

Mahmood, T., Saddique, M. T., Naeem, A., Westerhoff, P., Mustafa, S., & Alum, A. (2011). Comparison of different methods for the point of zero charge determination of NIO. *Industrial & Engineering Chemistry Research*, *50*(17), 10017-10023. https://doi.org/10.1021/ie200271d

Mititelu, M., Stanciu, G., Drăgănescu, D., Ioniță, A. C., Neacșu, S. M., Dinu, M., Stefan-van Staden, R.-I., & Moroșan, E. (2022). Mussel shells, a valuable calcium resource for the pharmaceutical industry. *Marine Drugs*, *20*, 25. https://doi.org/10.3390/md20010025

Nakamura, A., De Almeida, A. C., Riera, H. E., De Araújo, J. L. F., Gouveia, V. J. P., De Carvalho, M. D., & Cardoso, A. V. (2014). Polymorphism of $CaCO_3$ and microstructure of the shell of a Brazilian invasive mollusc (Limnoperna fortunei). *Materials Research-ibero-american Journal of Materials*, *17*(suppl 1), 15–22. https://doi.org/10.1590/s1516-14392014005000044

Pokroy, B., Fieramosca, J. S., Von Dreele, R. B., Fitch, A. N., Caspi, E. N., & Zolotoyabko, E. (2007). Atomic structure of biogenic aragonite. *Chemistry of Materials*, *19*(13), 3244-3251. https://doi.org/10.1021/cm070187u

Qian, Y. (1999). Taxonomy and biostratigraphy of small shelly fossils in China. In Y. Qian (Ed.), *Taxonomy and Biostratigraphy of Small Shelly Fossils in China* (pp. 216-219). Science Press.

Qian, Y., & Bengtson, S. (1989). *Palaeontology and biostratigraphy of the early Cambrian Meishucunian Stage in Yunnan Province, South China*. Universitetsforlaget. https://doi.org/10.18261/8200374157-1989

Somasundaran, P., & Agar, G. (1967). The zero point of charge of calcite. *Journal of Colloid and Interface Science*, *24*(4), 433-440. https://doi.org/10.1016/0021-9797(67)90241-x

Spann, N., Harper, E. M., & Aldridge, D. C. (2010). The unusual mineral vaterite in shells of the freshwater bivalve *Corbicula fluminea* from the UK. *The Science of Nature*, *97*(8), 743-751. https://doi.org/10.1007/s00114-010-0692-9

Sverjensky, D. A. (1994). Zero-point-of-charge prediction from crystal chemistry and solvation theory. *Geochimica et Cosmochimica Acta*, *58*(14), 3123-3129. https://doi.org/10.1016/0016-7037(94)90184-8

USGS. (2001), U. S. USGS OFR01-041: X-Ray Diffraction Primer, U. S. Geological Survey Open-File Report 01-041, Retrieved on January 28, 2024 from https://pubs.usgs.gov/of/2001/of01-041/htmldocs/xrpd.htm

Yildiz, H., & Berber, S. (2010). Depth and seasonal effects on the settlement density of *Mytilus galloprovincialis* L. 1819 in the Dardanelles. *Journal of Animal and Veterinary Advances*, *9*, 756-759.

Yıldız, H., Acarlı, S., Berber, S., Vural, P., & Gündüz, F. (2013). A preliminary study on Mediterranean Mussel (*Mytilus galloprovincialis* Lamarck, 1819) culture in integrated multitrofik aquaculture systems in Çanakkale Strait. *Alınteri Journal of Agricultural Sciences*, *25*(2), 38-44.

Acta Nat. Sci. (2024) 5(1): 69-78
DOI: 10.61326/actanatsci.v5i1.8
e-ISSN: 2718-0638

Original Research Paper
info@actanatsci.com
www.actanatsci.com

ACTA NATURA ET SCIENTIA PRENSIP

Biometric Evaluations and Condition Factor of the Mudskipper, *Periophthalmus barbarous* (Linnaeus, 1766) From Ibaka Mangrove Swamp, Nigeria

Enenwan Precious Udoinyang[1] • Aniefiokmkpong O. Okon[1] • Victoria Folakemi Akinjogunla[2]✉ • Itoro J. Archibong[1] • Unwana J. Effiong[1] • Emmanuel A. Essien[1]

[1] University of Uyo, Faculty of Science, Department of Animal and Environmental Biology, Uyo, Akwa Ibom State, Nigeria, everjewel2002@yahoo.co.uk, aniefiokmkpongo@gmail.com, itoroarchibong@uniuyo.edu.ng, vicakin@yahoo.com, emeritusessien49@gmail.com

[2] Bayero University, Faculty of Agriculture, Department of Fisheries and Aquaculture, Kano, Kano State, Nigeria, vfakinjogunla.faq@buk.edu.ng

✉ Corresponding Author: vfakinjogunla.faq@buk.edu.ng

Please cite this paper as follows:
Udoinyang, E. P., Okon, A. O., Akinjogunla, V. F., Archibong, I. J., Effiong, U. J., & Essien, E. A. (2024). Biometric Evaluations and Condition Factor of the Mudskipper, *Periophthalmus barbarous* (Linnaeus, 1766) From Ibaka Mangrove Swamp, Nigeria. *Acta Natura et Scientia*, *5*(1), 69-78. https://doi.org/10.61326/actanatsci.v5i1.8

ARTICLE INFO

Article History
Received: 29.07.2023
Revised: 22.03.2024
Accepted: 22.03.2024
Available online: 13.06.2024

Keywords:
Condition factor
Eye diameter
Head length
Ibaka estuary
Length-weight

ABSTRACT

The length-weight relationship and Fulton condition factor (K) of 404 samples of the mudskipper, *Periophthalmus barbarus* from Ibaka mangrove swamp were investigated for six months (January to June 2022) using standard methods to accommodate both the dry and wet seasons. For the 404 samples, the mean total length was 11.22±0.11 cm while the mean body weight was 16.4±0.48 g. Other biometric data collected includes percentage eye diameter (ED%) ranging between 5.07 and 8.26 cm for May and February, respectively. Percentage head length (HL%) values were between 20.9 and 28.12 cm for May and January, respectively. For percentage body depth (BD%), the least was recorded in April (19.49 cm) while the highest was observed in February (24.55 cm). The Fulton condition factor (K) determined for most of the sampled months showed that the values were above unity (K>1), indicating good living conditions on account of food availability, absence of parasites/predators, and absence of disease. However, K was less than unity (K<1) in February and June, indicating a possible decline in food availability and other factors responsible for growth. The values of the length-weight relationship (b) were greater than 3 (b>3) in almost all the months except in April, having a value of 2.895, indicating that the species exhibited a positive allometric growth pattern. This implied that as the length of the fish increased, there was also a corresponding increase in the weight of *P. barbarus* from the Ibaka Mangrove Swamp.

INTRODUCTION

The Cross River Estuary is an aquatic ecosystem which inhabits diverse life forms of fauna which includes silver catfish, tilapias, mudfishes, mudskippers, shrimps, oysters, plants and wildlife. The water found in this region is brackish salty water at the upper and lower stretch of the estuary. It is also a useful medium for the sustenance of livelihood and economic enhancement (Bisong et al., 2007). Mudskipper, *Periophthalmus barbarus* belonging to order Gobiiformes and family Oxudercidae is the only species of genus in West Africa (Abiaobo & Udo, 2017).

It inhabits the warmer and muddy part of the estuary and spends most of its life out of the water using large, specialized pectoral fins to walk on land. They burrow during high tide to protect themselves from predators as they are morphologically and physiologically adapted to live both on land (ability to walk on land and climb trees) and in water (Bob-Manuel, 2011; Ravi, 2013). Mudskippers occupy a salient ecological niche and is a valued component of some artisanal catches being exploited either for use as baits in hook and line fisheries, for human consumption or for use in traditional medicinal preparations where aphrodisiac properties are attributed to its flesh (Clayton, 1993).

The study of the relationship of length-weight is an important diagnostic indication of the wellbeing of fish species under investigation to measure the variations from the expected weight or length of individual fish or groups of fishes. The investigating and managing of the fisheries species most of the time entails the utilization of fundamental tools and biometric interactions (length, width and weight) to convert data collected in the field into appropriate indexes for evaluation purposes such as indication of fatness, gonadial development and stock biomass assessment (Froese & Pauly, 2015; Akinjogunla & Moruf, 2019; Akinjogunla & Soyinka, 2022).

Morphometric activities depend majorly on the stage of growth, reproductive organs and ecological parameters (food quantity and quality, water temperature and salinity) (Dall et al., 1991). In the aspect of fish morphometry, species of similar sizes can be compared when dealing with characteristics that alter in size. Eye diameter, (ED), head length (HL), body depth (BD), and total length (TL) are some of the common data observed for morphological features of fish samples under any investigation of biometric studies (Pradhan et al., 2017).

The condition factor which shows the degree or state of wellbeing of the fish species in their natural environment is expressed by using the 'coefficient of condition'. The co-efficient of the condition is a measure of various ecological and biological factors such as gonad stages, degree of fitness and suitability of the environment with regards to the feeding condition (Gomiero & Braga, 2005; Akinjogunla & Soyinka, 2022).

Due to the importance of this estuarine fauna worldwide, a great effort to study their biology (length-weight, sex ratio, condition factor, food and feeding, nutrients composition, etc.) has been undertaken in recent years (Clayton, 1993; King, 1996; Lawson, 2010; Kumolu-Johnson & Ndimele, 2010; Manoharan et al., 2013, Naminata et al., 2014; Yapi et al., 2017; Akinjogunla et al., 2017, 2021; Akinjogunla & Moruf, 2018, 2019; Solitoke et al., 2020; Udoinyang et al., 2022; Akinjogunla & Soyinka, 2022).

The study of morphometry (length, weight and health status) of species is considered to be important in the determination of the size-length relationships between sexes of the species and the connection that occurs between the various size groups of the sampled population while the relationship between condition factor and Length-weight values are linked to growth performances (Isometric, positive or negative allometric) of the species. Yet, little is known about the morphometric changes, length-weight relationship and condition factor in the mudskipper from Ibaka mangrove swamp off Cross River Estuary. The increasing demand of aquatic products as food in southern Nigeria and the dearth of information on growth dimensions of *P. barbarus* in Nigeria has prompted this study. Therefore, this research aimed to evaluate the morphometry relationship (length-weight relationship and condition factor) of *P. barbarus* from Ibaka mangrove swamp, Cross River

Estuary, Nigeria. This study would serve as baseline information for other research on the topic currently under investigation. This baseline information will help to pose an optimal and efficient management of stock available.

MATERIAL AND METHODS

Study Area

Ibaka is the biggest, most dynamic, and strategically located fishing community in Mbo Local Government Area of Akwa Ibom State, Nigeria, compared to the adjourning fishing communities in Cross River State (Udoinyang et al., 2022). The study site lies between latitude 4.6478°N and longitude 8.2979°E in the southern part of Nigeria which alternates between the wet and dry seasons. Ibaka has a long stretch that opens into Gulf of Guinea and the water is brackish and highly saline. It is a good nursery ground for cultivation of blue crabs and breeding of different fish and sea food species for fishermen.

Sampling

Monthly samples of *P. barbarus* (Figure 1) were obtained at Ibaka mangrove swamp, off Cross River Estuary, Nigeria. A total of 404 samples were collected for six months (from January to June 2022) with the help of the local fishermen who used traditional fishing gears such as cast nets with 10-40 mm as mesh size along with periwinkle baits. The sampling was done using a randomized sampling techniques i.e., collection was done at random using sampling net and traps in the swamp at different points. The samples were transported with the aid of a robust container with lid to the wet laboratory in the Department of Animal Environmental Biology, University of Uyo, Uyo where the biometric data were collected.

Figure 1. *Periophthalmus barbarus* from Ibaka Mangrove Swamp (X 25 mag)

Laboratory Analysis

The samples on reaching the laboratory were preserved under iced condition in a refrigerator awaiting morphometric measurements. At each measurement period, the samples were brought out of the refrigerator and allowed to defrost under the laboratory working bench. Four measurable morphometric characters (total length, standard length, body weight and body depth) were used in this study. These morphometric characters were measured and recorded in proformas for each mudskipper (Shamsa et al., 2016). The length and width were measured in centimeters (cm) with the aid of graduated meter rule while the body weights, gut weights and liver weight were measured to the nearest 0.1 in gram (g) using the electronic weighting scale Camry (Model EHA1).

Growth patterns of *P. barbarus*

Length–Weight Frequency Distributions

The statistical length-weight relationships were established using the linear regression:

$$W = aL^b \quad \text{(Ricker, 1975b) (1)}$$

where W and L are the independent and dependent variables of allometric parameters, respectively. W is total weight in grams (g); L is length in centimeters (cm); ais rate of change of weight with length (intercept); and b is weight at unit length (slope). The equation (1) above and data obtained were transformed into natural logarithms and this gave a linear (straight line) relationship as given in equation (2):

$$\log W = \log a + b(\log L) \quad \text{(Parsons, 1988) (2)}$$

Fulton Condition Factor (K)

The Fulton condition factor of the fish indicates the state of general wellness of the fish and was estimated from the relation. The Fulton condition factor of the *P. barbarus* was determined using the formula given in equation (3):

$$K = \frac{W}{L^3} \times 100 \quad \text{(Ricker, 1975a) (3)}$$

where *K*: condition factor; *L*: length of the species (cm); *W*: body weight (g).

Data Analysis

Data generated were presented as descriptive statistics, it was carried out and the results presented as mean ± standard error (SE), maximum and minimum using analysis of variance (ANOVA) and Statistical Package for Social Sciences (SPSS version 21) while co-efficient of determination (r^2) was used to determine the linear regression. Lines and scattered graphs were used to depict trends in the distribution and relationships between length, width and weights of *P. barbarus* using Minitab 14.

RESULTS

A total of 404 samples of *P. barbarus* were measured, the mean total length was 11.22±0.11 cm and mean body weight was 16.4±0.48 g.

Morphometric Characteristics

Table 1 shows the measurement of the morphometric parameters of the samples as range and mean±SE within the six months of sampling. The least mean total length and mean body weight were recorded in the month of May (6.35±1.13 and 13.85±0.94, respectively) while the highest value for the mean total length was recorded in the month of June (12.22±1.34 cm). The month of April had the highest mean body weight (17.11±0.98 g). For body depth, May had the least mean value of 1.78±0.08 cm while the highest was observed in February (2.20±0.07 cm) and March (2.20±0.08 cm); for head length (hl), the least was in the month of May (1.11±0.07 cm) while the highest was in March (2.57±0.55 cm); for eye diameter (ED), the least mean value was in May (0.44±0.02 cm) and the highest was in March (0.77±0.35 cm); for eye diameter (ED), the least mean value was in May (0.27 cm) and the highest

Table 1. Biometric characteristics of *Periophthalmus barbarus* for January-June 2022

Biometrics (min - max)	**January**	**February**	**March**	**April**	**May**	**June**
TL (cm)	7.5 - 16.5	7.8 - 17.4	8.5 - 18.2	8.5 - 15.4	4.0 - 10.6	8.6 - 18.3
Mean TL	**10.4±1.17**	**11.95±1.24**	**11.52±0.49**	**11.49±0.21**	**6.35±1.13**	**12.22±1.34**
SL (cm)	6.3-11.6	6.8-14.3	7.0-14.7	7.6-12.9	6.9-14.0	6.3-14.6
Mean SL	**8.57±0.86**	**8.96±1.09**	**9.37±0.98**	**9.75±0.80**	**5.32±0.97**	**8.91±1.03**
ED (cm)	0.4 - 1.5	0.3 - 1.9	0.5 - 1.8	0.3 - 1.0	0.1 - 1.0	0.1 - 1.0
Mean ED	**0.65±0.15**	**0.74±0.38**	**0.77±0.35**	**0.62±0.02**	**0.44±0.02**	**0.45±0.02**
BD (cm)	0.7 - 3.2	1.2 - 4.2	1.2 - 3.8	1.3 - 3.0	0.5 - 3.0	1.4 - 3.70
Mean BD	**1.83±0.09**	**2.20±0.07**	**2.20±0.08**	**1.90±0.05**	**1.78±0.08**	**1.98±0.08**
SWT (g)	2.0 - 36.0	2.0 - 26.0	2.0 - 41.0	3.0 - 34.0	4.0 - 39.0	3.0 - 39.0
LWT (g)	0.1 - 0.5	0.1 - 0.5	0.1 - 0.5	0.1 - 0.5	0.1 - 0.5	0.1 - 0.6
BWT (cm)	5.0 - 48.0	5.0 - 54.0	5.0 - 47.0	6.0 - 44.0	1.0 - 44.0	1.7 - 48.0
Mean BWT	**17.07±1.09**	**14.61±0.98**	**14.71±0.98**	**17.11±0.98**	**13.85±0.94**	**15.99±1.14**
HL (cm)	0.7 - 4.3	1.5 - 3.4	1.2 - 10.0	1.4 - 3.0	0.8 - 12.0	1.0 - 3.2
Mean HL	**2.41±0.09**	**2.30±0.78**	**2.57±0.55**	**1.42±0.04**	**1.11±0.07**	**1.87±0.05**
GWT (cm)	0.1 - 0.7	0.1 - 0.6	0.1 - 0.6	0.1 - 0.4	0.1 - 0.5	0.1 - 0.5
Mean GWT	**0.28±0.03**	**0.25±0.04**	**0.28±0.04**	**0.18±0.05**	**0.10±0.06**	**0.24±0.05**
% ED of SL	7.60	8.26	8.21	6.36	5.07	7.72
% HL of SL	28.12	25.70	27.4	24.80	20.90	20.39
% BD of SL	21.35	24.55	23.48	19.49	19.92	21.06

Note: TL: Total length; SL: Standard length; ED: Eye diameter; BD: Body depth; HL: Head length; GWT: Gut weight; SWT: Somatic weight; LWT: Liver weight; min: Minimum; max: Maximum.

was in March (0.77 cm); for gut weight (GWT), the least was in May (0.10±0.06 g) while the highest was in January (0.28±0.03 g) and March (0.28±0.04 g).

Length-Weight Relationship of *P. barbarus*

The monthly functional equations for total length-weight relationships for *P. barbarous* are shown in Table 2. There was a positive correlation in the relationship as indicated in the r^2 values across the six months. There was a variation in the 'r^2' values recorded across the month for the length-weight relationship for *P. barbarus* (0.6482-0.8976 cm). The least value of 0.6482cm was calculated for January while the highest value of 0.8976 cm was in the month of March. Figures 2a–f show the plot of the monthly relationship that existed between total length and body weight of *P. barbarus*.

Fulton Condition Factor (K)

In this study, Figure 3 summarizes the monthly variation in the condition factor for *P. barbarus*. The Condition Factor (K) ranged from 0.91 to 1.94. The minimum condition factor was reported in the month of June (0.91), while the maximum condition factor was in the month of May (1.94). A value of 0.97 was recorded in February, 1.01 in March, 1.21 in April and 1.34 was recorded in January.

Table 2. Functional equations for the total length–weight relationship of *Periophthalmus barbarus*

Month	Relationship	a	b	r^2	Functional equation
January	W vs TL	- 0.5436	1.6238	0.6482	W =1.6238TL - 0.5436
February	W vs TL	- 1.749	2.7742	0.8656	W = 2.7742TL - 1.749
March	W vs TL	- 1.7278	2.7154	0.8976	W = 2.7154TL - 1.7278
April	W vs TL	- 1.9662	3.0077	0.8893	W = 3.0077TL - 1.9662
May	W vs TL	- 1.4517	2.5289	0.8111	W = 2.5289TL - 1.4517
June	W vs TL	-0.9162	2.0407	0.6791	W = 2.0407TL - 0.9162

Note: W: Weight; TL: Total length; a: Slope; b: Intercept; r^2: Regression.

Table 3. Correlation matrix of body composition of *Periophthalmus barbarous*

	TL	SL	ED	BD	HL	SWT	GWT
TL	1	0.933*	0.894*	0.879*	0.622	0.835*	0.605
SL		1	0.837*	0.853*	0.770	0.877*	0.511
ED			1	0.968*	0.802*	0.542	0.864*
BD				1	0.831*	0.591	0.742
HL					1	0.438	0.658
SWT						1	0.104
GWT							1

Note: TL: Total length; SL: Standard length; ED: Eye diameter; BD: Body depth; HL: Head length; SWT: Somatic weight; GWT: Gut weight. The values with the asterisk (*) indicate significant difference.

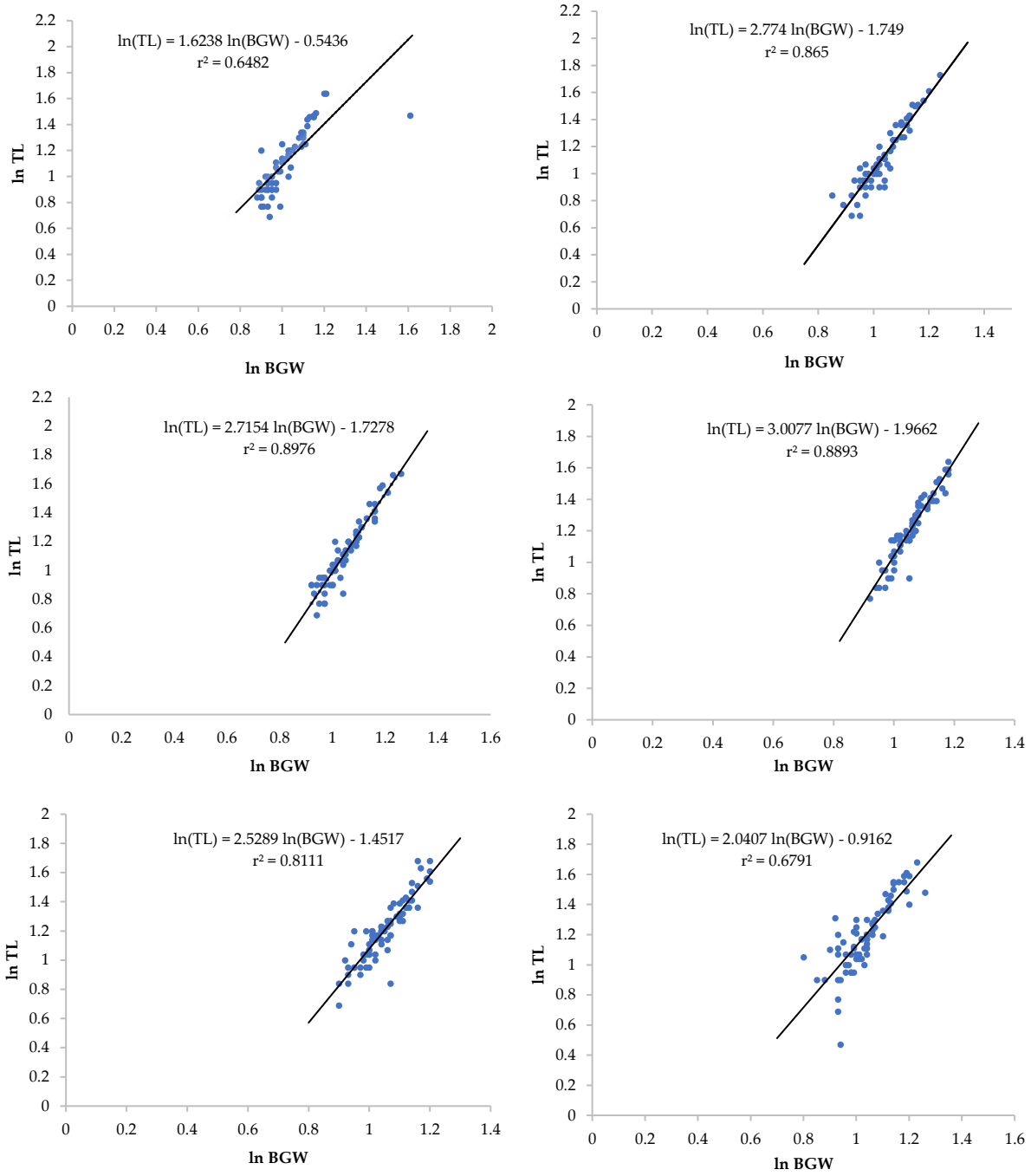

Figure 2. Length and weight relationship of *Periophthalmus barbarous* from a) January to e) June, 2022

DISCUSSION

In this study, specimens with total length between 6.35 and 12.22 cm were examined from the Ibaka mangrove ecosystem. Fish weight is considered to be a function of length (Naminata et al., 2014). For an ideal fish which maintains dimensional equality, the isometric value of '*b*' would be 3.0. Wotton (1990) and Naeem et al. (2010) stated that if the value of $b = 3$, the growth is isometric and allometric if $b \neq 3$ (negative allometric if $b < 3$ and positive allometric if $b > 3$). Positive allometric growths were observed ($b > 3$) during the sampled months except in the month of April where negative allometric growth rate was recorded. The negative allometric growth recorded for April is an indication of a decline in the growth performance of the fish. The sharp decline may be because it falls within the onset of the wet season where there is sharp change in the environmental parameters and the possibility of limited or reduced availability of quality and quantity food in their habitat.

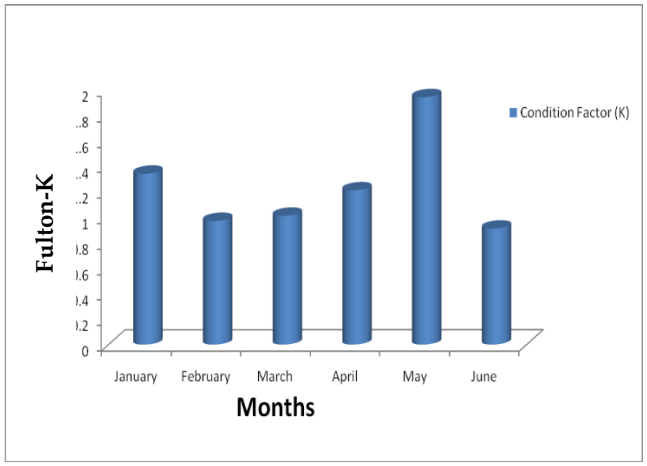

Figure 3. Monthly variation in the Fulton condition factor (K) of *Periophthalmus barbarus* from Ibaka mangrove swamp

The results of length-weight relationship of *Clarias gariepinus* obtained from Ibaka Mangrove Swamp, Nigeria revealed allometric pattern of growth. The average "b" value (2.44) for *Clarias gariepinus* was less than 3.0, which indicated a negative allometric growth increase. This implies that there was a slower rate increased in the weight than the body length. This agrees with the study of Kumolu-Johnson & Ndimele (2011) which reported similar growth for *Clarias gariepinus* in Ologe Lagoon, Lagos. Negative allometric growth pattern in freshwater fishes has also been reported in studies such as Abowei & Ezekiel (2013); Naminata et al., (2014); Akinjogunla & Soyinka (2022). The fish's weight is determined by length's function (Odedeyi et al., 2007). This study was in relation with researches from inland water bodies in Nigeria. This was noticeable among fish length-weight encompasses the outcomes of Peter & Diyaware (2014). Also, the allometric growth pattern experimented observations was similar to evaluation of length-weight relationship of fish species in Ebonyi River (Ude et al., 2011).

The inconsistencies in these results may be attributed to some internal (gonad maturity, sex, fish activities, health, seasonal growth and food habits) and external factors (habitat, temperature and availability of food) (Froese, 2006; Cazorla, 2008; Isa et al., 2010). The condition of fish upon capture such as stomach fullness, health and maturity can affect length-weight relationships (Cherif et al., 2008). The variability in the length-weight relationship can also be as a result of population variability and sampling error (Frosta et al., 2004). From the observation of this study, the rate of increase in length is considered to be directly proportional to increase in weight for *P. barbarus*.

The relative condition factor was studied to determine the general well-being or condition of fish. It can also be referred to as "ponderal index", "coefficient of condition", "condition factor and "length-weight factor" (Williams, 2000). The condition factor (K) for any species will have the value of 1, regardless of the unit measurement. For K value less than 1, it indicates slow growth rate in a fish which may be caused by disease and high population density (Anderson & Neumann 1996). In general, a high condition factor indicates favorable environmental conditions such as habitat and food availability while in contrast, a low condition factor indicates less favorable environmental condition factor (Blackwell et al., 2000).

The underlying hypothesis for this factor is that for a given length, a heavier fish is said to be in a better condition (Sivashanthini & Abeyrami 2003). In this study, the condition factor for *P. barbarus* varies among months of study (January to June). For January, March, April and May, condition factor, K values were 1.34, 1.01, 1.21 and 1.94, respectively, which indicated good favorable conditions of food availability, lack of predation, among other factors necessary for growth were available in those months. However, February and June had the lowest condition factor of 0.97 and 0.91, respectively, which showed that the conditions for optimum living were low in those months.

CONCLUSION

The morphometric features of *P. barbarus* from Ibaka mangrove swamp were investigated for six (6) months (dry season- January, February and March; rainy season – April, May and June) upon which length - weight relationship (LWR) and condition factor (K) were determined. The morphometry analysis carried out included measurement of weight, standard length, total length, length of head, eye diameter. The mean value for length–weight relationship (b) was greater than three (b > 3) across

the months with exception of the month of April that had b value less than 3 (b < 3). The condition factor (K) across the sampled months was found to be greater or equal to unity (≥ 1) especially during the rainy season indicating that the environmental conditions were favorable to the population of *P. barbarus*.

Compliance with Ethical Standards

Authors' Contributions

EPU, AOO, IJA, UJE and EAE: Manuscript design, Conducted the survey, Reviewing and Editing.

VFA: Drafting of manuscript

VFA, UJE and EAE: Data analysis, Editing

VFA and EAE: Reviewing

All authors read and approved the final manuscript.

Conflict of Interest

The author declares that there is no conflict of interest.

Ethical Approval

For this type of study, formal consent is not required.

Funding

Not applicable.

Data Availability

The data that support the findings of this study are available from the first author, (EPU) upon request.

REFERENCES

Abiaobo, N. O., & Udo, M. T. (2017). The population dynamics of the mudskipper, *Periophthalmus barbarus* (Linnaeus 1766) (Teleostei, Gobiidae) and the implication for conservation and management in the mangrove swamp of Iko River Estuary, Southeastern Nigeria. *Journal of Applied Life Sciences International, 14*(4), 1-19. https://doi.org/10.9734/JALSI/2017/37007

Abowei, J. F. N., & Ezekiel, E. N. (2013). The length-weight relationship and condition factor of *Chrysichthys nigrodigitatus* (Lacepède, 1803) from Amassoma River flood plains. *Science and Agriculture, 3*, 30-37.

Akinjogunla, V. F., & Moruf, R. O. (2018). The ecology and growth biology of *Farfante penaeusnotialis* (Pérez-farfante, 1967) from an open tidal estuary in Nigeria. *Nigerian Journal of Fisheries, 15*(1), 1326-1335.

Akinjogunla, V. F., & Soyinka, O. O. (2022). Morphometric assessment and condition factor of the mangrove oyster from a tropical mangrove swamp, off Lagos Lagoon, South-West, Nigeria. *Omni-Akuatika, 18*(1), 62-71. https://doi.org/10.20884/1.oa.2022.18.1.957

Akinjogunla, V. F., & Moruf, R. O. (2019). Shell growth pattern and percentage flesh yield of the West African Clam, g*alatea paradoxa* (born, 1778) from Itu Creek, Niger Delta, Nigeria. *Nigerian Journal of Basic and Applied Science, 27*(2), 119-126. https://doi.org/10.4314/njbas.v27i2.16

Akinjogunla, V. F., Lawal-Are, A. O., & Soyinka, O. O. (2017). Proximate composition and mineral contents of mangrove oyster (*Crassostrea gasar*) from Lagos Lagoon, Lagos, Nigeria. *Nigerian Journal of Fisheries and Aquaculture, 5*(2), 36-49.

Akinjogunla, V. F., Mudi, Z. R., Akinnigbagbe, O. R., & Akinnigbagbe, O. E. (2021). Biochemical profile of the mangrove oyster, *Crassostrea gasar* (Adanson, 1757) from the mangrove swamps, South-West, Nigeria. *Tropical Journal Natural Products and Research, 5*(12), 2137-2143.

Anderson, R. O., & Neumann, R. M. (1996). Length-weight, and associated structural indices. In B. R. Murphy & D. W. Willis (Eds.), *Fisheries techniques* (pp. 447-482). 2nd edition. American Fisheries Society.

Bisong, F. E., Andrew-Essien, E. E., Ambo, M. E., Offiong, R., & Okon I. E. (2007). Cross River Estuary: Changing trends resource utilization patterns. *Global Journal of Environmental Sciences, 6*(2), 76-87. https://doi.org/10.4314/gjes.v6i2.2495

Blackwell, B. G., Brown, M. L., & Willis, D. W. (2000). Relative weight (Wr) status and current use in fisheries assessment and management. *Reviews in Fisheries Science, 8*(1), 1-44. https://doi.org/10.1080/10641260091129161

Bob-Manuel, F. G. (2011). Food and feeding ecology of the mudskipper (*Periopthalmus koelreuteri*) (Pallas) Gobiidae at Rumuolumeni Creek, Niger Delta, Nigeria**.** *Agriculture and Biology Journal of North America, 6*, 897-901.

Cazorla, S. H. (2008). The reproductive biology of the *Limanda limanda* (L.) in the North Sea: Gonadosomatic index, hepatosomatic index and condition factor. *Journal of Fish Biology, 13*, 369-378. https://doi.org/10.1111/j.1095-8649.1978.tb03445.x

Cherif, M., Zarrad, R., Gharbi, H., Missaoui, H., & Jarboui, O. (2008). Length-weight relationships for 11 fish species from the gulf of Tunis (SW Mediterranean Sea, Tunisia). *Pan-American Journal of Aquatic Sciences, 3*(1), 1-5.

Clayton, M. T. (1993). Morphometric relationship and reproductive maturation of the mudskippers *Periopthalmus barbarus* from subsistence catches in the mangrove swamps of Imo estuary Nigeria. *Journal of Environmental Science, 14*(2), 221-226.

Dall, W., Hill, B. J., Rothlisberg, P. C., & Sharples, D. J. (1991). The biology of the Penaeidae. In J. H. S. Blaxter, & A. J. Southward (Eds.), *Advances in marine biology: Volume 27* (pp. 1-489). Academic Press.

Froese, R., & Pauly, D. (Eds.) (2015). FishBase. World Wide Web electronic publication. Retrieved on July 29, 2023, from http://www.fishbase.org

Froese, R. (2006). Cube law, condition factor and weight-length relationships: history, meta-analysis and recommendations. *Journal of Applied Ichthyology, 22*(4), 241-253. https://doi.org/10.1111/j.1439-0426.2006.00805.x

Frosta, L. O., Costa, P. A. S., & Braga, A. C. (2004). Length-weight relationships of marine fishes from the central Brazilian coast. *NAGA, WorldFish Center Quarterly*, *27*(1 & 2), 20-26.

Gomiero, L. M., & Braga, F. M. S. (2005). The condition factor of fishes from two river basins in Sao Paulo State, South-East of Brazil. *Acta Scientiarum: Biological Sciences*, *27*(1), 73-78. https://doi.org/10.4025/actascibiolsci.v27i1.1368

Isa. M. M., Godfrey, T. S., & Adebiyi, F. (2010). Length–weight relationships of freshwater fish species in Kerian River Basin and Pedu Lake. *Research Journal of Fisheries and Hydrobiology, 5*(1), 1-8.

King, R. P. (1996). Population dynamics of the mudskipper *Periophthalmus barbarus* (Gobiidae) in the estuarine swamp of Cross River, Nigeria. *Journal of Aquatic Science,11*, 31-41.

Kumolu-Johnson, C. A., & Ndimele, P. E. (2010). Length-weight relationship and condition factors of twenty-one fish species in Ologe lagoon, Lagos Nigeria. *Asian Journal of Agricultural Sciences, 2*(4), 233-236. https://doi.org/10.12691/ajrd-8-1-2

Kumolu-Johnson, C. A., & Ndimele, P. E. (2011). Length-weight relationship and condition factor of nine species from Ologe Lagoon, Lagos, Nigeria. *African Journals Biotechnology, 10*(2), 16-32. https://doi.org/10.5897/AJB10.870

Lawson, E. O. (2010). Morphometric measurements and meristic counts in mudskipper (*Periophthalmus papilio*) from mangrove swamps of Lagos lagoon, Nigeria. *Journal of Applied Biosciences, 34*, 2166-2172.

Manoharan, J., Gopalakrishnan, A., Varadharajan, D., Udayakumar, C., & Priyadharsini, S. (2013). Length-weight relationship of crescent perch *Terapon jarbua* (Forsskal) from Parangipettai coast, south east coast of India. *Journal of Aquaculture Research & Development, 4*(4), 1000181. https://doi.org/10.4172/2155-9546.1000181

Naeem, M., Salam, A., Ishtiaq, S., & Shafique, S. (2010). Length weight relationship and condition factor of farmed hybrid *Catla catla* from Multan Pakistan. *Sindh University Research Journal, 42*, 35-38.

Naminata, K., Kraidy, A. B. B., Gnonleba, B. F. H., & Koumelan, E. P. (2014). Length-weight relationship and population parameters of *Periophthalmus barbarus* (Linnaeus 1760) Boulengar. *International Journal of Biosciences, 5*(4), 149-158.

Odedeyi, D. O., Fagbenro, O., Bello-Olusoji, O. and Adebayo, O. (2007). Length-weight relationship and condition factor of the elephant fish, *Mormyrus rume* (Valenciennes, 1846) in River Ose, South Western Nigeria. *Animal Research International*, *4*(1), 617-620.

Parsons, R. (1988). *Statistical analysis: A decision making approach*. Second edition. Harper & Row.

Peter, K. J. & Diyaware, M. Y. (2014). The length-weight, condition factor and fecundity of *Clarias gariepinus* in Luhu Reservoir, Michika Local Government Area, Adamawa State Nigeria. *Nigerian Journal of Fisheries and Aquaculture*, *2*, 1-5

Pradhan, R. K., Deshmukh, V. D., Chakraborty, S. K. Chellapan, A., Jaiswar, A. K. & Roul, S. K. (2017). Length-weight relationship and morphological studies of the big eye shad, *Ilisha filigera* (Valenciennes, 1847) in Mumbai waters. *Indian Journal of Geo Marine Sciences*, *46*(01), 102-106.

Ravi, V. (2013). Food and Feeding Habits of the Mudskipper, *Boleophthalmus boddarti* (Pallas, 1770) from Pichavaram Mangroves, Southeast Coast of India. *International Journal of Marine Science, 3*(12), 98-104.

Ricker, W. E. (1975a). Handbook of computations and interpretations of biological statistics of fish production. *Bulletin of Fisheries Research Board of Canada*, *191*, 382 p.

Ricker, W. E. (1975b). Computation and Interpretation of biological statistics of fish population. *Journal of the Fisheries Research Board of Canada*, *191*, 1-382.

Shamsa, A., Jang, A. J. Y., & McGee, T. M. (2016). Documentation of instrumental vaginal deliveries: The benefits of a pro forma. *Health Information Management Journal*, *45*(3), 116-120. https://doi.org/10.1177/1833358316647547

Sivashanthini, K., & Abeyrami, B. (2003). Length-weight relationship and relative condition of a silver biddy, *Gerrus oblongus* (Pisces: Perciformes) from the Jaffna lagoon, Sri Lanka. *Indian Journal of Marian Sciences, 32*(3), 252-254.

Solitoke, H. D., Afiademanyo, K. M., Ouro-Sama, K., Tanouayi,g., Badassan, T. E., & Gnandi, K. (2020). Aspects of population dynamics of the mangrove oyster, *Cassostrea gasar* Dautzenherg (1891) (Ostreida: Ostreidae) from the Lake Zowla-Aného Lagoon system in Togo. *Journal of Fisheries and Aquaculture Research*, *5*(1), 93-106.

Ude, E. F., Ugwu, L. L. C., Mgbenka, B. O. and Nwani, C. D. (2011). Evaluation of length-weight relationship of fish species of Ebonyi River, Nigeria. *Nigerian Journal of Fisheries, 8*(1), 136-144.

Udoinyang, E. P., Okon, A. O. Akinjogunla, V. F. & Isangedighi, R. F. (2022). Proximate and selected mineral compositions in *Periophthalmus barbarus* from the Ibaka mangrove ecosystem, Akwa-Ibom State, Nigeria. *Journal of Innovative Research in Life Sciences*, *4*(1), 80-91.

Williams, J. E. (2000). The coefficient of condition of fish. In J. C. Schneider (Ed.), *Manual of Fisheries Survey Method II* (pp. 151-153). Michigan Department of Natural Resources.

Wotton, R. J. (1990). *Ecology of teleost fishes. Fish and fisheries series 1*. Champman and Hall.

Yapi, J. N., Ble, M. C., Etchian, A. O., Kadjo, V., & Yao, K. (2017). Population dynamics of mangrove oyster, *Crassostrea gasar* of the Lagoons Ebrié and Aby (Côte d'Ivoire). *International Journal of Sciences: Basic and Applied Research, 36*(8), 122-137.

Acta Nat. Sci. (2024) 5(1): 79-88
DOI: 10.61326/actanatsci.v5i1.9
e-ISSN: 2718-0638

Original Research Paper
info@actanatsci.com
www.actanatsci.com

ACTA NATURA ET SCIENTIA PRENSİP

Çanakkale Koşullarında Farklı Dikim Yöntemlerinin Nanede (*Mentha spp.*) Verim ve Bazı Tarımsal Karakterlere Etkisi

Bahri İzci[1]✉

[1] Çanakkale Onsekiz Mart University, Faculty of Agriculture, Department of Field Crops, 17020, Çanakkale, Türkiye

✉ Corresponding Author: bizci@comu.edu.tr

Please cite this paper as follows:
İzci, B. (2024). Çanakkale Koşullarında Farklı Dikim Yöntemlerinin Nanede (*Mentha spp.*) Verim ve Bazı Tarımsal Karakterlere Etkisi. *Acta Natura et Scientia*, *5*(1), 79-88. https://doi.org/10.61326/actanatsci.v5i1.9

MAKALE BİLGİSİ

Makale Geçmişi
Geliş: 27.03.2024
Düzeltme: 25.06.2024
Kabul: 25.06.2024
Çevrimiçi Yayınlanma: 27.06.2024

Anahtar Kelimeler:
Nane
Mentha × *piperita* L. var Mitcham
Mentha piperita
Mentha spicata
Verim

ÖZET

Çanakkale koşullarında üç farklı nane tür ve tipinde (*Mentha* × *piperita* L. var Mitcham, *M. piperita* ve *M. spicata*), dört dikim zamanının (18 Ekim, 18 Kasım, 5 Nisan ve 5 Mayıs) verim ve tarımsal özellikleri üzerine olan etkinin araştırıldığı bu çalışma 2019-2020 yıllarında Çanakkale ili Sarıcaeli Köyünde gerçekleştirilmiştir. Denemeye alınan 3 nane tür ve tipinde, Ekim ve Kasım dikimlerinde (18 Ekim ve 18 Kasım) Nisan ve Mayıs dikimlerine (5 Nisan ve 5 Mayıs) nazaran çok daha fazla drog herba ve uçucu yağ verimleri elde edilmiştir. Denemeye alınan naneler arasında en fazla toplam taze ve drog herba, drog yaprak ve uçucu yağ verimleri *M. spicata* tipi nanede saptanmıştır. Sonrasında en yüksek değerler *Mentha* × *piperita* L. var Mitcham tipi nanede gerçekleşmiştir. *Mentha* × *piperita* L. var Mitcham tipi nanede ise Ekim ve Kasım dikimlerinde, toplam drog yaprak veriminin düşük olmasına rağmen uçucu yağ oranının yüksek olması sebebiyle daha fazla toplam uçucu yağ verimi saptanmıştır. Çanakkale koşullarında *M. spicata* tipi nane genelde incelenen özellikler açısından ilk sırada yer almıştır. *M. spicata* nane tipinin hem 2019 hem de 2020 yılında iyi bir sonuç ortaya koyması ve bölge ekolojik koşullarında, özellikle Ekim ve Kasım aylarında dikimin daha uygun olacağı ve bu alanlarda üretiminin rahatlıkla yapılabileceği ortaya çıkmıştır.

Effect of Different Planting Times on Yields and Agricultural Characters of Different Mint (*Mentha spp.*) Varieties Under the Çanakkale Plain Conditions

ARTICLE INFO

Article History
Article History
Received: 27.03.2024
Revised: 25.06.2024
Accepted: 25.06.2024
Available online: 27.06.2024

Keywords:
Mint
Mentha × piperita L. var Mitcham
Mentha piperita
Mentha spicata
Yield

ABSTRACT

This study investigated the effects of different planting times (October 18, November 18, April 5 and May 5) on the yield and some agricultural characteristics of different mint species and types (*Mentha × piperita* L. var Mitcham, *M. piperita* and *M. spicata*). It was carried out in Sarıcaeli Village of Çanakkale province in 2019-2020 in Çanakkale conditions. In the 3 mint species and types tested, much higher drug herb and essential oil yields were obtained in October and November plantings (October 18 and November 18) than in April and May plantings (April 5 and May 5). Among the mints included in the experiment, the highest total fresh and drug herb, drug leaf and essential oil yields were determined in *M. spicata* type mint. Afterwards, the highest values were observed in *M. piperita* Mitcham type mint. In *Mentha × piperita* L. var Mitcham type mint, higher total essential oil yield was determined in October and November plantings due to the high essential oil content, although the total drug leaf yield was low. In Çanakkale conditions, *M. spicata* type mint generally ranked first in terms of the examined characteristics. It has been revealed that the *M. spicata* mint type showed good results in both 2019 and 2020 and that planting will be more suitable in the ecological conditions of the region, especially in October and November, and production can be easily done in these areas.

GİRİŞ

Türkiye florasında doğal olarak yetişen 9000 bitkiden 500 tanesi tıbbi olarak değerlendirilmekte ve çeşitli amaçlar için etkili madde temininde kullanılmaktadır (Ekim, 1990). Bu bitkilerin büyük çoğunluğu doğadan toplama yoluyla ve küçük bir kısmı da kültür tarımı yapılarak üretilmekte, iç ve dış piyasada çeşitli alanlarda değerlendirilmektedir. Kültürü yapılan bitkilerden naneden elde edilen uçucu yağ, dünya piyasalarında büyük bir ticarete sahiptir. Dünyada uçucu yağ ticaretinde ikinci sırada yer alan naneden yılda 6000-8000 ton nane uçucu yağı elde edilmektedir (Başer, 1993). Nane yağı üretiminde en yüksek paya sahip ülke Amerika olup, bunu Fransa, Brezilya ve Arjantin takip etmektedir. Batı Avrupa ülkeleri, Çin, Peru, Tayland ve Kore de yüksek miktarda nane yağı üretimine sahiptir (Ceylan vd., 1994). Kültürü yapılan nane bitkisi ülkemizde 2019 yılında 9800 ton üretime ulaşmış (TÜİK, 2024) ve o dönemki yıllık verilere bakıldığında yaklaşık 20 milyon dolarlık bir dış ticareti gerçekleşmiştir. Bu dış satıma karşılık, aynı yıl içerisinde farklı ülkelerden 52.865 kg nane yağı ithal edilerek toplam 930.500 $, ilave olarak da 18.325 kg mentol için 400 bin $ ödenmiştir (TÜİK, 2021). Bu tarz çalışmalarla yurt içi ihtiyacı karşılanarak döviz kaybının önlenmeli ve verimi de artırılıp dış satım gerçekleştirilerek ekonomiye katkı sağlanmalıdır. Bu sebeple, uçucu yağ oranı ve kalite içeriği yüksek naneleri ve bu nane tür ve tiplerinin yetiştirilme tekniklerini belirlemek oldukça yararlı olacaktır.

Nane, bulundurduğu uçucu yağlarından dolayı tıbbi faydası yüksek bitkilerden birisidir. Nane, çoğunlukla sindirim sistemi rahatsızlıklarında yıllarca tedavi amacıyla kullanılmıştır. Mide ağrıları ve bağırsak gazdan oluşan kramplarda nane antispazmodik özelliği sayesinde oldukça etkilidir. Son yıllarda önem arz eden nanenin insan sağlığı ve gıda sanayisinde kullanımı oldukça yaygınlaşmakta ve ekonomik değer açısından da önemli bir unsur haline gelmektedir. Nane üretimi için 1950'li yıllarda 400–500 dekarlık olan üretim alanı, 1980'li ve 1990'lı

yıllarda 600–750 dekara ve 2000'li yıllarda ise 4080-7500 dekara kadar artış göstermiştir. Nane üretim miktarı ise 2004 yılında 6500 ton iken 2023 yılında 26.198 tona kadar ulaşmıştır (TÜİK, 2024).

Nane Labiatae familyasına ait *M. piperita*'nın ana vatanının Akdeniz Bölgesi, Mısır ve Anadolu olduğu bildirilmektedir. Genellikle kök, gövde ve yaprak çelikleriyle üretilen nanenin tohumla da üretimi mümkündür. Vejetatif ve generatif gelişmesini aynı yıl içinde tamamlayan nane çok yıllık bir tıbbi aromatik bitkidir. Mayıs ayı başında generatif gelişmeye başlayan naneler çiçeklenmeden sonra Ağustos'ta generatif gelişmesine başlar. Kıştan önce toprak üstü aksamı kurur ve toprak altı kök gövdesi ile kış periyodunu geçirir. Sonraki yıl kök gövdesinden yeni sürgünler meydana getirerek gelişimine devam eder. Saçak kök görünümünde olan kökün derinliği 100 cm'ye kadar uzayabilir.

Nanenin Türk tarımı tarihinde yeri oldukça eskiye dayanmaktadır. Birçok uygarlıkta kullanılan nane, Osmanlı ve Türk tıbbında da *Mentha piperitae*'dan elde edilen, nane yaprağı ve nane uçucu yağı, oldukça yoğun olarak kullanılan bir baharattır. Birçok rahatsızlık için tedavi edici özelliğinden faydalanılmıştır.

Bahçe nanesi (*Mentha piperita*) yoğun olarak yetiştirilen nane türüdür. Yaprakları özellikle salatalarda taze sebze olarak yenen nanenin kurutularak baharat olarak da değerlendirilmesi sebebiyle daha çok Avrupa, Asya ve Kuzey Amerika'da yoğun tarımı yapılmaktadır. Vejetasyon periyodunda morumsu pembe çiçekleri açtıktan sonra toplanarak kurutulmuş yapraklardan elde edilen çay, mide bulantılarında önleyici ve gaz söktürücüsü etkisi sebebiyle kullanılmaktadır. Yapraklarda bulunan mentol renksiz, keskin kokulu ve serinletici bir özelliğe sahiptir.

Çanakkale ve yöresinde doğal olarak yetişen nanenin bazı yerli tipleri, pazarlarda ve aktarlarda taze ve kuru olarak tüketilmek üzere satılmakta olup tüketim ve ticaret amacıyla küçük alanlarda yetiştiriciliği yapılmaktadır. Çanakkale ve çevresinde yüksek verimli ve kaliteli nane çeşitleri ve bunların yetiştirme tekniklerindeki bazı önemli noktalar belirlenerek yöredeki nane tarımının yaygınlaştırılması hem bölge hem de ülke tarımı açısından önemli bir kazanç olacaktır. Bu bağlamda, bu çalışma Çanakkale koşullarına adapte, yüksek verimli ve kaliteli kültür çeşitlerinin belirlenmesi, kalite yönünden yüksek değerlere sahip uçucu yağın elde edilebileceği en uygun dikim zamanlarının tespit edilmesi amacıyla gerçekleştirilmiştir.

MATERYAL VE YÖNTEM

Bu çalışma Çanakkale ili Merkez ilçesi Sarıcaeli Köyünde gerçekleştirilmiştir. Deneme yerinin toprağı, organik madde açısından iyi durumda, alüvyal özellikte, düz ve eğimsiz, derin profilli topraklardır. Deneme alanı pH değeri 7,2-7,6 arasında ve organik maddece iyi, katyon değişim kapasitesi de yüksektir (Dinç vd., 1988).

Denemenin yapıldığı dönemde Temmuz, Ağustos ve Eylül aylarında hiç yağış gözlenmemiş olup Ekim ayında ise geçmiş yıllara oranla az yağış gerçekleşmiştir. Vejetasyon döneminde elde edilen oransal nem değerleri, uzun yıllar ortalamasına paralellik göstermiştir. Güneşlenme süresi değerleri, uzun yıllar ortalama değerlerine benzer değerlerde tespit edilmiştir.

Materyal

Çanakkale Onsekiz Mart Üniversitesi Ziraat Fakültesi Tarla Bitkileri Bölümünde bulunan Balıkesir ve Çanakkale'nin farklı yerlerinden temin edilen *Mentha* × *piperita* L. var Mitcham, *M. piperita* ve *M. spicata* tipi naneler çalışmanın materyalini oluşturmaktadır.

Yöntem

Çalışma, bölünmüş parseller deneme desenine göre üç tekerrürlü planlanarak kurulmuş, naneler (*Mentha* × *piperita* L. var Mitcham, *M. piperita* ve *M. spicata*) ana parselleri, dikim zamanı (18 Ekim. 18 Kasım, 5 Nisan ve 5 Mayıs) alt parselleri oluşturmuştur. Birden fazla biçim yapılan nane, bitki boyu ve uçucu yağ oranında elde edilen verilerin değerlendirilmesinde, bölünen bölünmüş parseller deneme deseni kullanılmıştır. Nane tipleri ana parselleri, dikim zamanları alt parselleri oluşturmuştur.

Alt parseller beş sıradan oluşup parsel alanı 8 m^2 (5×2=10 m^2), dikim sıklığı 20×40 cm şeklinde planlanmıştır. Biçimlerde, kenar tesiri olarak birer sıra ve parsel başlarından yarım metre kenar tesiri bırakılarak, geri kalan alanda ölçüm ve gözlem yapılmıştır. Bir vejetasyon döneminde üç biçim alınabilmiştir.

2019 ve 2020 yıllarında her dikim zamanında ayrı ayrı hazırlanan parsellere dikimler yapılmıştır. Her parsele dikimde saf madde hesabı yapılarak dekara 5 kg N, 5 kg P_2O_5 ve 6 kg K_2O'lu gübre ve biçimlerden sonrada dekara 5 kg N hesabıyla gübre verilmiştir. Dikimlerde yağmurlama sulama yapılmıştır. Her iki deneme yılında da herhangi bir zararlı veya hastalıkla karşılaşılmadığından kimyasal ilaç kullanılmamıştır. Gerektiğinde yabancı ot mücadelesi hem mekanik yöntemle hem de biçimler sonrasında elle yapılmıştır. Biçimler bütün parsellerde çiçeklenme başlangıcında yapılmıştır.

Çalışmada, bitki boyları cetvelle ölçülerek cm olarak, toplam taze herba verimi, toplam drog herba verimi ve toplam drog yaprak verimi hassas terazi ile tartılarak kg/da olarak hesaplanmıştır. Kuru madde ve uçucu yağ oranları % ve toplam uçucu yağ verimi ise l/da olarak saptanmıştır.

Bitki boyu ve uçucu yağ oranları verileri Bölünen Bölünmüş Parseller, diğerleri ise Bölünmüş Parseller deneme desenine göre TARİST paket programında değerlendirilmiştir.

BULGULAR VE TARTIŞMA

Denemenin her iki yılında bitki boyu ve uçucu yağ oranı açısından, nane tür ve tipleri, dikim zamanları ve biçim zamanları arasındaki farklılıklar önemli bulunmuş ($p<0,05$), incelenen diğer karakterlerde ise nane tür ve tipleri ve dikim zamanları arasındaki farklılıkların da istatistiksel olarak önemli olduğu saptanmıştır($p<0,01$).

Bitki Boyu

Yıllara göre farklı biçimlerde, nanelerin dikim zamanlarından elde edilen bitki boyu değerleri ve ortalamaları Tablo 1'de verilmiştir. En yüksek bitki boyu değerleri 18 Ekim ve 18 Kasım dikimlerinde belirlenirken, en düşük bitki boyu değerleri her iki yılda da 5 Mayıs dikimlerinde gözlenmiştir. Sonbaharda yapılan dikimlerin bitki boyu değerlerinin ilkbaharda yapılan dikimlerin değerlerinden daha yüksek olduğu tespit edilmiştir. Bu durum sonbahar dikimlerinde ilkbaharda yapılan dikimlere göre daha uzun bir vejetasyon süresinin oluşması ve sonbahar dikimlerinin ilkbahar dikimlerine nazaran gelişmeye daha erken başlaması ve daha avantajlı olmalarından kaynaklanmaktadır.

Nane tipleri açısından değerlendirildiğinde, en yüksek ortalama bitki boyu değeri bir vejetasyonda üç biçimin alınabildiği *M. spicata* tipi nanede saptanırken, en düşük bitki boyu *M. piperita* tipinden elde edilmiştir. Nane tiplerindeki farklılık, değişik genotipe sahip bitkilerin farklı ekolojik koşullarda gösterdiği olumlu ya da olumsuz tepkilerden kaynaklanmaktadır.

Biçim zamanları açısından değerlendirildiğinde genel olarak ilk biçimlerde bitki boyu için en yüksek değerler elde edilmiştir. Bu sonuçlar literatürde ilk biçimde yüksek bitki boyu elde eden bazı araştırmalarla uyum göstermektedir (Kothari vd., 1987; Özgüven vd., 1995). Ayrıca bitki boyu değerleri bazı araştırıcıların bildirdikleri değerlerden düşük (Morton, 1977; Ceylan, 1978; Kothari vd., 1987), bazılarının değerlerine benzer veya yüksek bulunmuştur (Özgüven vd., 1995). Bitki boyu değerlerinin literatürdeki bazı çalışmalardan daha düşük olmasının bölgede yaz aylarının sıcak ve nisbi nem oranının düşük olmasından kaynaklandığı düşünülmektedir (Genç & Tükel, 1988).

Toplam Taze Herba Verimi

Denemenin iki yılında da toplam taze herba verimi en yüksek 18 Ekim dikimlerinde ve üç kez biçimin alınabildiği *M. spicata* tipi nanede saptanmıştır. Ortalama değerler incelendiğinde, geciken dikimlere bağlı olarak toplam taze herba verimi değerleri düşmüş ve sonbahar yapılan dikimlerinden ilkbahar dikimlerine nazaran daha yüksek değerler elde edilmiştir (Tablo 2).

Table 1. Plant height values and averages (cm) obtained from planting times of mint in different forms in 2019 and 2020

Tablo 1. *2019 ve 2020 yıllarında farklı biçimlerde, nanelerin dikim zamanlarından elde edilen bitki boyu değerleri ve ortalamaları (cm)*

Dikim Zamanı	Biçimler	2019				2020			
		Nane Tipleri			*Ort.*	*Nane Tipleri*			*Ort.*
		a	*b*	*c*		*a*	*b*	*c*	
18 Ekim	1. Biçim	61,43	54,80	64,63	**60,29**	58,28	46,98	60,78	**55,35**
	2. Biçim	61,53	44,35	56,80	**54,23**	50,05	39,33	58,48	**49,29**
	3. Biçim	41,24	36,54	48,75	**42,18**	32,25	25,36	54,80	**37,47**
Ortalama		**54,73**	**45,23**	**56,73**	**52,23**	**46,86**	**37,22**	**58,02**	**47,37**
18 Kasım	1. Biçim	63,83	57,20	64,23	**61,75**	56,88	50,45	54,48	**53,94**
	2. Biçim	57,50	47,95	59,65	**55,03**	49,73	45,03	59,45	**51,40**
	3. Biçim	36,45	31,25	46,10	**37,93**	26,56	35,25	54,03	**38,61**
Ortalama		**52,59**	**45,47**	**56,66**	**51,57**	**44,39**	**43,58**	**55,99**	**47,98**
5 Nisan	1. Biçim	60,35	40,58	55,35	**52,09**	40,00	32,72	55,06	**42,59**
	2. Biçim	44,63	36,15	58,73	**46,50**	34,25	30,30	55,85	**40,13**
	3. Biçim	24,56	24,58	45,68	**31,61**	26,00	18,25	41,48	**28,58**
Ortalama		**43,18**	**33,77**	**53,25**	**43,40**	**33,42**	**27,09**	**50,80**	**37,10**
5 Mayıs	1. Biçim	46,78	40,08	43,83	**43,56**	44,10	31,75	51,70	**42,52**
	2. Biçim	42,20	37,73	49,38	**43,10**	41,15	27,03	52,18	**40,12**
	3. Biçim	22,12	13,54	19,90	**18,52**	21,66	12,35	40,15	**24,72**
Ortalama		**37,03**	**30,45**	**37,70**	**35,06**	**35,64**	**23,71**	**48,01**	**35,79**
Genel Ortalama		**46,89**	**38,73**	**51,09**	**45,57**	**40,08**	**32,90**	**53,20**	**42,06**
EGF. (%5)		3,12 (çeşit), 1,35 (dikim zamanı)				0,81 (çeşit), 1,03 (dikim zamanı)			

Not: a) *Mentha × piperita* L. var Mitcham; b) *Mentha piperita*; c) *Mentha spicata*

Table 2. Comparison of total fresh herb yield values (kg/da) in 2019 and 2020 in terms of planting times

Tablo 2. *2019 ve 2020 yılları toplam taze herba verimi değerlerinin (kg/da), dikim zamanları yönünden karşılaştırılması*

Dikim Zamanı	Biçimler	2019				2020			
		Nane Tipleri			*Ort.*	*Nane Tipleri*			*Ort.*
		a	*b*	*c*		*a*	*b*	*c*	
18 Ekim	1. Biçim	3504,2	2950,0	4681,9	**3712,0**	2587,5	2329,1	4400,0	**3105,5**
	2. Biçim	3489,0	2895,3	4586,2	**3656,8**	2577,1	2319,8	4382,4	**3093,1**
	3. Biçim	3452,2	2886,1	4532,1	**3623,5**	2566,8	2310,5	4364,8	**3080,7**
Ortalama		**3481,8**	**2910,4**	**4600,1**	**3664,1**	**2577,1**	**2319,8**	**4382,4**	**3093,1**
18 Kasım	1. Biçim	3438,2	2674,3	4368,7	**3493,7**	2697,6	2251,0	4239,5	**3062,7**
	2. Biçim	3424,4	2663,6	4351,3	**3479,7**	2686,8	2242,0	4222,6	**3050,5**
	3. Biçim	3410,7	2652,9	4333,9	**3465,8**	2676,1	2233,0	4205,7	**3038,3**
Ortalama		**3424,5**	**2663,6**	**4351,3**	**3479,8**	**2686,8**	**2242,0**	**4222,6**	**3050,5**
5 Nisan	1. Biçim	2559.7	1133.3	3913.1	**2535,4**	2114.5	1791.6	3439.5	**2448,6**
	2. Biçim	2549,5	1128,8	3897,5	**2525,2**	2106,1	1784,4	3425,8	**2438,8**
	3. Biçim	2539,3	1124,3	3881,9	**2515,1**	2097,7	1777,3	3412,1	**2429,0**
Ortalama		**2549,5**	**1128,8**	**3897,5**	**2525,2**	**2106,1**	**1784,5**	**3425,8**	**2438,8**
5 Mayıs	1. Biçim	2288.9	1429.5	2375.3	**2031,2**	2211.4	1797.9	3422.9	**2477,4**
	2. Biçim	2279,7	1423,8	2365,8	**2023,1**	2202,6	1790,7	3409,2	**2467,5**
	3. Biçim	2270,6	1418,1	2356,3	**2015,0**	2193,7	1783,5	3395,5	**2457,6**
Ortalama		**2279,8**	**1423,8**	**2365,8**	**2023,1**	**2202,6**	**1790,7**	**3409,2**	**2467,5**
Genel Ortalama		**2933,9**	**2031,7**	**3803,7**	**2923,1**	**2393,2**	**2034,3**	**3860,0**	**2762,5**
EGF. (%5)		138,7 (çeşit), 125,4 (dikim zamanı)				28,6 (çeşit), 52,8 (dikim zamanı)			

Not: a) *Mentha × piperita* L. var Mitcham; b) *Mentha piperita*; c) *Mentha spicata*

Table 3. Comparison of total drug herb yield values (kg/da) in 2019 and 2020 in terms of planting times

Tablo 3. *2019 ve 2020 yılları toplam drog herba verimi değerlerinin (kg/da), dikim zamanları yönünden karşılaştırılması*

Dikim Zamanı	Biçimler	2019				2020			
		Nane Tipleri			*Ort.*	*Nane Tipleri*			*Ort.*
		a	*b*	*c*		*a*	*b*	*c*	
18 Ekim	1. Biçim	936,0	704,4	1106,2	**915,5**	795,5	604,1	986,8	**795,5**
	2. Biçim	931,3	700,8	1100,6	**910,9**	791,6	601,1	981,8	**791,5**
	3. Biçim	922,0	693,8	1089,6	**901,8**	783,6	595,1	972,0	**783,6**
Ortalama		**929,8**	**699,7**	**1098,8**	**909,4**	**790,2**	**600,1**	**980,2**	**790,2**
18 Kasım	1. Biçim	966,6	698,6	983,2	**882,8**	793,1	587,5	953,9	**778,2**
	2. Biçim	961,7	695,1	978,3	**878,4**	789,1	584,5	949,2	**774,3**
	3. Biçim	952,1	688,2	968,5	**869,6**	781,2	578,7	939,7	**766,5**
Ortalama		**960,1**	**694,0**	**976,7**	**876,9**	**787,8**	**583,6**	**947,6**	**773,0**
5 Nisan	1. Biçim	668,1	318,9	908,7	**631,9**	640,1	491,9	718,7	**616,9**
	2. Biçim	664,8	317,3	904,1	**628,7**	636,9	489,4	715,1	**613,8**
	3. Biçim	658,1	314,1	895,1	**622,5**	630,5	484,5	708,0	**607,7**
Ortalama		**663,7**	**316,8**	**902,6**	**627,7**	**635,8**	**488,6**	**713,9**	**612,8**
5 Mayıs	1. Biçim	611,0	404,1	523,6	**512,9**	624,3	467,4	653,4	**581,7**
	2. Biçim	607,9	402,0	521,0	**510,3**	621,2	465,1	650,2	**578,8**
	3. Biçim	601,8	398,0	515,8	**505,2**	615,0	460,4	643,7	**573,0**
Ortalama		**606,9**	**401,4**	**520,1**	**509,5**	**620,2**	**464,3**	**649,1**	**577,9**
Genel Ortalama		**790,1**	**527,9**	**874,6**	**730,9**	**708,5**	**534,2**	**822,7**	**688,5**
EGF. (%5)		54,46 (çeşit), 40,98 (dikim zamanı)				21,75 (çeşit), 20,84 (dikim zamanı)			

Not: a) *Mentha* × *piperita* L. var Mitcham; b) *Mentha piperita*; c) *Mentha spicata*

Elde edilen değerler, sonbahar yapılan dikimlerde bitkilerin uzun bir vejetasyon süresine sahip olmalarından, gelişmeye daha erken ve avantajlı başlamalarından ve ilkbahar dikimlerinde kullanılan rizomların sürgün vermeye başlamış olmaları nedeniyle depo besinlerinin bir kısmını kullanmış olmalarından kaynaklanmaktadır (Singh vd., 1977, 1986; Singh & Nand, 1979a, 1979b; Adamovic vd., 1982; Ruminska vd., 1984). Ayrıca, sonbahar dikimlerinden yüksek verim alınması genç nanelerin bir süre soğukta kalmalarının verimi artırmasından kaynaklanabilir (El-Moursi vd., 1986).

Toplam taze herba verimi değerlerimizin nane tür ve tiplerine göre değişim göstermesi, bazı araştırıcıların bildirdikleriyle benzerlik göstermektedir (Özgüven vd., 1995). Denemenin iki yılında da elde edilen toplam taze herba verimi değerleri bazı araştırıcıların (Morton, 1977; Singh vd., 1977, 1986; Ceylan, 1978; Singh & Nand, 1979b; Franz vd., 1984; Özgüven vd., 1995) bildirdikleri değerlerden yüksek bulunmuştur. Bu sonuç, bölgemize vejetasyon dönemindeki gece ile gündüz sıcaklıkları arasındaki farklılığın fazla olmasından kaynaklanabilir (Reda vd., 1985).

Toplam Drog Herba Verimi

Toplam drog herba verimi değerleri toplam taze herba verimi değerlerine büyük oranda benzerlik göstermektedir. Hem 2019 hem de 2020 yılında en fazla toplam drog herba verimi 18 Ekim dikiminde ve yılda üç biçimin alınabildiği *M. spicata*'da saptanmıştır. Ortalamalar açısından değerlendirildiğinde geciken dikimler sebebiyle toplam drog herba verimi değerlerinin belirgin olarak düştüğü ve sonbahar yapılan dikimden ilkbahar yapılan dikime oranla yüksek değerler elde edildiği gözlenmiştir (Tablo 3).

Toplam taze herba veriminin yüksek olmasının sonbahar yapılan dikimlerde kuru madde birikiminin yüksek olmasından kaynaklandığı düşünülmektedir. Çalışmada elde edilen bulgular geç yapılan dikimlerde kuru madde miktarının azaldığını rapor eden Prasad & Saxsena (1980) ve sonbahar yapılan dikimlerden yüksek drog herba verimi elde eden Adamovic vd. (1982)'nin bulgularıyla uyum göstermektedir. Ayrıca, her iki yılda elde edilen toplam drog herba verim değerleri bazı araştırıcıların

(Ceylan, 1978; Özgüven vd., 1995) bildirdiği değerlerden yüksek bulunmuştur.

Toplam Drog Yaprak Verimi

Toplam drog yaprak verimi değerlerinde toplam taze ve drog herba verimi değerlerinde de olduğu gibi geç yapılan dikimlere paralel olarak oldukça yüksek seviyede düşüşler olduğu gözlemlenmektedir (Tablo 4). Her iki yılda da en yüksek toplam drog yaprak verimi değerleri sonbahar dikimlerinde saptanmıştır. Ayrıca, nane tiplerinden en yüksek değerler *M. spicata*'da ve en düşük değerler ise *Mentha* × *piperita* L. var Mitcham ve *M. piperita'*da tespit edilmiştir.

Çalışmada sonunda elde edilen bulgular sonbaharda yetiştirilen nanelerin yaz döneminde yetiştirilenlere oranla daha yüksek miktarda yaprak elde edildiğini, yaprak oranının geç yapılan dikimlere paralel olarak düştüğünü ve dikim zamanının yaprak oranını önemli derecede etkilediğini bildiren araştırıcıların bulgularıyla uyum göstermektedir (Singh & Singh, 1970; Singh & Nand, 1979b; Franz vd., 1984; Sing vd., 1986). Bununla birlikte, her iki yılda da toplam drog yaprak verimi değerleri, bazı araştırıcıların (Ceylan, 1978; Franz vd., 1984; Özgüven vd., 1995) bildirdikleri değerlerden yüksek bulunmuştur.

Uçucu Yağ Oranı

2019 yılında ortalama en yüksek uçucu yağ oranı değerleri 18 Kasım ve 5 Nisan dikimlerinden, 2020 yılında ise 5 Nisan ve 5 Mayıs dikimlerinden elde edilmiştir. Naneler arasında ortalama en yüksek uçucu yağ oranı 1. yıl *Mentha* × *piperita* L. var Mitcham tipi nanede, 2. yıl ise *M. spicata* tipi nanede saptanmıştır. Her iki yılda farklı biçimlerde, nane tür ve tiplerine göre dikim zamanlarından elde edilen uçucu yağ değerleri incelendiğinde ilk biçimlerde genellikle geç yapılan dikimlerde uçucu yağ oranlarında bir artış, diğer biçimlerde ise tam tersi gözlenmiştir. Bu sonuca bağlı olarak, en yüksek uçucu yağ oranları ilk biçimlerde ilkbahar dikimlerinden elde edilmiştir. İkinci biçimlerde de en yüksek değerler çoğunlukla sonbaharda yapılan dikimlerde saptanmıştır (Tablo 5). Sonbaharda dikimi yapılan naneler, ilkbaharda yapılan dikimlere kıyasla daha erken biçime gelmektedir. Bunun sebebi genelde serin bir periyodu geçirmelerinden kaynaklanmaktadır. Bulgularımız sıcaklığın belirli oranda artması ile nanede uçucu yağ oranının artığını bildiren Ceylan'ın (1978) bulgularıyla uyumludur. Ayrıca, uçucu yağ oranının türlere, biçimlere ve dikim zamanlarına göre değiştiği birçok araştırmacı tarafından da belirtilmiştir (Ceylan, 1978; Reda vd., 1985; El-Moursi vd., 1986; Duriyaprapan vd., 1986; Kothari vd., 1987; Hadipoentyanti, 1990; Özgüven vd., 1995).

Uçucu yağ oranına ilişkin tespit edilen değerler bazı araştırıcıların (Morton, 1977; Ruminska vd., 1984; Sing vd., 1986; Kothari vd., 1987; Hadipoentyanti, 1990) değerlerinden yüksek iken, bazılarının (Ceylan, 1978; Franz vd., 1984; Özgüven vd., 1995) bildirdiği değerlere benzerlik göstermektedir.

Table 4. Comparison of total drug leaf yield values (kg/da) in 2019 and 2020 in terms of planting times
Tablo 4. *2019 ve 2020 yılları toplam drog yaprak verim değerlerinin (kg/da), dikim zamanları yönünden karşılaştırılması*

Dikim Zamanı	**2019**				**2020**			
	Nane Tipleri			***Ort.***	***Nane Tipleri***			***Ort.***
	a	***b***	***c***		***a***	***b***	***c***	
18 Ekim	532,71	371,27	618,79	**507,59**	485,28	364,72	577.59	**425,00**
18 Kasım	573,54	370,07	561,98	**501,86**	498,04	313,77	540,56	**450,79**
5 Nisan	409,49	185,13	534,29	**376,30**	419,98	342,02	455,69	**405,90**
5 Mayıs	381,16	221,14	331,18	**311,16**	395,26	311,75	414,42	**373,81**
Ortalama	**474,23**	**286,90**	**511,56**	**424,23**	**449,64**	**333,07**	**470,22**	**413,87**
EGF. (%5)	20,89 (çeşit), 23,21 (dikim zamanı)				19,29 (çeşit), 11,28 (dikim zamanı)			

Not: a) *Mentha* × *piperita* L. var Mitcham; b) *Mentha piperita*; c) *Mentha spicata*

Table 5. Essential oil content values and averages (%) obtained from planting times according to mint species and types in different forms in 2019 and 2020

Tablo 5. *2019 ve 2020 yıllarında farklı biçimlerde, nane tür ve tiplerine göre dikim zamanlarından elde edilen uçucu yağ oranı değerleri ve ortalamaları (%)*

Dikim Zamanı	**2019**				**2020**			
	Nane Tipleri			***Ort.***	***Nane Tipleri***			***Ort.***
	a	***b***	***c***		***a***	***b***	***c***	
18 Ekim	2,48	2,33	1,69	**2,17 b**	2,30	3,20	2,70	**2,73 b**
18 Kasım	2,60	3,00	1,78	**2,46 b**	2,40	3,13	2,35	**2,63 b**
5 Nisan	2,60	3,68	2,48	**2,92 a**	3,55	3,25	2,70	**3,17 a**
5 Mayıs	3,00	3,50	2,70	**3,07 a**	3,45	3,45	3,35	**3,42 a**
Ortalama	**2,67 b**	**3,13 a**	**2,16 c**	**2,65**	**2,93 b**	**3,45 a**	**2,78 b**	**2,99**
EGF. (%5)	0,048 (çeşit), 0,058 (dikim zamanı)				0,14(çeşit), 0,062 (dikim zamanı			

Not: a) *Mentha* × *piperita* L. var Mitcham; b) *Mentha piperita*; c) *Mentha spicata*

Table 6. Comparison of total essential oil yield values (l/da) in 2019 and 2020 in terms of planting times

Tablo 6. *2019 ve 2020 yılları toplam uçucu yağ verimi değerlerinin (l/da), dikim zamanları yönünden karşılaştırılması*

Dikim Zamanı	**2019**				**2020**			
	Nane Tipleri			***Ort.***	***Nane Tipleri***			***Ort.***
	a	***b***	***c***		***a***	***b***	***c***	
18 Ekim	14,44	12,54	16,23	**14,40 a**	9,51	13,24	16,98	**13,24 a**
18 Kasım	15,65	14,70	14,85	**15,07 a**	9,30	11,10	15,39	**11,93 b**
5 Nisan	10,67	6,50	14,67	**10,61 b**	9,33	11,07	14,54	**11,65 b**
5 Mayıs	9,08	7,19	8,71	**8,33 c**	8,26	9,62	13,29	**10,39 c**
Ortalama	**12,46 b**	**10,23 c**	**13,62 a**	**12,10**	**9,10 c**	**11,26 b**	**15,05 a**	**11,80**
EGF. (%5)	0,735 (çeşit), 0,7216 (dikim zamanı)				0,755 (çeşit), 0,502 (dikim zamanı)			

Not: a) *Mentha* × *piperita* L. var Mitcham; b) *Mentha piperita*; c) *Mentha spicata*

Toplam Uçucu Yağ Verimi

2019 ve 2020 yıllarında elde edilen en yüksek toplam uçucu yağ verimi değerleri Ekim ve Kasım dikimlerinde saptanmış ve geciken dikimlerde ise uçucu yağ veriminde oldukça önemli bir düşüş gözlenmiştir (Tablo 6). Ayrıca, naneler içerisinde en yüksek değerler *M. spicata* tipi nanede saptanmış ve bunu *Mentha* × *piperita* L. var Mitcham tipi nanenin izlediği ve en düşük değerlerin 1. yıl *M. piperita* tipi nanede gözlendiği, 2. yılda da verimlerin gerileyerek benzer durum sergilediği tespit edilmiştir.

Bütün nane tür ve tiplerinde Nisan ve Mayıs dikimlerinde toplam uçucu yağ verimlerinde belirgin düşüşler gözlenmiştir. Ayrıca, Ekim ve Kasım dikimlerindeki toplam uçucu yağ verim değerleri, Nisan ve Mayıs dikimlerine göre nazaran yüksek miktarlarda toplam uçucu yağ elde edilmiştir (Tablo 6). Bu durum, sonbahar dikimlerinden daha yüksek toplam drog yaprak verimleri alınmasından kaynaklanmaktadır.

Çalışma sonunda elde edilen bulgular sonbahar dikimlerinden ilkbahar dikimlerine göre daha yüksek toplam uçucu yağ verimi aldığını ve geciken dikimlere paralel olarak uçucu yağ verimin düştüğünü göstermektedir. Bu durum gözlenen düşüşün yaprak verimindeki düşüşten kaynaklandığını bildiren araştırıcıların (Singh & Nand, 1979b; Adamovic vd., 1982; Sing vd., 1986) bulgularıyla benzerlik göstermektedir.

Toplam uçucu yağ verimleri bakımından nane tür ve tipleri arasında farklı sonuçlar alınması değişik genotiplere sahip olan nanelerin ekolojik faktörlere karşı, farklı tepki göstermelerinden ve toplam drog yaprak verimlerinden kaynaklanmaktadır. Ayrıca bazı araştırıcılar uçucu yağ veriminin nane tür ve tiplerine göre değişim gösterdiğini bildirmektedir (Ceylan, 1978; Franz vd., 1984; Özgüven vd., 1995).

Her iki yılda elde edilen toplam uçucu yağ verimi değerleri (6,50-16,98 l/da), Kothari vd. (1987) tarafından rapor edilen değerlerin (15,06-20,53 kg/da) alt sınırına yakın, bazı araştırıcıların (Singh & Nand, 1979b; Clark & Menary, 1984; Singh vd., 1986; Özgüven vd., 1995) değerlerine (7,94-16,59 l/da) benzer ve bazılarının (Morton, 1977; Hadipoentyanti, 1990) bildirdiği değerlerden (0,68-10,0 l/da) ise yüksek bulunmuştur.

SONUÇ

İncelenen özellikler bakımından Çanakkale koşullarında, *M. spicata* tipi nane genelde ilk sırada yer almıştır. Bu nane tipinin her iki deneme yılında da iyi bir performans göstermesi ve bölge ekolojik koşullarında, özellikle sonbahar dikimi şeklinde üretiminin rahatlıkla yapılabileceği ortaya çıkmıştır. Çanakkale koşullarında tüm dikim zamanlarında toplam taze herba, toplam drog herba, toplam drog yaprak ve uçucu yağ verimlerinin literatür değerleri ile aynı paralelde veya daha yüksek olması ve deneme süresince bitkilerde önemli bir hastalık ve zararlının görülmemesi, bu ekolojinin nane tarımı için uygun olduğunu ortaya koymaktadır. Tüm nane tür ve tiplerinde, sonbahar dikimlerinde (18 Ekim ve 18 Kasım) ilkbahar dikimlerine (5 Nisan ve 5 Mayıs) göre çok daha yüksek drog ve uçucu yağ verimlerinin tespit edilmesi, bölge koşullarında nane için en uygun dikim zamanının sonbahar olduğunu göstermektedir. Nane tür ve tipleri arasında en yüksek toplam taze herba, toplam drog herba, toplam drog yaprak ve uçucu yağ verimleri *M. spicata* tipi nanede saptanmış ve ikinci sırada *Mentha* × *piperita* L. var Mitcham tipi nane yer almıştır. *Mentha* × *piperita* L. var Mitcham tipi nanede sonbahar dikimlerinde toplam drog yaprak veriminin düşük olmasına rağmen uçucu yağ oranının yüksek olması nedeniyle daha yüksek toplam uçucu yağ verimi saptanmıştır. Ancak, bu nane tipinin özellikle sıcaklığın artması ile gelişmesinin yavaşlaması, birinci biçimlerden sonra gelişmenin yok denecek kadar az olması, ikinci yıl yeniden gelişmenin çok az olması ve dolayısıyla drog verimlerinin düşük olmasından ötürü, bölge için uygun olmadığı kanaatine varılmıştır. Bununla birlikte, yüksek uçucu yağ ve mentol içeren bu tür ile ilgili ek araştırmaların bölgede yapılması faydalı olacaktır.

Etik Standartlara Uygunluk

Çıkar Çatışması

Yazar herhangi bir çıkar çatışması olmadığını deklare etmektedir.

Etik Onay

Yazar bu çalışma için resmi etik kurul onayının gerekli olmadığını bildirmektedir.

Veri Kullanılabilirliği

Yazar, bu çalışmanın bulgularını destekleyen verilerin makale içinde mevcut olduğunu onaylamaktadır.

KAYNAKLAR

Adamovic, D., Kisgeci, J., Stanacev, S., & Sapevak, P. (1982). Effect of planting time and growing area on the yield and quality of Mitcham peppermint. *Bilten za Hmelj i Sirak*, *14*(39), 63-73.

Başer, H. (1993). Uçucu yağların dünya ticareti. *Tıbbi ve Aromatik Bitkiler Bülteni*, *9*, 15-17.

Ceylan, A. (1978). *Menemen ekolojik koşullarında Mentha piperita L. ve Mentha spicata L. türlerinin bazı agronomik ve teknolojik özellikleri üzerinde araştırma*. E.Ü. Ziraat Fakültesi, Yayın No: 379.

Ceylan, A., Yılmaz, G., Gürbüz, B., & Bayram, E. (1994). İlaç ve aromatik bitkilerin tüketim projeksiyonları ve üretim hedefleri. *Türkiye Ziraat Mühendisliği 4. Teknik Kongresi Bildiriler Kitabı*, Türkiye, ss. 571-576.

Clark, R. J., & Menary, R. C. (1984). The effect of two harvests per year on the yield and composition of Tasmanian peppermint oil (*Mentha piperita* L.). *Journal of the Science of Food and Agriculture*, *35*, 1191-1195. https://doi.org/10.1002/jsfa.2740351109

Dinç, U., Şenol, S., Sayın, M., Kapur, S., Güzel, N., Derici, R., Yeşilsoy, M. Ş., Yegingil, İ., Sarı, M., Kaya, Z., Aydın, M., Kettaş, F., Berkman, A., Çolak, A. K, Yılmaz, K, Tunçgögüs, B., Özbek, H., Gülüt, K. Y., Karaman, C., Dinç, U., Öztürk, N., & Kara, E. E. (1988). Harran ovası toprakları. Çukurova Üniversitesi Ziraat Fakültesi Toprak Bölümü. TÜBİTAK - TOAG 534 Nolu Proje.

Duriyaprapan, S., Britten, E. J., & Basford, K. E. (1986). The effect of temperature on growth, oil yield and oil quality of Japanese mint. *Annals of Botany*, *58*, 729-736. https://doi.org/10.1093/oxfordjournals.aob.a087236

Ekim, T. (1990). İhraç edilen yabani bitkilerimiz ve geleceği. *TOK Dergisi*, *53*, 9-12.

El-Moursi, A., Shedeed, M. R., Reda, F., & EL-Din, K. G. (1986). Effect of cold hardening on growth and essential oil content of *Mentha piperita* L. *Journal of Agronomy Crop Science*, *156*, 260-265. https://doi:10.1111/j.1439-037X.1986.tb00035.x

Franz, Ch., Hölzl, J., Ceylan, A., & Vömel, A. (1984). Influence of the growing site on the quality *Mentha piperita* L. oil. *Acta Horticulturae*, *144*, 145-150. https://doi.org/10.17660/ActaHortic.1984.144.18

Genç, İ., & Tükel, T. (1988). *Tarımsal ekoloji*. Ç.Ü. Ziraat Fakültesi, Ders Kitabı. No: 29, Adana.

Hadipoentyanti, E. (1990). Yield stability analysis of oil yield and quality of *Mentha spp*. *Pemberitaan Penelitian Tanaman Industri*, *16*(1), 18-23.

Kothari, S. K., Singh, V., & Singh, K. (1987). Effect of rates and methods of phosphorus application on herb and oil yields and nutrient concentrations in Japanese mint (*Mentha arvensis* L.). *The Journal of Agricultural Science*, *108*(3), 691-693. https://doi.org/10.1017/S0021859600080163

Morton, J. F. (1977). *Major medicinal plants: Botany, culture, and uses*. Charles C Thomas.

Özgüven, M., Kırıcı, S., & Mengel, C. (1995). *Nane (Mentha) türlerinin farklı ekolojilerde araştırılması*. Tıbbi ve Aromatik Bitkiler Workshop, İzmir.

Prasad, S., & Saxsena, M. C. (1980). Effect of date of planting and row spacing on the growth and development of peppermint (*Mentha piperita* L.) in Taria. *Indian Journal of Plant Physiology*, *23*(2), 119-126.

Reda, F., Shedeed, M. R., El-Moursi, A., & El-Din, K. G. (1985). Effect of heat hardening on growth and essential oil content of peppermint plants. *Egyptian Journal of Botany*, *28*(1-3), 37-45.

Ruminska, A., Suchorska, K., & Weglarz, Z. (1984). Growth and development of peppermint (*Mentha piperita L.*) in the first and second year of cultivation. *Annals of Warsaw Agricultural University SGGW-AR, Horticulture*, *12*, 33-39.

Sing, K., Ram, P., Sing, V., & Kothari, S. K. (1986). Effect of dates of planting and nipping on herb and oil yield *of Mentha arvensis* L. *Indian Journal Agronomy*, *41*(2), 128-130.

Singh, J. N., & Singh, D. P. (1970). Effect of phosphate fertilisation and seasonal variations on Japanese mint (*M. arvensis L. var. piperascens*). *Soil Science and Plant Nutrition*, *16*(3), 95-101. https://doi.org/10.1080/00380768.1970.10432824

Singh, K., Singh, V., Kothari, S. K. (1986). Effect of planting materials and spacing on herb, oil and sucker production in *Mentha arvensis* L. *Annals of Agricultural Research*, *7*(2), 313-316.

Singh, N. P., & Nand, K. (1979a). Influence of planting time and row spacing on yield of spearmint. *Indian Perfumer*, *XXIII*(1), 53-54.

Singh, N. P., & Nand, K. (1979b). Response of *Mentha citrata Ehrh*. to dates of planting and row spacing. *Indian Perfumer*, *XXIII*(1), 50-52.

Singh, N. P., Saxena, M. C., & Nand, K. (1977). Effect of dates of planting, row spacing and rates of nitrogen application on herb yield of *Mentha arvensis* Linn. *Indian Perfumer*, *XXI*(2), 83-85.

TÜİK. (2021). *Dış ticaret istatistikleri*. Türkiye İstatistik Kurumu. https://www.tuik.gov.tr/ Erişim tarihi: 24.06.2024

TÜİK. (2024). *Bitkisel üretim istatistikleri*. Türkiye İstatistik Kurumu. https://www.tuik.gov.tr/ Erişim tarihi: 24.06.2024

ACTA NATURA ET SCIENTIA

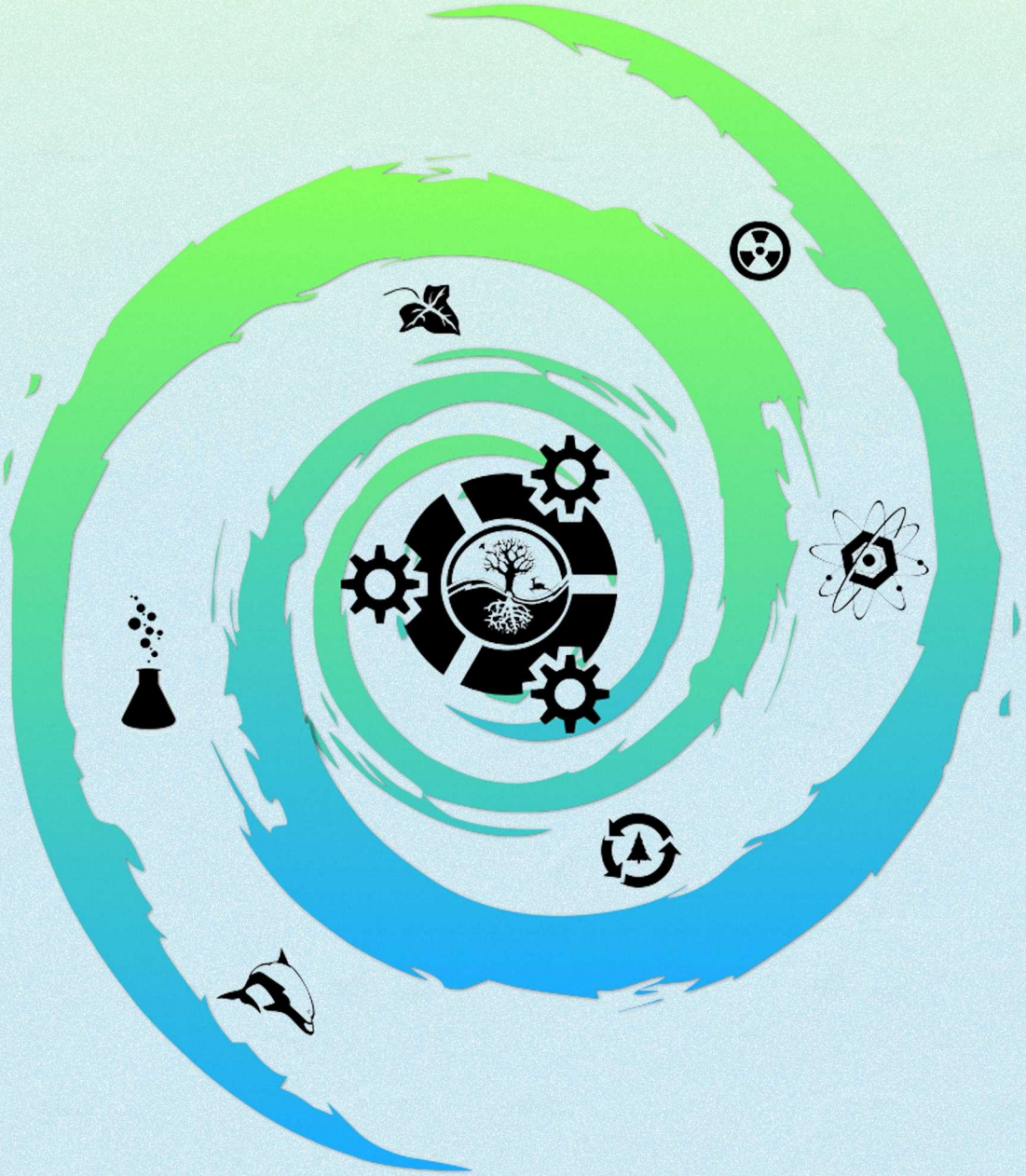

e-ISSN: 2718-0638

www.actanatsci.com